ROLE OF INTERLEUKIN-17 IN ENDOTHELIAL CELL ACTIVATION AND VASCULAR FUNCTION

A Dissertation
Submitted to the
Temple University Graduate Board

In Partial Fulfillment of the
Requirement for the
Degree of Doctor of Philosophy

By
Jietang Mai
May, 2014

Dissertation Examining Committee Members:

Dr. Xiao-Feng Yang, Department of Pharmacology (Dissertation Advisor)
Dr. Hong Wang, Department of Pharmacology (Dissertation Co-advisor)
Dr. Barrie Ashby, Department of Pharmacology (Dissertation Examining Committee Chair)
Dr. Michael Autieri, Department of Physiology
Dr. Victor Rizzo, Department of Anatomy and Cell Biology
Dr. Nicholas Sibinga, Albert Einstein College of Medicine of Yeshiva University (External Examiner)

ABSTRACT

ROLE OF INTERLEUKIN-17 IN ENDOTHELIAL CELL ACTIVATION AND VASCULAR FUNCTION

Jietang Mai

Doctor of Philosophy

Temple University, 2014

Doctoral Advisory Committee Chair: Xiao-Feng Yang, MD, PhD

Endothelial cell (EC) activation is a change of the endothelium from a quiescent state to one that is involved in immune reactions. Activation of ECs is associated with the inception of atherosclerosis. Atherosclerosis is a chronic inflammatory disease that involves adaptive and innate immunity. There are many pro-inflammatory stimuli which activate the endothelium. The pro-inflammatory cytokine interleukin-17 (IL-17) has been shown to activate lung microvascular ECs. Enhanced expression of the IL-17 receptor by synovial ECs is associated with rheumatoid arthritis. These studies suggest that IL-17 plays an important role in EC biology. Nevertheless, the role of IL-17 in EC activation and endothelial dysfunction in the context of hyperlipidemia-induced atherosclerosis has not been studied.

In the current study, we investigated the role of IL-17 in EC activation *in vitro* with mouse aortic ECs and human aortic ECs. In addition, we used the IL-17/ApoE double knock-out mouse to determine the role of IL-17 in vessel function and atherosclerosis development. First, we found that hyperlipidemia increased the number of

IL-17-producing cells in the spleens from wild type mice and ApoE$^{-/-}$ mice that were fed a Western diet when compared to their respective normal chow diet controls. We also found that after treatment with the pro-atherogenic factor, oxidized LDL, there was an increase in the expression of IL-17 receptor by ECs. Using an EC specific array, we found that IL-17 induced significant up-regulation of four genes that are associated with EC activation in mouse aortic ECs. The four genes induced in IL-17-treated mouse aortic ECs were Cxcl1, Cxcl2, Il6, and Csf2. Moreover, we also found that IL-17 induced these four genes in human aortic ECs, and we showed that enhanced monocyte adhesion to ECs was dependent on these four genes.

It was previously observed that a Western diet induced vessel dysfunction in the aortas of ApoE$^{-/-}$ mice. Thus, we sought to determine whether IL-17-deficiency rescues impaired endothelium-dependent relaxation in ApoE$^{-/-}$ mice that were fed a Western diet with the Wire Myograph System. We found that ApoE$^{-/-}$ mice on a 3-week Western diet had impaired endothelium-dependent relaxation when compared to IL-17$^{-/-}$ApoE$^{-/-}$ mice. Endothelium-independent relaxation in response to sodium nitroprusside (SNP) and contraction responses induced by potassium chloride (KCl) and phenylephrine (PE) were not different in ApoE$^{-/-}$ mice and IL-17$^{-/-}$ApoE$^{-/-}$ mice.

Since our *in vitro* studies and vessel function assay pointed to a pro-atherogenic role for IL-17, we investigated lesion formation in ApoE$^{-/-}$ mice and IL-17$^{-/-}$ApoE$^{-/-}$ mice. Lesion formation was assessed with Sudan IV staining of the whole aorta and Oil red O

staining of aortic sinus cross sections. IL-17 deficiency in ApoE$^{-/-}$ mice did not affect atherosclerotic lesion formation in our study.

Hyperlipidemia is a well-established risk factor for atherosclerosis so we investigated whether the pro-atherogenic role of IL-17 may have been compromised by lipid levels *in vivo*. The lipid profiles of mice which measured the levels of LDL, HDL, triglyceride, non-esterified free fatty acid, and total cholesterol were determined. The lipid profiles showed that IL-17 deficiency in ApoE$^{-/-}$ mice modulated the levels of the lipids in the plasma.

Taken together, our data suggest that IL-17 is up-regulated in hyperlipidemia and IL-17 induces aortic EC activation. IL-17 also contributes to endothelial dysfunction in ApoE$^{-/-}$ mice induced by a Western diet. Moreover, IL-17 may modify lipid metabolism in mice. The effects of IL-17 on lipid levels may weaken its pro-atherogenic potential and contribute to the lack of an atherosclerotic phenotype in our atherosclerosis study. Our current work has shed light on the role of IL-17 on EC biology and has provided insights into the effects of IL-17 on EC activation, lipid modification, and vascular function. These important findings may serve as the stepping stone to the development of therapeutics that target vascular inflammation and its underlying mechanisms.

The studies in this dissertation were supported by grants from the National Institutes of Health (NIH) and a fellowship from the American Heart Association (AHA).

ACKNOWLEDGEMENTS

Over the past 5^{+} years, I have received tremendous support and encouragement from a number of wonderful individuals. I would like to thank my advisor, Dr. Xiao-Feng Yang, for welcoming me into his laboratory. Dr. Yang has guided me in my thesis direction and manuscript writing, and he has taught me many indispensable laboratory techniques. I am continued to be captivated by his passion for his work as a professor, researcher, and mentor. Dr. Yang's commitment to science is contagious and I thank him for inspiring and driving me towards scientific research. I would like to thank Dr. Hong Wang, our laboratory's longtime collaborator, for her constructive criticisms and insights during our joint lab meetings and journal clubs. I am also grateful that she is part of my thesis committee. I am also thankful for other members of my committee, Dr. Barrie Ashby, Dr. Michael Autieri, and Dr. Victor Rizzo for their ideas, help, and words of encouragement during each of our meetings. I am grateful for Dr. Nicholas Sibinga, my external examiner, for his kindness and his generosity with his time.

I would like to thank all the members (past and present) of Dr. Wang and Dr. Yang's laboratories for all their help and collaborations. I want to extend a special thank you to Xiaohua Jiang, our lab manager, for all her help. I am grateful to have had Xiaohua to take care of all my needs in the lab. I am grateful for Dr. Fang Liu who helped me in initiating the "IL-17 project" while I was still taking my graduate courses. Fang was always willing to help and teach the graduate students in the lab; I hope to encounter more post-doctoral fellows like her. I am grateful to have had Xinyu Xiong to

teach me techniques in molecular cloning. Although these skills were not incorporated in this thesis, I am thankful that I was taught an essential laboratory skill. I would like to thank Michael Jan for all his help and guidance. Michael is an extremely knowledgeable person; he was always willing to share his expertise. He helped and taught everyone in the lab with enthusiasm. Also, I would like to thank Jiyeon Yang who taught me how to isolate primary human monocytes and provided me cells and plasmas for my assays. Jiyeon is an extremely dedicated scientist who was very collaborative and always willing to extend her help. I am grateful to have had Shu Meng's help. Dr. Shu Meng is extremely knowledgeable and she always asked challenging questions and took interest in others' projects. I would like to thank Dr. Ya-Feng Li for his help with the microarray data analysis and insightful discussions about a career in science. I am grateful to have had Dr. Huimin Shan's help in the intravital study as well as in maintaining the lab. I am thankful to have Dr. Xiaojin Sha's help with the flow cytometry in our lab. I would like to thank Dr. Zhongjian Cheng for her help with the vessel relaxation assay and for all the wonderful discussions about science and life.

More importantly, I am thankful to have had Meghana Pansuria (now Dr. Meghana Pansuria) as a colleague and friend during my study. I thank her for all her help, motivation, and positive outlooks. She was always there to assure that everything "is okay." I would like to thank Ying Yin (now Dr. Ying Yin) for all her help. Ying was always knowledgeable regarding the methods that we used in the lab. I am grateful to have had Ying's guidance whenever I began a new experiment. I would like to thank Anthony Virtue for his encouragement and help. Anthony is the most productive person

in the lab. His positive attitude towards his work is inspiring and I thank him for all his encouragement during the dissertation writing process.

I am also grateful to have all the wonderful individuals in our administrative department who had helped me over the years, especially to Dolores (Lor) Hatch for all her support, encouragement, and prayers. I would like to thank Dr. Xiaoxuan Fan, manager of the Flow Cytometry Facility, for all his help with my FACS needs. Also, I would like to thank Dr. Yoichiro Iwakura of the University of Tokyo for providing our lab with the IL-17$^{-/-}$ mice.

Lastly, I want to thank all my friends and family for all their prayers and support. I am grateful for their words of encouragement and comfort. I am especially grateful to have my family's blessing and love. Most importantly, I thank God for the Love He has given to all of us. :)

DEDICATION

To my dearest…

TABLE OF CONTENTS

LIST OF FIGURES

LIST OF TABLES

LIST OF ABBREVIATIONS

WHO	World Health Organization
CVDs	Cardiovascular diseases
PAD	Peripheral artery disease
VSMC(s)	Vascular smooth muscle cell(s)
EC(s)	Endothelial cell(s)
TAG(s)	Triacylglycerol(s)
VLDL	Very-low-density lipoproteins
IDL	Intermediate-density lipoproteins
LDL	Low-density lipoproteins
HDL	High-density lipoproteins
ApoB	Apolipoprotein B
OxLDL	Oxidized low-density lipoproteins
ApoE	Apolipoprotein E
LDLR	Low-density lipoprotein receptor
WT	Wild type
HF	High fat
NO	Nitric oxide
GPCR(s)	G protein-coupled receptor(s)
CD	Cluster of differentiation
Th	T helper
Treg(s)	Regulatory T cell(s)

CCR	Chemokine C-C motif receptor
CXCR	CXC-chemokine receptor
IFN-γ	Interferon-gamma
IL	Interleukin
TNF-α	Tumor necrosis factor-alpha
LT	Lymphotoxin
EAE	Experimental autoimmune encephalomyelitis
CTL	Cytotoxic T lymphocyte
Ctla8	Cytotoxic T lymphocyte associated antigen 8
STAT	Signal Transducer and Activator of Transcription
TGF-β	Transforming growth factor-beta
SOCS	Suppressor of cytokine signaling
HUVEC(s)	Human umbilical venous cord endothelial cell(s)
HMVEC(s)	Human dermal microvascular endothelial cell(s)
VEGF	Vascular endothelial growth factor
PGE	Prostaglandin E
MIP-2	Macrophage inflammatory protein 2
CXCL	Chemokine C-X-C motif ligand
bFGF	Basic fibroblast growth factor
HGF	Human growth factor
LMVEC(s)	Lung microvascular endothelial cell(s)
ICAM-1	Intracellular cell adhesion molecule-1

VCAM-1	Vascular cell adhesion molecule-1
MAPK	Mitogen-activated protein kinase
BBB	Blood-brain barrier
ROS	Reactive oxygen species
ACh	Acetylcholine
SNP	Sodium nitroprusside
IACUC	Institutional Animal Care and Use Committee
PCR	Polymerase chain reaction
NaCl	Sodium chloride
EDTA	Ethylenediaminetetraacetic acid
SDS	Sodium dodecyl sulfate
Bp	Base pair
APC	Allophycocyanin
PE	Phycoerythrin
PE-Cy	Phycoerythrin-Cyanine
FITC	Fluorescein isothiocyanate
HRP	Horseradish Peroxidase
IgG	Immunoglobulin G
Anti-phospho	Antibody against phosphorylation
HAEC(s)	Human aortic endothelial cell(s)
FBS	Fetal bovine serum
ECGS	Endothelial cell growth supplement

PSA	Penicillin, streptomycin, and amphotericin
DMEM	Dulbecco's modified eagle medium
ELISA	Enzyme-linked immunosorbent assay
ACK	Ammonium-Chloride-Potassium
PMA	Phorbol 12-myristate 12-acetate
PFA	Paraformaldehyde
PBS	Phosphate buffered saline
MAEC(s)	Mouse aortic endothelial cell(s)
EGM	Endothelial growth medium
DBPS	Dulbecco's Phosphate-Buffered Saline
DiI-Ac-LDL	1,l'-dioctadecyl-3,3,3',3'-tetramethylindocarbocyanine-acetyl-low density lipoprotein
DAPI	4', 6-diamidino-2-phenylindole
ACD	Acid Citrate Dextrose
THP-1 cells	Human acute monocytic leukemia cells
RPMI	Roswell Park Memorial Institute
HPBMC(s)	Human peripheral blood monocyte(s)
BCA	bicinchoninic acid
ECL	Enhanced chemiluminescence
cDNA	Complementary DNA
qRT-PCR	Quantitative real-time PCR
i.p.	Intraperitoneal

$NaHCO_3$	Sodium bicarbonate
$CaCl_2•2H_2O$	Calcium chloride dehydrate
KCl	Potassium chloride
KH_2PO_4	Monopotassium phosphate
$MgSO_4•7H_2O$	Magnesium sulfate heptahydrate
PE	phenylephrine
eNOS	Endothelial nitric oxide synthase
GC	Guanylyl cyclase
cGMP	Cyclic guanosine monophosphate
HEPES	4-(2-hydroxyethyl)-1-piperazineethanesulfonic acid
HBSS	Hank's Balanced Salt Solution
OCT	Optimal Cutting Temperature compound
WD	Western diet
Csf2	Colony stimulating factor 2
GM-CSF	Granulocyte-Macrophage Colony-Stimulating Factor
SSC	Side-scattered
FSC	Forward-scattered
MNC(s)	Mononuclear cell(s)
FFA	Free fatty acid
RefSeq	Reference Sequence
ApoAI	Apolipoprotein A-I

CHAPTER 1

GENERAL INTRODUCTION

According to the World Health Organization (WHO), cardiovascular diseases (CVDs) including ischemia heart disease and stroke are the number one cause of deaths worldwide. CVDs contribute to 3 of every 10 deaths - accounting for an estimate of 17.3 million deaths in 2008 (WHO, 2011b). Ischemic heart disease (coronary artery disease) is the disease of the blood vessels supplying the heart muscle whereas a cerebrovascular accident or stroke occurs when blood flow to a part of the brain stops. The underlying pathological process of coronary artery disease and stroke is atherosclerosis. Atherosclerosis is the thickening and hardening of arteries due to the buildup of plaques along the inner walls of blood vessels (WHO, 2011a).

Atherosclerosis can occur in any artery in the body, including arteries of the heart, brain, kidneys, and extremities. In the heart, atherosclerosis can cause coronary heart disease. In the brain, it can lead to ischemic stroke and transient ischemic attack. In the kidneys, it can lead to renal impairment and hypertension. And in the extremities, it can cause peripheral artery disease (PAD) (Powell-Braxton et al., 1998). The clinical consequence of atherosclerosis is predominantly due to the rupture of a plaque, which exposes pro-thrombotic materials to the blood and triggers a clot to form. A blood clot can further narrow the artery or completely occlude the artery and stop blood flow in that artery.

Atherosclerosis

Atherosclerosis was originally regarded as a lipid storage and metabolism disease associated with aging since some hardening of arteries normally occurs as people grow older. Recent advances in fundamental science have established atherosclerosis as a chronic inflammatory disease in which inflammation plays a critical role through all stages of the disease (Powell-Braxton et al., 1998) (Figure 1). During the initial step of atherosclerosis, the endothelium is activated and inflamed due to insults such as pro-atherogenic factors. Activated endothelial cells (ECs) express high levels of adhesion molecules and pro-inflammatory chemokines and cytokines which attract circulating leukocytes. At the same time, the inflamed endothelium allows leukocytes to transmigrate to the sub-endothelium as well as circulating lipids to accumulate in the intima of arteries. The accumulated lipids are modified (e.g. by oxidation) and transformed into pro-inflammatory stimuli. Meanwhile, in response to the inflammatory signals initiated in ECs, vascular smooth muscle cells (VSMCs) are induced to release chemokines, which act together with the inflamed endothelium in orchestrating the recruitment of monocytes and T cells into the arterial wall. Transmigrated monocytes differentiate into macrophages which form foam cells within the intima by taking up modified lipids; these foam cells form a fatty streak. Macrophages along with activated T cells in the sub-endothelium produce additional pro-inflammatory cytokines. These pro-inflammatory stimuli aggravate the inflammatory process by driving additional immune cell recruitment and proliferation of VSMCs; the inflammatory process becomes one that is chronic. Proliferating VSMCs synthesize collagen and elastin which form a fibrous

cap, and a lipid core is formed by the accumulation of T cells, foam cells, and lipids in the sub-endothelium. As more lipid material and cells accumulate within the fibrous cap, the atherosclerotic plaque becomes necrotic and vulnerable to rupture. Ultimately, a lesion ruptures and exposure of thrombogenic material in the core initiates a thrombotic event, which causes stenosis or blockage in an artery leading to an ischemic event, with potential fatal consequences of a myocardial infarction or a cerebrovascular accident.

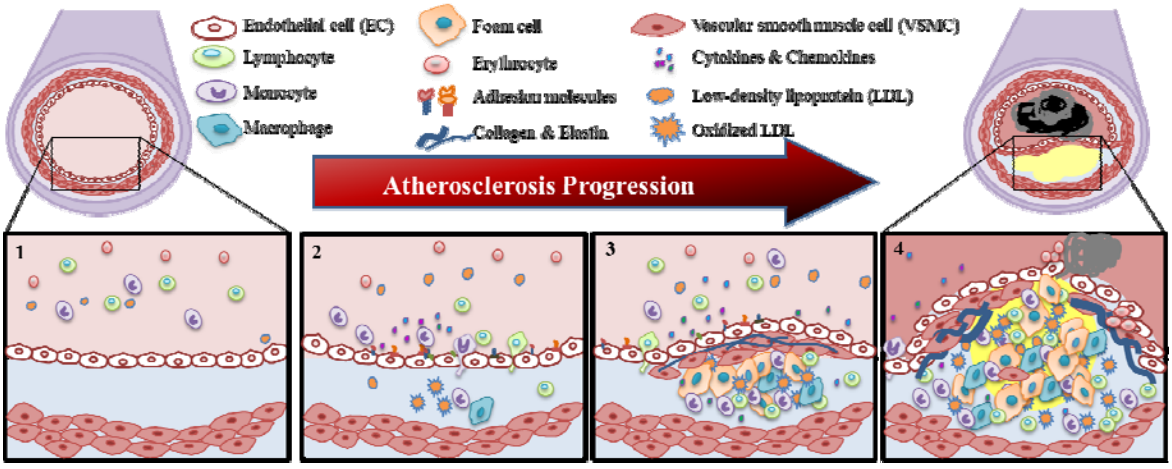

Figure 1. Multi-step of atherosclerosis progression

Illustration of the multiple steps in atherosclerosis development. 1. A normal vessel is lined by a monolayer of ECs called the endothelium that carries out many essential physiological functions. **2.** During the initial steps of atherosclerosis, blood leukocytes adhere to the activated endothelial monolayer and transmigrate into the intima where maturation of monocytes into macrophages, and their uptake of lipids, yield foam cells. **3.** Lesion progression involves the recruitment of additional leukocytes into the sub-endothelium and the proliferation and migration of VSMCs from the media to the intima. Synthesis of extracellular matrix macromolecules such as collagen and elastin by VSMCs forms a fibrous cap around the lesion. **4.** The rupture of a lesion leads to the ultimate complication of atherosclerosis - thrombosis. A thrombus that partially blocks the vessel lumen impedes the blood flow in the vessel and a thrombus that completely occludes a vessel causes ischemia.

Hyperlipidemia, a Risk Factor for Atherosclerosis

Many genetically and environmental risk factors for atherosclerosis has been established, including elevated blood cholesterol levels, high blood pressure, smoking, insulin resistance, diabetes mellitus, obesity, and hyperhomocysteinemia (Glass & Witztum, 2001). Animal, epidemiological, and clinical studies have established that hypercholesterolemia, a form of hyperlipidemia, promotes atherosclerosis. Hyperlipidemia is characterized by abnormally elevated levels of any or all lipids and/or lipoproteins in the blood. Lipids in the body including triacylglycerols (TAGs), phospholipids, cholesterol, and fatty acids are transported in the circulatory system via lipoproteins. Chylomicrons, very-low-density lipoproteins (VLDL), intermediate-density lipoproteins (IDL), low-density lipoproteins (LDL), and high-density lipoproteins (HDL) are the five major classes of lipoproteins classified based on their hydrated density, size, electrophoretic mobility, and relative content of triglyceride, cholesterol, and protein (Cox & Garcia-Palmieri, 1990).

Cholesterol is essential for physiological processes. It has two main functions within the body; it serves as a crucial structural component in the cell membrane of vertebrates, and it participates in the synthesis of steroid hormones, bile acids, and vitamin D. Cholesterol within the lipid bilayer of cell membranes is distributed heterogeneously and it is important for establishing and maintaining the fluidity and permeability of the membrane. Cholesterol not only contributes to the integrity of the cell

membrane, it also affects cellular processes. It interacts with other lipids and proteins within the cell membrane. Cholesterol in the body is derived from two sources: diet and *de novo* synthesis which mainly occurs in the liver but other cells can also produce cholesterol. Due to its importance in biological processes, the synthesis, metabolism, transfer, and storage of cholesterol within the body is tightly controlled (Ikonen, 2008).

Most cells are able to fulfill their membrane cholesterol needs by endogenous synthesis, but many cells have mechanisms to internalize exogenous sources of cholesterol such as those derived from diet. Hormone-producing cells may take up external cholesterol for use during acute steroid hormone synthesis (Lin et al., 1995). Macrophages are known to have numerous receptors that mediate the uptake of external lipids. Macrophages and smooth muscle cells internalize lipoproteins that are present in the arterial wall, which reduce the insult of lipoproteins on the endothelium. Thus, uptake of lipids by cells is physiological and protective. However, internalization of exogenous cholesterol suppresses the ability of cells to produce endogenous cholesterol and disrupts the homeostatic regulation of cholesterol biosynthesis. Excess uptake of extracellular cholesterol also leads to repression of LDL receptor (LDLR) expression, a protective mechanism to prevent cholesterol overload (Applebaum-Bowden et al., 1984). Hepatocytes eliminate excess diet-derived cholesterol in the plasma to prevent lipid overload of other cells via a process known as reverse cholesterol transport. Excess cholesterol in forms of lipoproteins is taken up by the liver to synthesize bile acid which is excreted from the body (Lewis & Rader, 2005).

In humans, LDL is the major carrier of cholesterol in blood, whereas in mice, HDL is the major player. HDL is often referred to as the "good" cholesterol and LDL is the "bad" cholesterol. Studies have suggested an inverse relationship between plasma HDL levels and CVD risk in humans (Boden, 2000). HDL is important in maintaining cellular cholesterol homeostasis; it mobilizes cholesterol during reverse cholesterol transport which reduces the lipid load of non-hepatic cells and decreases the plasma cholesterol concentrations. HDL has been shown to have anti-atherogenic properties (Assmann & Gotto, 2004). Contrary to HDL, LDL has been shown to contribute to the initiation and progression of atherosclerosis. Retention of apolipoprotein B (ApoB)-containing lipoprotein in the sub-endothelial space is a hallmark event in the initiation of atherosclerosis. ApoB is the major apolipoprotein of LDL, which serves as a ligand for LDLR on various cells. Foam cells of early lesion are macrophages that have taken up lipoproteins such as LDL in the sub-endothelium (Tabas, Williams, & Boren, 2007). It is important to note that the uptake of native LDL does not induce cholesterol accumulation and foam cell formation since internalization of exogenous lipoproteins leads to down-regulated LDLR expression, which prevents lipid overload. However, it should also be noted that there are other receptors on macrophages which mediate the uptake of lipids. It has been shown that it is the uptake of modified LDL, especially oxidized low-density lipoproteins (OxLDL), that causes cholesterol accumulation (Boullier et al., 2001). Studies support the correlation of OxLDL levels and atherogenesis. Oxidized LDL is found in atherosclerotic lesions but not in normal arteries of animals (Rosenfeld, Palinski, Yla-Herttuala, Butler, & Witztum, 1990). Transient increases of circulating OxLDL are

detected prior to lesion development in mice (Kato et al., 2009). More importantly, studies demonstrated that macrophages internalize OxLDL more efficiently than native LDL to form foam cells (Goldstein, Ho, Basu, & Brown, 1979; Maor, Mandel, & Aviram, 1995).

Mouse Models of Atherosclerosis

Apolipoprotein E-deficient ($ApoE^{-/-}$) and LDLR-deficient ($LDLR^{-/-}$) mice are two very useful and well-characterized mouse models for studying the mechanisms of atherogenesis. ApoE and LDLR are important in cholesterol metabolism and targeted deletions of the genes encoding these molecules have rendered mice that are hypercholesterolemic (Figure 2).

ApoE is a glycoprotein that is mainly produced by the liver. It is presented in all plasma lipoproteins that transport dietary- and liver-derived cholesterols except LDL. ApoE is important in mediating the uptake of cholesterol. It is a ligand for cell-surface lipoprotein receptors such as chylomicron remnant receptors and LDLR which mediate the uptake of chylomicrons and VLDL remnants by the liver, respectively. Thus, genetic modification of the *Apoe* gene leads to drastic consequences for lipoprotein metabolism. The ApoE-deficient mouse was created in two different laboratories practically simultaneously by target inactivation of the *Apoe* gene (Plump et al., 1992; Zhang, Reddick, Piedrahita, & Maeda, 1992). These mice have at least a 5-fold increase in plasma cholesterol levels compared with their wild type (WT) counterparts. These mice spontaneously form atherosclerotic lesion and the lesion composition of $ApoE^{-/-}$ mice is

closely similar to atherosclerotic plaques found in humans. Fatty streaks were first observed in 3-month old mice on a normal chow diet. Foam cell lesions were detected by light microscopy as early as 10 weeks with a normal chow diet (Plump et al., 1992). With a pro-atherogenic, Western diet or high fat (HF) diet, $ApoE^{-/-}$ mice developed more severe atherosclerotic plaques that were accompanied with further elevated plasma cholesterol levels. In addition, earlier foam cell lesions were observed in mice that were fed a pro-atherogenic diet; foam cell lesions were observed at 8 weeks of age after 3 weeks of a high fat diet (Zhang, Reddick, Burkey, & Maeda, 1994).

Another important and widely used mouse model for atherosclerosis is the $LDLR^{-/-}$ mouse generated by Ishibashi and colleagues via homologous recombination in embryonic stem cells to produce mice lacking functional *Ldlr* genes (Ishibashi et al., 1993). $LDLR^{-/-}$ mice on a normal chow diet have mildly elevated cholesterol levels; they have about a two-fold higher level of total plasma cholesterol than their WT littermates. Unlike $ApoE^{-/-}$ mice which develop spontaneous atherosclerosis on a normal chow diet, no gross aortic lesion was detected in $LDLR^{-/-}$ mice that were fed a normal diet for up to 13 months. Upon histological examination, small accumulations of intimal foam cells within the walls of the coronary sinuses were found in mice fed a normal chow diet for 12 months. However, Ishibashi et al. demonstrated that $LDLR^{-/-}$ mice on a modified diet (chow supplemented with 1.25% cholesterol, 7.5% cocoa butter, 7.5% casein, and 0.5% sodium cholate.) for 7 months had massive atheromatous deposits within the proximal aorta that virtually blocked the coronary sinuses in some instances. The morphology of

the aortic lesions was well-developed with lipid-rich core and infiltration of foam cells (Ishibashi, Goldstein, Brown, Herz, & Burns, 1994).

The mouse is a widely used species in vascular pathology studies because an extensive amount of genetic information is available. Genetic manipulation of different strains is easily achieved. Atherogenic $ApoE^{-/-}$ and $LDLR^{-/-}$ mice have been routinely used in atherosclerosis research and have provided valuable insights into the progression of atherosclerosis. Since their conceptions, these two mouse strains have been crossed-bred with many other genetically manipulated mouse strains to elucidate the roles of other genes in atherogenesis.

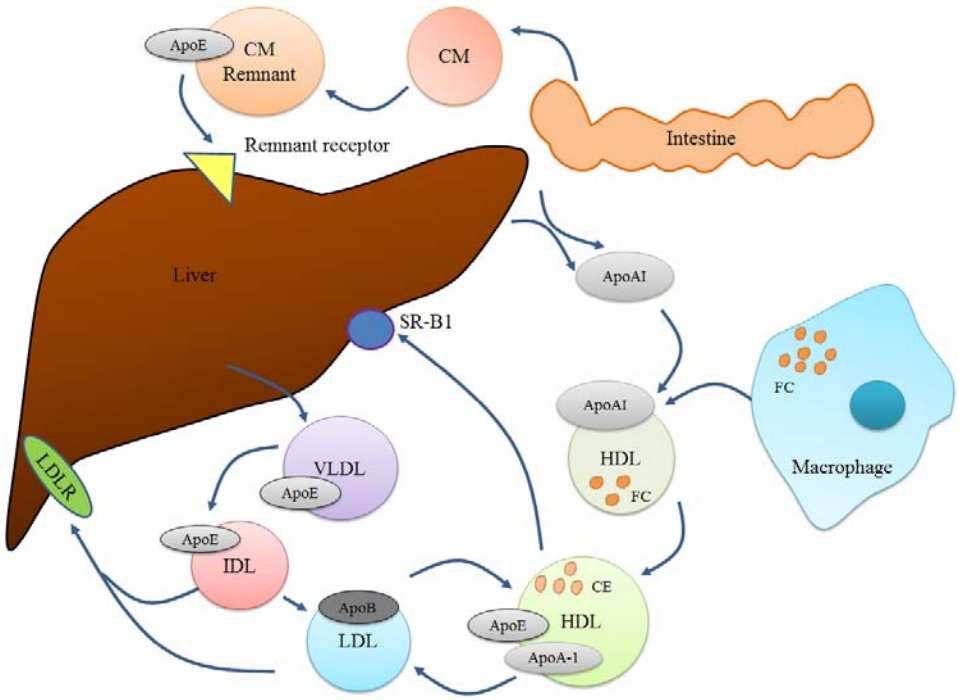

Figure 2. Roles of ApoE and LDLR in lipid metabolism and HDL in reverse cholesterol transport

Schematic of the role of HDL in reverse cholesterol transport and the roles of ApoE and LDLR in cholesterol metabolism. ApoE is a ligand for cell-surface lipoprotein receptors and LDLR mediate the uptake of chylomicrons remnant and VLDL remnant (IDL) by the liver. HDL is important for transferring cholesterol from non-hepatic tissues to the liver via the plasma in a process called reverse cholesterol transport. CM: Chylomicron; ApoE: Apolipoprotein E; LDLR: Low-Density Lipoprotein Receptor; VLDL: Very-Low-Density Lipoprotein; IDL: Intermediate-Density Lipoprotein; LDL: Low-Density Lipoprotein; ApoB: Apolipoprotein B; ApoAI: Apolipoprotein A-I; HDL: High-Density Lipoprotein; SR-B1: Scavenger Receptor Class B Member 1; FC: Free Cholesterol; CE: Cholesteryl Ester

Endothelial Cell

ECs are a heterogeneous population that fulfills many physiological processes. ECs form a single cell layer called the endothelium, which lines the vascular and lymphatic systems, forming a semi-permeable barrier between blood or lymph within vessels and the surrounding tissues. The endothelium is a highly specialized, dynamic, and disseminated organ. The endothelium is an important regulator of vascular homeostasis with many essential functions in physiological processes. Besides serving as a physical barrier, ECs have a wide array of functions which are characterized into three major categories: trophic, tonic, and trafficking. Under physiological conditions, ECs are involved in the modulations of metabolic homeostasis (trophic function), vascular hemodynamics (tonic function), vascular permeability, coagulation, and cell extravasation (trafficking function) (Davidson, 2010). In a quiescent state, ECs balance the release of various vasodilating or vasoconstricting factors such as nitric oxide (NO), prostacyclins, and endothelin to maintain vascular tone, blood pressure, and blood flow (Moncada & Higgs, 2006). Furthermore, the endothelium is crucial in regulating coagulation, utilizing both anti-coagulation and pro-coagulation mechanisms. Under standard physiological conditions, ECs express inhibitors of the tissue factor pathway and thrombomodulin, which prevents the activation of pro-coagulation molecules including factor X, thrombin, and fibrin. However, once the endothelium is injured, the EC changes to an activated state in which the EC surface quickly transforms to a pro-coagulant state by inducing tissue factors that initiate the extrinsic coagulation cascade (Cines et al., 1998). In addition to coagulation, ECs have an essential role in modulating

vascular permeability. This function regulates the ability of cells to move to and from the circulatory system during inflammatory responses. Under normal physiological conditions, endothelium basal permeability only allows for the easy diffusion of solutes such as glucose, ions, and other metabolites to underlying cells. However, during states of acute and chronic inflammation, endothelial permeability is increased, allowing for additional trafficking of immune cells. Excessive or prolonged increases in permeability, as seen in cases such as chronic inflammation, can have deleterious effects resulting in tissue edema. Endothelial permeability is mediated via two pathways; paracellular and transcellullar (Bazzoni & Dejana, 2004; Minshall & Malik, 2006). The inability of ECs to adequately carry out these or any other basal functions is referred to as endothelial dysfunction, and is a hallmark of several CVDs.

EC Activation

Endothelial cell activation is a change of ECs from a quiescent state to one that is involved in immune responses (Figure 3). EC activation may be classified into two types, Type I and Type II. Type I activation includes rapid responses that are independent of new gene expression. These responses are mediated by ligands binding to the extracellular domains of heterotrimeric G protein-coupled receptors (GPCRs) and signal through the intracellular G-protein α_q subunit. Type II activation is a relatively slower response that depends on new gene expression but delivers a more sustained inflammatory response (Pober & Cotran, 1990). Once activated, ECs up-regulate cell surface adhesion molecules and pro-thrombotic molecules. Moreover, activated ECs can

generate and secrete pro-inflammatory cytokines and chemokines. In their basal state, cultured ECs have detectable mRNA levels of numerous pro-inflammatory and anti-inflammatory cytokines and growth factors (Nilsen et al., 1998). However, the expression of pro-inflammatory cytokines is marginal, possibly inhibited by basal production of NO which maintains endothelium quiescence (De Caterina et al., 1995).

Endothelial Dysfunction

EC activation is characterized by the endothelial expression of cell-surface adhesion molecules which is typically induced by pro-inflammatory cytokines, whereas endothelial dysfunction is defined as the decreased production, release, and/or activity of endothelium-derived NO. The reduction of NO bioavailability leads to the disruption in the functional integrity of the endothelium. NO is important for the maintenance of vascular quiescence by inhibiting inflammation, coagulation, and thrombosis. Moreover, endothelial dysfunction results in increased adhesion and migration of leukocytes, platelet aggregation, and VSMC proliferation (Liao, 2013).

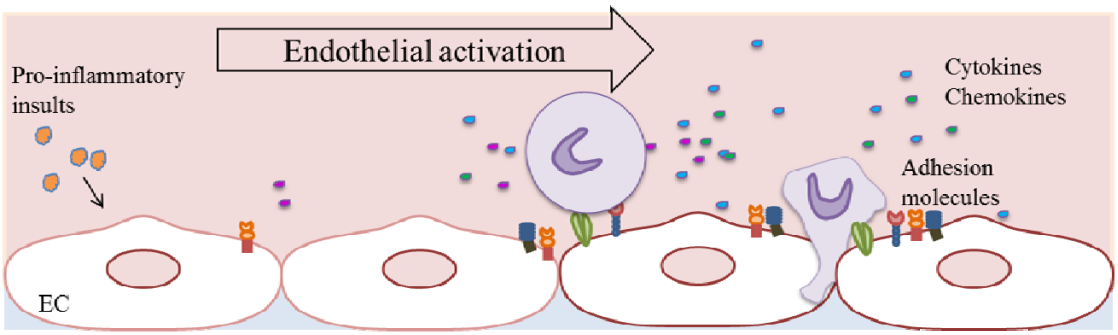

Figure 3. Endothelial cell activation

Endothelial cell activation is a response of the endothelium to pro-inflammatory insults. In response to pro-inflammatory stimuli, the endothelium is activated; it transitions from a quiescence phenotype to one that is involved in immune responses. The activated endothelium up-regulates the expression of adhesion molecules on its surface which enhances the interactions of ECs with leukocytes. Activated ECs also increase the production of pro-inflammatory cytokines and chemokines which serve as chemoattractants for leukocytes.

Immune System and Atherosclerosis

As described, atherosclerosis is a chronic inflammatory disease that involves various vascular and inflammatory cells (J. W. Park, Merz, & Braun, 1998), and both the innate and adaptive immune systems partake in this process. ECs and macrophages contribute to the innate immune responses in atherogenesis. Macrophage and endothelial-derived cytokines mediate the recruitment of other inflammatory cells such as T-lymphocytes to lesions and promote the adaptive immune responses. T cells within lesions are memory effector cells including $CD4^+$ T helper (Th) cells, $CD8^+$ cytotoxic T cells, and regulatory T cells (Tregs).

Th cells are the dominant T cells in plaques, and atherosclerosis has been shown to be driven by Th1 response. Associated with the cell surface expression of chemokine receptors CCR5 (Chemokine C-C motif receptor 5) and CXCR3 (CXC-chemokine receptor 3), Th1 cells also are defined by the expression of cell surface molecules CD26 and lymphocyte activation gene 3. The primary cytokine secreted by Th1 cells is interferon-gamma (IFN-γ), though they also produce interleukin (IL)-2, tumor necrosis factor-alpha (TNF-α), and lymphotoxin (LT). These cytokines are important in mediating delayed-type hypersensitivity reactions and macrophage activation. Functionally, Th1 cells play a key role in cellular immunity against viruses and intracellular pathogens. The signature cytokine of Th1 cells, IFN-γ was found within lesions and had pathogenic effects (Hansson, Robertson, & Soderberg-Naucler, 2006). $ApoE^{-/-}$ mice deficient in IFN-γ or its receptor had decreased atherosclerotic lesions (Gupta et al., 1997). Administration

of exogenous IFN-γ to ApoE$^{-/-}$ mice exacerbated atherosclerosis development (Whitman, Ravisankar, Elam, & Daugherty, 2000). Similar results were found with IL-12, a key Th1-related cytokine. IL-12 is produced by macrophages and it drives the differentiation and maturation of Th1 cells. IL-12 deficiency in ApoE$^{-/-}$ mice attenuated atherosclerosis and injection of IL-12 aggravated lesion formation (Davenport & Tipping, 2003; T. S. Lee, Yen, Pan, & Chau, 1999). IL-18, another Th1-promoting cytokine, was shown to have pro-atherogenic effect. IL-18$^{-/-}$ApoE$^{-/-}$ mice had reduced lesions (Elhage et al., 2003) whereas ApoE$^{-/-}$ mice injected with IL-18 was shown to enhance lesion development via an IFN-γ-mediated mechanism (Whitman, Ravisankar, & Daugherty, 2002). Furthermore, targeted deletion of *Tbx21*, a gene that encodes T-bet, transcription factor required for Th1 differentiation, produced athero-protective effects in LDLR$^{-/-}$ mice (Buono et al., 2005).

Th2 cells differ from Th1 cells in a number of characteristics. They are identified by the expression of chemokine receptors CCR3 and CCR4 (Bonecchi et al., 1998; Lohmann et al., 2002; Sallusto, Lenig, Mackay, & Lanzavecchia, 1998) and surface molecules CD62L, T1/ST2, and CD30 (Okazaki et al., 2002). Moreover, IL-4 is the most important cytokine produced by Th2 cells although they also secrete IL-5, IL-9, IL-10, and IL-13 to a lesser extent. Differentially, Th2 cells play a critical role in humoral immunity, aid in B cell proliferation, and are important in allergic responses and in protecting against infections by helminthic parasites (Anthony, Rutitzky, Urban, Stadecker, & Gause, 2007; Mosmann & Coffman, 1989). Studies on Th2-mediated responses in atherosclerosis have yet to yield a clear role. The cytokine profile of Th2

cells includes pro-inflammatory and anti-inflammatory mediators. The Th2 signature cytokine, IL-4 was shown to have pro-atherosclerotic effects by some reports (Davenport & Tipping, 2003; King, Szilvassy, & Daugherty, 2002) while other found it had no effect on lesion size (King, Cassis, & Daugherty, 2007). In addition, study with IL-5 suggested an atheroprotective role (Daugherty, Rateri, & King, 2004). IL-10-deficiency in $ApoE^{-/-}$ mice was shown to have atheroprotective effects (Caligiuri et al., 2003). However, it should be noted that IL-10 is not solely produced by Th2 cells.

For a long time, studies in atherosclerosis have been focused on Th1 and Th2 responses. It has been over 20 years since Mosmann and Coffman proposed the Th1-Th2 cell paradigm, which explained how hosts are able to initiate T cell responses in order to eradicate the invasion of various pathogens (Mosmann & Coffman, 1989). Until recently, this paradigm has been the cornerstone to our perception of T cell responses. However, as several complicated pathological conditions which could not be illuminated by the basic Th1-Th2 model became evident; the replacement of the paradigm became warranted. A long held belief that supported the Th1-Th2 model was the idea that autoimmune diseases were primarily driven by auto-reactive Th1 cells. This concept was supported by T cell passive transfer. For example, Th1 cells were thought to have a pathogenic function in the development of experimental autoimmune encephalomyelitis (EAE), which suggested that IFN-γ-producing Th1 cells have specificity for self-antigen and are pathogenically required for the induction of organ-specific autoimmunity in EAE. However, experimental data which examined the depletion of IFN-γ gave contradictory results. IFN-γ-deficient and IFN-γ receptor-deficient mice and mice lacking other factors

involved in Th1 lineage differentiation developed a more severe disease rather than being protected from the disease as predicted by the Th1-Th2 model (Krakowski & Owens, 1996; Tran, Prince, & Owens, 2000). Furthermore, the relationship between IL-12 and IL-23 demonstrates another example of how the Th1-Th2 paradigm fails to address autoimmunity. IL-12 and IL-23 both contain two subunits, a common p40 subunit, and a unique p35 (IL-12) or p19 (IL-23) subunit (Oppmann et al., 2000), respectively. It was shown that loss of the unique IL-23 subunit rendered animals highly resistant to the development of autoimmunity and inflammation, whereas the lack of the IL-12 subunit did not. Since IL-12 is central in Th1 differentiation, this result suggests that Th1 cells are not required for the induction of autoimmune-mediated inflammation (Cua et al., 2003). The shortcomings of the Th1-Th2 paradigm brought investigators to the recent identification of Th cells with cytokine profile and transcription factors unique from Th1 and Th2 cells and led to the proposition of a new multi-subset paradigm for regulating immune processes including atherosclerosis.

Interleukin-17

Interleukin-17A (IL-17) is a member of the IL-17 cytokine family. The *Il17a* gene was first cloned in 1993 from a murine cytotoxic T lymphocyte (CTL) hybridoma cDNA library thus originally named the cytotoxic T lymphocyte associated antigen 8 (Ctla8) gene (Rouvier, Luciani, Mattei, Denizot, & Golstein, 1993). Subsequently, the identification of IL-17 led to the characterization of a new lineage of $CD4^+$ T helper cells, Th17 (Harrington et al., 2005). IL-17 is the signature cytokine of Th17 cells but other

cells including macrophages (Arca, Quagliarini, Pigna, Catalano, & Napoli, 2011), neutrophils (Szypula, Kotulska, Szopa, Pieczyrak, & Kucharz, 2009), dendritic cells (Rocha et al., 2013), CD8 T cells (Zhang et al., 1992), αβ T cells (Mueller, Beutner, Teupser, Ceglarek, & Thiery, 2008), γδ T Cells (Dervisoglu, Turgut, & Yilmaz, 2007), and natural killer T cells (Gonzalez-Navarro et al., 2007) also produce IL-17. Since its characterization, IL-17 has been shown to aid in host defense against extracellular bacterial and fungal infections including *Klebsiella pneumonia, Bordetella pertussis, Mycoplasma pneumonia, Mycobacterium tuberculosis,* and *Candida albicans* (Curtis & Way, 2009). In addition, Th17 and IL-17 are implicated in many inflammatory and autoimmune diseases including multiple sclerosis (Hofstetter et al., 2005), psoriasis (Lowes et al., 2008), inflammatory bowel disease (Ogawa, Andoh, Araki, Bamba, & Fujiyama, 2004), and rheumatoid arthritis (Nakae, Nambu, Sudo, & Iwakura, 2003).

Interestingly, the capacity to hinder the differentiation of Th17 cells has been attributed to cytokines and transcription factors produced by cells of other subsets. Both Th17 development and IL-17 expression is negatively regulated by IFN-γ and IL-4 which are secreted by Th1 and Th2 cells respectively. Th17 cell development is also hindered by specific Th1 and Th2 transcriptional factors including STAT1 (Signal Transducer and Activator of Transcription 1), STAT4, T-bet, STAT6, and GATA3 (Harrington et al., 2005; H. Park et al., 2005). Furthermore, Th17 promoting cytokines such as transforming growth factor-beta (TGF-β) and IL-23 maintain the ability to suppress the development of other T cell lineages as well (Korn, Oukka, Kuchroo, & Bettelli, 2007). This fact implies that the balance of the T cell lineage is regulated by the products of each subset, and that

during an infection, the proper T helper cell activation is crucial for the host to effectively combat and control the infection.

IL-17 exists as a homodimer or heterodimer with IL-17F, another IL-17 family cytokine produced by Th17 cells. IL-17 cytokine family members (IL-17A to IL-17F) interact with a unique family of IL-17 receptors (IL-17RA to IL-17RE). IL-17 signals through IL-17RA and IL-17RC which form a complex together in humans. However, in mouse the IL-17RC does not bind to IL-17 (Kuestner et al., 2007; Toy et al., 2006). Pro-inflammatory genes that are up-regulated by IL-17 are induced by binding of IL-17 to IL-17R and followed by recruitment of essential adaptor molecule ACT1 [also called TRAF3IP2 (tumor necrosis factor receptor-associated factors 3 interacting protein 2)] to the IL-17R via the similar expression to fibroblast growth factor genes and IL-17R (SEFIR) domain. Downstream of ACT1 lies two signaling cascades; one is dependent on TRAF6 and another is TRAF-6 independent. TRAF-6-dependent IL-17 signaling activates the transcription factor NF-κB and leads to induction of pro-inflammatory genes. Meanwhile, the TRAF-6-independent cascade of IL-17 signaling involves TRAF2 and TRAF5 which leads to mRNA stabilization of pro-inflammatory molecules (May, 2011). IL-17R expression is widespread with high levels in hematopoietic tissues. Gene targets of IL-17 include pro-inflammatory chemokines and cytokines. Chemokines induce chemotaxis of cells such as immune cells to the site of infection or inflammation whereas pro-inflammatory cytokines enhance the inflammatory effects of immune cells. IL-17 also induces matrix metalloproteinases, implicating its role in cellular behavior such as proliferation and migration (Shen & Gaffen, 2008).

IL-17 and Atherosclerosis

The role of IL-17 and Th17 cells in promoting inflammatory diseases suggests their potential involvement in atherosclerosis. In fact, IL-17 and IL-17-producing T cells are found in atherosclerotic plaques (de Boer et al., 2010; Eid et al., 2009). However, the role of IL-17 cells and whether it is pro-atherogenic or anti-atherogenic remains a debate. Using neutralizing approaches, several studies showed that IL-17 has a pro-atherogenic role. Inhibition of IL-17, by an adenovirus-produced soluble IL-17 receptor or by monoclonal antibody against IL-17, attenuated lesion formation in $ApoE^{-/-}$ mice (Erbel et al., 2009; Smith et al., 2010). In addition, a $LDLR^{-/-}$ mouse bone marrow transfer model resulting in the disruption of IL-17R signaling led to a reduction in atherosclerosis (van Es et al., 2009). Meanwhile, other experimental evidence indicated an anti-atherogenic role for IL-17. Suppressor of cytokine signaling (SOCS) 3 protein is a negative regulator of Th17 cell formation since its genetic deficiency leads to enhanced Th17 generation and increased IL-17 production (Chen et al., 2006). In regards to atherosclerosis, a loss of SOCS3 expression in T cells of $LDLR^{-/-}$ mice via bone marrow reconstitution resulted in an atheroprotective phenotype. Specifically, this model enhanced IL-17 and IL-10 production, induced an anti-inflammatory phenotype in macrophages, and reduced atherosclerosis formation. Moreover, neutralization of IL-17 with monoclonal antibody in the mouse chimera increased lesion formation (Taleb et al., 2009). Based on these studies, utilization of neutralization and bone marrow transfer strategies has yielded conflicting results in the role of IL-17 in atherosclerosis.

Citing that previous methods used in depleting IL-17 may lack specificity or fail to completely eliminate the cytokines, several laboratories have generated IL-17$^{-/-}$ApoE$^{-/-}$ mice and ApoE$^{-/-}$IL-17R$^{-/-}$ mice in an attempt to clarify the previous inconsistency. Madhur et al. found that IL-17 deficiency had no effect on atherosclerotic plaque area in ApoE$^{-/-}$ mice after three months of high fat feeding. However, they found that vascular inflammation was decreased in IL-17/ApoE double knock-out mice when compared to ApoE$^{-/-}$ mice. Specifically, leukocytes and dendritic cells were decreased in the aorta while macrophage within atherosclerotic plaques was reduced. The authors of this study concluded that IL-17 may play a role in some aspect of vascular inflammation and function, but IL-17 inhibition was not adequate to reduce plaque burden (Madhur et al., 2011). In another study, Butcher et al. showed that IL-17 deficiency in ApoE$^{-/-}$ background reduced atherosclerotic lesion size in the whole aorta after 15 weeks of high fat diet by 35% when compared to controls. Similarly, IL-17R deficiency in ApoE$^{-/-}$ mice yielded a 25% reduction in lesion size. In addition, CD45^{+} leukocytes and CD3^{+} T cells were also found to be reduced in the double knock-out mice (Butcher, Gjurich, Phillips, & Galkina, 2012). Data from both laboratories suggest that IL-17 has a pro-atherogenic role. Although there was no consensus on the effect of IL-17 in lesion formation, both studies found that vascular inflammation was diminished by IL-17 deficiency as judged by leukocyte, T cell, and macrophage numbers in the atherosclerotic aorta (Butcher et al., 2012; Madhur et al., 2011). It should be noted, that in another study using IL-17/ApoE double knock-out mice, Danzaki and colleagues observed results that were contradictory to those previously found. IL-17 deficiency was found to accelerate

atherosclerotic lesion formation in ApoE$^{-/-}$ mice after high fat feeding for 8 or 16 weeks. In addition, increased MOMA-2 positive macrophages were found to infiltrate into atherosclerotic lesions. Moreover, increased CD4^{+}IFN-γ^{+} Th1 cells and IFN-γ production were found in ApoE$^{-/-}$IL-17$^{-/-}$ mice (Danzaki et al., 2012). The authors of these findings suggested that IL-17 deficiency may induce a pro-atherogenic response by modulating cytokine production and altering Th1 responses. In fairness, Butcher et al. did not find any effect of IL-17 or IL-17R deficiency on the generation and maintenance of Th1 cells in their models (Butcher et al., 2012). These conflicting reports demonstrate that despite significant progress, the roles of IL-17 in atherosclerosis remain undefined. Further investigation is warranted to elucidate these conflicting results.

IL-17 and Vascular Function

IL-17 promotes angiogenesis and tumor growth *in vitro* with mouse fibroblasts, human umbilical venous cord endothelial cell (HUVECs), tumor cell lines, and human dermal microvascular endothelial cell (HMVECs). In order to promote angiogenesis, IL-17 up-regulates pro-angiogenic factors such as vascular endothelial growth factor (VEGF), Prostaglandin E1 (PGE1), PGE2, keratinocyte-derived cytokines, and macrophage inflammatory protein 2 [MIP-2; also called Chemokine C-X-C motif ligand 2 (CXCL2)] (Numasaki et al., 2003) found in fibroblasts and tumor cells. In human EC culture, IL-17 was found to enhance the effects of various growth factors, such as basic fibroblast growth factor (bFGF), human growth factor (HGF), and VEGF, to induce proliferation of vascular ECs (Takahashi, Numasaki, Lotze, & Sasaki, 2005).

Additionally, the levels of IL-6, IL-10, IL-12, and PGE2 were induced (Jovanovic et al., 1998). IL-17 maintains the ability to induce IL-6 production through a STAT3 pathway in ECs, $CD11c^+$, $CD11b^+$, melanoma, MEF, splenic, and tumor cells (Wang et al., 2009). The pro-angiogenic effects of IL-17 were shown to contribute to the pathogenesis of rheumatoid arthritis. It was found that IL-17 concentrations present in rheumatoid arthritis joints were sufficient to promote human lung microvascular EC migration and tube formation suggesting an important role for IL-17 in rheumatoid arthritis angiogenesis (Pickens et al., 2010).

Additionally, the effects of IL-17 on ECs were found to be important in chronic airway diseases. IL-17 receptor expressions were increased in bronchoscopic biopsy tissues from asthmatic patients with strong labeling in epithelial cells as well as ECs. Lung microvascular endothelial cells (LMVECs), in response to IL-17, increased the mRNA expressions of intracellular cell adhesion molecule-1 (ICAM-1), vascular cell adhesion molecule-1 (VCAM-1), and E-selectin in a P38 mitogen-activated protein kinase (MAPK)-dependent manner. In addition to adhesion molecules in LMVECs, IL-17 also induced the production of CXCL8, a potent neutrophil chemoattractant. Thus, it was found that IL-17-treated LMVECS selectively enhanced the migration of neutrophils (Roussel et al., 2010). In another study, IL-17 and TNF-α were found to synergistically enhance the expression of P-selectin and E-selectin in cultured mouse heart ECs. In the mouse cremaster muscle, IL-17 and TNF-α were found to synergistically increase the rolling interaction of leukocytes with microvascular endothelium as well as to increase the transendothelial migration of leukocytes *in vivo* (Griffin et al., 2012). These results

show that IL-17 is an activator of the endothelium which leads to the enhance recruitment of neutrophils and leukocytes to the sites of inflammation.

However, it is worth to point out that Taleb et al. found that IL-17-treated mice had lower expression of ICAM-1 on ECs in atherosclerotic lesions (Taleb et al., 2009). Similarly, IL-17 was found to mitigate TNF-α-induced VCAM-1 mRNA and protein expression in human aortic smooth muscle cells (Madhur et al., 2010).

The development of EAE, rodent model of multiple sclerosis, was suppressed in IL-17$^{-/-}$ mice demonstrating that IL-17 contributes to the pathogenesis of EAE (Komiyama et al., 2006). The breakdown of the blood-brain barrier (BBB) is a crucial event in the pathogenesis of multiple sclerosis and it was found that IL-17 induced disruption of the BBB. Treatment of bEnd.3 cells, an immortalized mouse brain EC line, with IL-17 showed that IL-17-induced BBB disruption via formation of reactive oxygen species (ROS) which were responsible for the down-regulation and reorganization of tight junction molecules, occuldin and zona occludens 1, respectively (Huppert et al., 2010).

IL-17 was found to be critical in angiotensin II-induced hypertension. Human patients with hypertension were found to have increase serum levels of IL-17. In mice, angiotensin II induced the production of IL-17 from T cells which leads to the notion that IL-17 may play a role in angiotensin II-induced hypertensive phenotype. IL-17$^{-/-}$ mice infused with angiotensin II were shown to have the similar initial hypertensive characteristic as WT mice; however after 3 weeks of angiotensin II treatment, blood

pressures of IL-17$^{-/-}$ mice began to decline whereas WT mice remained hypertensive. Moreover, IL-17$^{-/-}$ mice infused with 4 weeks of angiotensin II had improved vessel relaxation in response to acetylcholine (ACh) and sodium nitroprusside (SNP) when compared to angiotensin II-treated WT mice. These results suggest that IL-17 is important in endothelium-dependent and endothelium-independent vascular relaxation in angiotensin II-induced hypertension (Madhur et al., 2010).

Key Knowledge Gaps, Rationale, and Hypothesis of Dissertation

Atherosclerosis is a chronic inflammatory disease that involves both the innate and adaptive immune responses. ECs are important in mediating the innate immune responses whereas T-lymphocytes, especially Th cells, are critical for the adaptive functions in atherogenesis. Th17 cells are a relatively new subset of Th cells that have been shown to have a role in atherosclerosis. IL-17 is the signature cytokine of Th17 cells and the function of IL-17 in atherosclerosis has garnered much interest. However, studies on the role of IL-17 in atherosclerosis have yet to reach a consensus.

Undisrupted endothelium integrity is important in maintaining its normal physiological functions. As the cells that line the blood vessels, ECs are the first to sense pro-inflammatory and pro-atherogenic insults presented in the blood. EC activation due to pro-atherogenic and pro-inflammatory stimuli is the initiating step of atherosclerosis. Pro-inflammatory cytokines such as IL-17 have been shown to induce EC activation. However, the role of IL-17 in EC activation and endothelial dysfunction in the context of hyperlipidemia-induced atherosclerosis has not been explored. Several key knowledge gaps including whether IL-17 is increased in hyperlipidemia, does IL-17 activates aortic ECs, and whether IL-17 contributes to vascular dysfunction and early atherosclerosis in $ApoE^{-/-}$ mice are needed to be bridged. To fill these knowledge gaps, we hypothesize IL-17 that is up-regulated during hyperlipidemia contributes to EC activation, which leads to endothelial dysfunction and early atherosclerosis development in $ApoE^{-/-}$ mice.

Our hypothesis will be tested with the following specific aims:

Specific aim 1 – Determine whether hyperlipidemia induces IL-17 production

Study 1 – Determine whether IL-17-expressing cells in splenocytes and plasma IL-17 level differ in WT mice and atherogenic hypercholesterolemia ApoE$^{-/-}$ mice

Study 2 – Determine whether IL-17 receptor expression in ECs is changed in response to the pro-atherogenic factor, OxLDL

Specific aim 2 – Determine whether IL-17 induces aortic EC activation

Study 1 – Determine whether IL-17 induces mouse aortic EC activation

Study 2 – Determine whether IL-17 induces human aortic EC activation and affects monocyte adhesion to ECs

Specific aim 3 – Determine whether IL-17 gene deletion attenuates endothelial dysfunction and atherogenesis

Study 1 – Determine whether IL-17 disturbs vascular function of mouse aorta

Study 2 – Determine whether leukocyte adhesion to endothelium is affected by IL-17

Study 3 – Determine whether IL-17 affects monocyte infiltration into the aorta

Study 4 – Determine whether IL-17 promotes lesion formation during early atherosclerosis

CHAPTER 2

MATERIAL AND METHODS

Animals

All animal experiments were performed in accordance with the Institutional Animal Care and Use Committee (IACUC) Guidelines and Authorization for the use of Laboratory Animals and approved by the Experimental Animal Committee of Temple University School of Medicine.

All mice used were on a C57BL/6 background. IL-17$^{-/-}$ mice were generated and provided by Dr. Yoichiro Iwakura's laboratory at the Center for Experimental Medicine of the Institute of Medical Science, University of Tokyo (Japan). ApoE mutant mice or commonly known as ApoE$^{-/-}$ mice (strain name: B6.129P2-Apoetm1Unc/J) and WT mice were purchased from The Jackson Laboratory (Bar Harbor, ME). All animals were housed in the Temple University Central Animal Facility under controlled temperature (23±1°C) with a 12-hour light-dark cycle. Animals had *Ad libitum* access to standard chow diet and water. IL-17$^{-/-}$ApoE$^{-/-}$ mice were generated by crossing IL-17$^{-/-}$ mice with ApoE$^{-/-}$ mice. Age-matched male mice were used for all experiments.

Mouse Genotype

Mice were genotyped for specific gene of interest with polymerase chain reaction (PCR) followed by agarose gel separation of the products. Mouse tail or ear tissue was

collected and digested with 600µl of tissue lysis buffer [10mM tris (pH 8.0), 100mM sodium chloride (NaCl), 10mM ethylenediaminetetraacetic acid (EDTA, pH 8.0), and 0.5% sodium dodecyl sulfate (SDS)] containing 0.4mg/ml proteinase K at 55°C overnight. Tissue lysate was centrifuged at 13,000rpm (Fisher Scientific Accuspin Micro R Centrifuge) for 20 minutes. Supernatant containing genomic DNA was collected and DNA was precipitated in 100% ethyl alcohol and dissolved in distilled deionized water at 37°C overnight.

Mouse genomic DNA was amplified with specific primer sets by PCR. Mouse IL-17A allele was examined using primers developed by Dr. Yoichiro Iwakura's laboratory: IL-17 common primer 5'-ACTCTTCATCCACCTCACACGA-3', IL-17 wild type primer 5'-GTACACCAGCTATCCTCCAGATAG-3', and IL-17 knock-out primer 5'-TCCTTGAAGTCGATGCCCTTCA-3'. The PCR condition was 94°C for 15 seconds, 64°C for 30 seconds, and 72°C for 30 seconds for a total of 40 cycles. The PCR product was realized by gel electrophoresis with a 2% agarose gel. The wild type band is 700bp and knock-out band is 500bp. ApoE allele was examined using primers: ApoE common primer 5'-GCCTAGCCGAGGGAGAGCCG-3', ApoE wild type primer 5'-TGTGACTTGGGAGCTCTGCAGC-3', and ApoE mutant primer 5'-GCCGCCCCGACTGCATCT-3'. The PCR condition was 94°C for 30 seconds, 68°C for 40 seconds, and 72°C for 60 seconds for 35 cycles. The PCR product was separated by a 2% agarose gel with gel electrophoresis. The ApoE wild type band is 155bp whereas the mutant band is 245bp.

Antibodies and Chemicals

All reagents and chemicals were from Sigma-Aldrich (St. Louis, MO) unless otherwise indicated. Recombinant human IL-17A cytokine, antibodies against human IL-6, GM-CSF, and CXCL1/2/3, and mouse IgG1 isotype control were purchased from R&D Systems (Minneapolis, MN). Allophycocyanin (APC)-conjugated Ly6C and Phycoerythrin (PE)-conjugated CD11b mouse antibodies were purchased from BD Biosciences (San Jose, CA). Phycoerythrin-Cyanine-7 (PE-Cy7)-conjugated F4/80 mouse antibody was purchased from eBioscience (San Diego, CA). LIVE/DEAD® Fixable Violet Dead Cell Stain Kit was from Life Technologies (Carlsbad, CA). PE-IL-17RA human antibody was from eBioscience and APC-IL-17RC human antibody was from R&D Systems. Human oxidized low density lipoprotein and human low density lipoprotein were purchased from Biomedical Technologies, Inc. (Stoughton, MA). IL-2, CD28, CD3e, Fluorescein isothiocyanate (FITC)-CD4, PE-CCR6, and APC-IL-17 mouse antibodies, mouse IL-6 and IL-23 recombinant proteins, and human TGFβ-1 recombinant protein were from eBioscience.

Anti-phospho P38 (Thr180/Tyr182), Anti-P38, Anti-phospho JNK1/2 (Thr183/Tyr185), Anti-JNK1/2, and Anti-phospho eNOS (Ser1177) were purchased from Cell Signaling Technology (Beverly, MA). Anti-phospho-eNOS (thr495) and anti-eNOS were from BD Biosciences. Horseradish Peroxidase (HRP)-conjugated anti-rabbit and anti-mouse immunoglobulin G (IgG) antibodies were purchased from GE Healthcare Life

Scicences (Piscataway, NJ). All PCR primers were purchased from Integrated DNA Technologies, Inc. (Coralville, IA).

Cell Culture

Human aortic endothelial cells (HAECs) (Lonza, CC2535) were cultured in medium M199 (Hyclone laboratories, Logan, UT) supplemented with 15% fetal bovine serum (FBS; HyClone), endothelial cell growth supplement (ECGS, 50μg /mL; BD Biosciences), heparin (50μg/mL), and 1% penicillin, streptomycin, and amphotericin (PSA; Invitrogen, Carlsbad, CA). HAECs were grown on 0.2% gelatin-coated flasks, plates, or dishes and they were used between passages 8 to 9.

Plasma IL-17 Concentration by Enzyme-linked Immunosorbent Assay

Whole blood was collected from anesthetized animals via the inferior vena cava in mini-centrifuge tubes coated with EDTA. Plasma was separated by centrifugation and plasma IL-17 concentration was determined by Enzyme-linked Immunosorbent Assay (ELISA) with the Mouse IL-17A ELISA MAX™ Deluxe kit (Biolegend, San Diego, CA) following the manufacturer's instruction.

Mouse Splenocyte IL-17 Staining and Flow Cytometry

Mouse spleen was excised and homogenized with two frost glass slides in Dulbecco's modified eagle medium (DMEM; HyClone) containing 2% FBS. Red cells were lysed with Ammonium-Chloride-Potassium (ACK; 0.15M NH_4Cl, 10mM $KHCO_3$, 0.1mM EDTA) lysis buffer, and cell debris and aggregates were removed by passing the

cell suspension through a 70µm pore cell strainer. Splenocytes were re-suspended at $1.5x10^6$ cells per mL of complete medium [DMEM-low glucose supplemented with 10% FBS, 1% penicillin and streptomycin, 2mM L-glutamine (HyClone), 11.4mM HEPES buffer (HyClone), and 0.22µM 2-mercaptoethanol] and 3mL of cells were seeded in each well of a 6-well plate that had been coated with anti-mouse CD3e (5µg/mL) and anti-mouse CD28 (1µg/mL). Cells were incubated with anti-mouse IL-2 (1µg/mL), mouse recombinant IL-23 (10ng/mL) and IL-6 (20ng/ml), human recombinant TGF-β (1ng/ml), BD GolgiStop protein transport inhibitor containing monensin (BD Biosciences), Phorbol 12-myristate 12-acetate (PMA), and ionomycin for 6 hours. Cells were stained with LIVE/DEAD® Fixable Violet Dead Cell Stain Kit at room temperature for 30 minutes. Then cells were washed and stained with FITC-CD4 and PE-CCR6 for 30 minutes at 4°C. Following permeabilization and fixation with BD Cytofix/Cytoperm Plus Fixation/Permeabilization Kit (BD Biosciences), cells were stained with APC-IL-17 for 30 minutes at 4°C. Cells were fixed overnight at 4°C with 2% paraformaldehyde (PFA) prior to Fluorescence-activated cell sorting (FACS).

HAEC Staining and Flow Cytometry

HAECs grown and treated in 6-well plate were washed once with ice-cold Phosphate buffered saline (PBS) and 200µL of Trypsin-EDTA was added to each well to detach cells. Cells were washed once with FACS buffer (2% FBS in PBS). Cells were stained with antibodies for 30 minutes at 4°C. After washing with FACS buffer, cells were fixed overnight with 2% PFA prior to FACS.

Mouse Aortic EC Isolation and Culture

Mouse aortic endothelial cells (MAECs) were isolated and cultured as previous described with modifications (Hasty et al., 2001). Briefly, the entire mouse thoracic aorta was exposed and an incision was made at the distal end where the aorta passed through the diaphragm. The aorta was perfused with PBS containing 1000U heparin via an incision at just after the aortic arch. The aorta was filled with DMEM containing 300 U/mL collagenase type 2 (Worthington Biochemical Corp., Freehold, NJ) with ligation at both ends. The aorta was then isolated and incubated in DMEM containing 20% FBS at 37°C for 1 hour. The fluid inside the aorta was flushed out with DMEM containing 20% FBS into a 15-mL tube containing 10 mL of endothelial growth medium (EGM) [DMEM supplemented with 40% Ham's F-12 nutrient mixture (Invitrogen), 10% FBS, 0.3% ECGS, 10 U/mL Heparin, and 1% Penicillin and Streptomycin]. The cells were centrifuged at 1,500rpm for 3 minutes. Cells were collected and re-suspended with fresh EGM. The cells were then transferred into collagen-coated 35mm dishes (2 aortas per dish) and incubated for 1 hour. The non-adhered cells were then washed away by Dulbecco's Phosphate-Buffered Saline (DPBS; Hyclone) and the MAECs were cultured with EGM until 80% confluence.

The specificity of ECs was determined by 1,l'-dioctadecyl-3,3,3',3'-tetramethylindocarbocyanine-acetyl-low density lipoprotein (DiI-Ac-LDL; Biomedical Technologies Inc.) uptake and CD31 staining. Briefly, DiI-Ac-LDL was added into the culture medium at the final concentration of 10μg/ml. MAECs were incubated with the

labeled lipoprotein for 4 hours at 37°C. The cells were then washed twice with DPBS and fixed with 4% PFA for 20 minutes. Following fixation, cells were stained with 4', 6-diamidino-2-phenylindole (DAPI) (1μg/mL) for 5 minutes and visualized via fluorescence microscopy. For CD31 staining, MAECs were cultured on a collagen-coated cover slip in a 12-well plate and fixed with 4% PFA for 20 minutes before staining. Rat anti-mouse CD31 antibody (1:200 dilution; BD Biosciences) and FITC-conjugated rabbit anti-rat antibody (1:200 dilution; Jackson ImmunoResearch Laboratories, West Grove, PA) were used. All images were visualized and captured with the Zeiss Axioscope microscope.

Mouse EC PCR Array

RNA from WT mouse treated with mouse IL-17(100ng/ml) for 24 hour was isolated using the RNeasy Plus Mini Kit (Qiagen). RNA was converted to cDNA with the RT² First Strand Kit (SABiosciences) and used following the direction of the Mouse Endothelial Cell RT² Profiler™ PCR Array (SABiosciences). Data was analyzed with the SABiosciences PCR Array Data Analysis Software.

Peripheral Blood Monocyte Isolation

Blood was drawn from informed healthy volunteers into one-sixth volume of Acid Citrate Dextrose (ACD) Solution (85mM sodium citrate, 111mM glucose, 71.4mM citric acid) according to a protocol approved by the Institutional Review Board of Temple University. Whole blood was carefully layered onto an equal amount of histopaque-1077

and centrifuged at 500g for 30 minutes at room temperature. The cloudy-white interface containing mononuclear cells was transferred into a tube with 20mL of DPBS containing 2% FBS. The cells were washed twice with DPBS containing 2% FBS and re-suspended in 10mL of DMEM and transferred to a T75 flask coated with 2% gelatin. The cells were incubated for 1 hour at 37°C with 5% CO_2 for monocytes to adhere. Non-adherent cells were removed by three washes with DMEM. Adherent monocytes were harvested by incubation with 5mL of monocyte culture medium [DMEM supplemented with 10% FBS, 1% penicillin and streptomycin, 1% L-Glutamine (200mM) and 1% Non-essential amino acids (HyClone)] plus 5mL of EDTA (10mM) for 10 minutes. Monocytes were collected and re-suspended in monocyte culture medium after centrifugation. Monocytes were incubated for 1 hour in monocyte culture medium prior to use.

Monocyte-EC Static Adhesion Assay

HAECs (passage 9) were cultured in 24-well plates and treated with human IL-17 (100ng/ml). THP-1 cells (Human acute monocytic leukemia cell line; American Type Culture Collection, Manassas, VA) were maintained in Roswell Park Memorial Institute (RPMI) 1640 medium with 10% FBS, 1% penicillin/streptomycin, and 2mM L-Glutamine. Human peripheral blood monocytes (HPBMCs) were freshly isolated as described in the previous section. THP-1 cells or HPBMCs ($5x10^6$ cells/mL) were stained with 2μM calcein AM (Invitrogen) fluorescence dye for 30 minutes at 37ºC. THP-1 cells or HPBMCs ($1x10^6$ cells/mL) were suspended in complete RPMI 1640 medium and complete M199 medium (1:1) or DMEM monocyte culture medium and

complete M199 medium (1:1), respectively, and added to HAEC monolayer. After 1 hour incubation at 37ºC, unattached THP-1 cells or HPBMCs were removed by careful wash with PBS supplemented with $CaCl_2$ and $MgCl_2$. Fluorescence was measured with a microplate fluorescence reader (FLx800, Bio-tek, Winooski, VT) at 494nm/517nm. The percentage of adherent cells to HAEC monolayer was determined as a percentage of the no treatment control group. For assays with blocking antibodies, 100ng/ml anti-GM-CSF, 50ng/ml anti-CXCL1/2, and 10ng/ml anti-IL-6 were added to treated ECs 30 minutes prior to the adhesion assay.

Protein Extraction and Western Blot Analysis

Protein extracts were prepared from mouse aorta. Protein concentrations were determined by the bicinchoninic acid (BCA) assay with BSA standards. Proteins were separated on 8% SDS-polyacrylamide gels and transferred onto nitrocellulose membranes. Membranes were blocked by 5% non-fat milk in tris buffered saline containing 0.01% Tween 20 [TBST, 50mM Tris (pH 7.5), 150mM NaCl, and 0.1% Tween 20 (v/v)]. Membranes were incubated with primary antibodies overnight at 4°C or at room temperature for 1-2 hours. Membranes were then washed extensively with TBST and incubated with the appropriate horseradish peroxidase-labeled secondary antibodies for 1 hour at room temperature. Afterward, membranes were incubated with enhanced chemiluminescence (ECL) substrate for horseradish peroxidase (Pierce/Thermo, Rockford, IL) and the ECL intensity was detected by X-ray film exposure in a dark room. The X-ray films were developed by the SRX-101A medical film processor. The

expression levels of proteins as indicated by the ECL intensity were measured with ImageJ software (NIH, Bethesda, MD).

RNA Extraction and Real-Time PCR

Total RNA was isolated from HAECs with TRIzol® Reagent (Invitrogen). HAECs grown in 60mm culture dishes were rinsed with iced-cold PBS then lysed with 1ml of TRIzol® Reagent. Lysed cells were incubated for 5 minutes at room temperature for complete dissociation of nucleoprotein complex. Then 200µl of chloroform was added to each sample and the mixture was shaken vigorously for 15 seconds then the sample was centrifuged at 13,000rpm for 15 minutes at 4°C. The upper aqueous phase was collected and RNA was precipitated by addition of equal volume of isopropanol. After centrifugation, the RNA pellet was washed twice with 75% ethyl alcohol in nuclease-free water (Qiagen, Valencia, CA). The RNA was solubilized in 30µl nuclease-free water. RNA quality and concentration was determined by the Nanodrop 2000 (Thermo Scientific, Wilmington, DE). Two µg of total RNA was reverse transcribed to generate complementary DNA (cDNA) using the High Capacity cDNA Reverse Transcription Kit (Invitrogen).

The mRNA expression levels of genes were determined by quantitative real-time PCR (qRT-PCR) with the SYBR-green dye (Invitrogen) on the StepOnePlus PCR system (Applied Biosystems, Foster City, CA). The primers used are listed in Table 1.

Table 1. List of primers used in qRT-PCR

Human	
Gene	Sequence (5'-3')
Beta-actin	ACCTTCTACAATGAGCTGCG CCTGGATAGCAACGTACATGG
GM-CSF	ACTTTCTGCTTGTCATCCCC CCATCCTGAGTTTCTAGCTCTTG
CXCL1	TGCTCCTGCTCCTGGTAG GGACTTCACGTTCACACTTTG
CXCL2	AACCGAAGTCATAGCCACAC AGGAACAGCCACCAATAAGC
IL6	CCACTCACCTCTTCAGAACG CATCTTTGGAAGGTTCAGGTTG
ICAM-1	CAATGTGCTATTCAAACTGCCC CAGCGTAGGGTAAGGTTCTTG
VCAM-1	TCTACGCTGACAATGAATCCTG AGGGCCACTCAAATGAATCTC
E-selectin	AAGTTCGCCTGTCCTGAAG CAGAAAGTCCAGCTACCAAGG
Mouse	
Gene	Sequence (5'-3')
Beta-actin	CTGTATTCCCCTCCATCGTG GCCTCGTCACCCACATAG
IL17ra	GGTTTTCCTTCAGCCACTTTG TCTTCATCTTGCTGTCCTCAC

Vascular Function Studies in Mouse Aorta

Endothelial-dependent and –independent vessel relaxation responses (Figure 4) were determined by myography with the Multi Wire Myograph System (model 610M, Danish Myo Technology, Denmark) (Figure 5). $ApoE^{-/-}$ mice and $IL\text{-}17^{-/-}ApoE^{-/-}$ mice were anesthetized using a cocktail of ketamine (80mg/kg), xylazine (15mg/kg), and acepromazine (2mg/kg) via intraperitoneal (i.p.) injections. The thoracic aorta was excised and dissected free of fat and connect tissues. Two segments of aorta (2mm each) from just after the subclavian artery bifurcation were dissected from each aorta and mounted on the myograph system. Aortic ring segments were maintained at 37°C in physiologic Krebs buffer [pH 7.4, NaCl (119mM), sodium bicarbonate ($NaHCO_3$, 25mM), glucose (11.1mM), calcium chloride dehydrate ($CaCl_2 \bullet 2H_2O$, 1.6mM), potassium chloride (KCl, 4.7mM), monopotassium phosphate (KH_2PO_4, 1.2mM), magnesium sulfate heptahydrate ($MgSO_4 \bullet 7H_2O$, 1.2mM)] aerated with 95% O_2 and 5% CO_2. The aortic rings were equilibrated for 1 hour at 37°C at a resting tension of 4.5mN. The presence of intact endothelium in the vascular preparation was confirmed by observing the relaxation response to 1μM ACh in aortic rings pre-contracted with 1μM phenylephrine (PE).

Endothelial-dependent and endothelial-independent vessel relaxation was determined by responses to cumulative concentrations of ACh (10nM - 33μM) and SNP (1nM - 10μM), respectively, in aortic rings pre-contracted with 1μM PE. Vascular contractile responses to 120mM KCl and 10nM - 33μM PE were examined as controls.

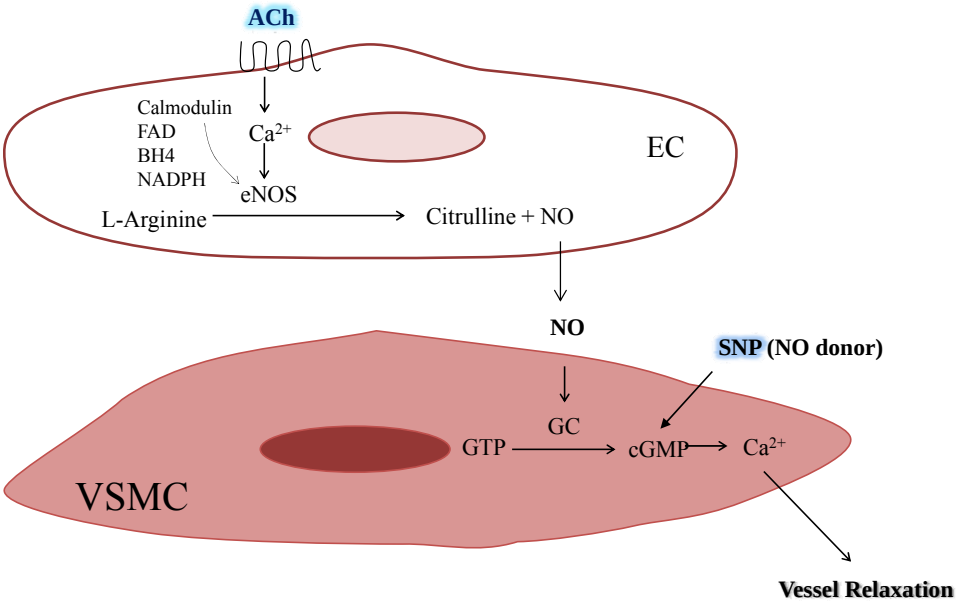

Figure 4. Vascular relaxation mechanism

Illustration of EC and VSMC vascular relaxation mechanism. Under normal conditions, NO is continuously produced by endothelial nitric oxide synthase (eNOS). The activity of eNOS is calcium and calmodulin dependent. Agonists such as ACh acts on its receptor on ECs to induce Ca^{2+} influx and eNOS activation. L-arginine is converted to L-citrulline by eNOS with subsequent production of NO. eNOS requires a number of cofactors including NADPH, FAD, calcium, calmodulin, and BH_4. NO diffuses to the smooth muscle cells where it activates guanylyl cyclase (GC), with a resulting increase in cyclic guanosine monophosphate (cGMP), which initiates processes that lead to vascular relaxation. SNP directly releases NO in VSMC and induces endothelium-independent relaxation. BH_4, tetrahydrobiopterin; FAD, flavin adenine dinucleotide; NADPH, nicotinamide adenosine diphosphate; Ca^{2+}, calcium; cGTP, cyclic guanosine triphosphate; GC, guanylyl cyclase; cGMP, cyclic guanosine monophosphate.

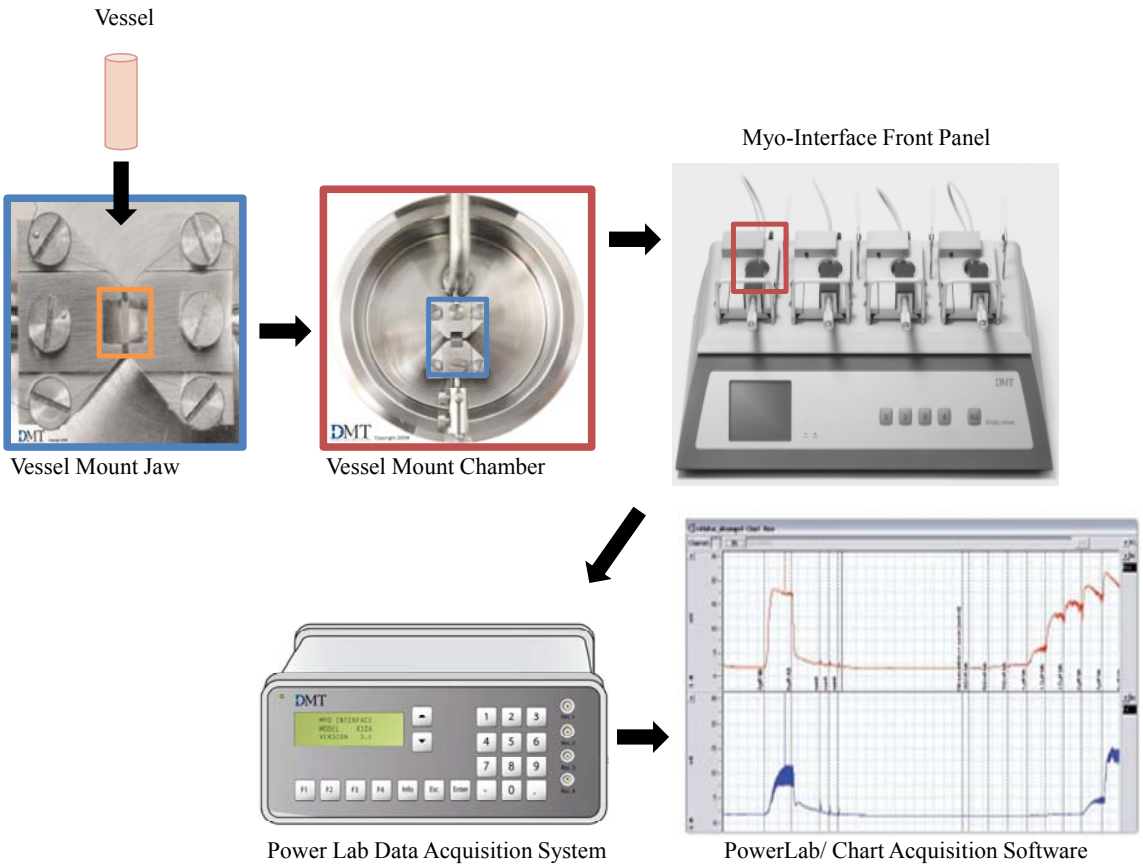

Figure 5. Multi Wire Myograph System

Schematic of the Wire Myograph System used to assess vessel function. A vessel segment is secured in the vessel mount jaw of the myograph chamber. The vessel mount chamber is connected with the myograph interface after vessel is mounted. The myograph interface is linked with a PowerLab Data Acquisition System. Data collected is analyzed with the PowerLab/Chart Acquisition software.

Intravital Microscopy

Male mice were anesthetized with 50mg/kg of pentobarbital via i.p. injection and maintained on a thermo-controlled rodent blanket at 37ºC. The cremaster muscle was exteriorized. Briefly, a midline incision was made through the scrotal skin and the cremaster muscle was dissected from the associated fascia and connective tissue. The distal end of the exposed muscle was pinned gently on a silicone pedestal and cremaster muscle was cauterized longitudinally. The testis and epididymis were separated from the underlying muscle and gently pushed back into the abdominal cavity. The cremaster muscle was spread out the pedestal and superfused continuously with bicarbonate-buffered saline (NaCl 127 mM, KCl 4.7 mM, $CaCl2{\cdot}2H_2O_2$ mM, $MgSO_4$ 1.2 mM, $NaHCO_3$ 28 mM, and glucose 5 mM) using a peristaltic pump. The buffer was aerated continuously with 95% N_2 and 5% CO_2 gas mixture to maintain a pH 7.35~7.45. The temperature of the buffer was maintained at 35ºC. The muscle was allowed to equilibrate for 15 minutes prior to observing leukocyte rolling and adhesion. Venules and arterioles that are 40~50μm in diameter as measured by the CellSens Dimension software (Olympus) were observed on a microscope (Olympus BX51WI) with a digital camera mounted (Olympus DP80). Leukocyte rolling was determined as the number of cells that rolled pass an imaginary line that is perpendicular to the vessels in 1 minute. Adhesion was determined as cells that adhered to the vessel wall for 1 minute on a 100μm length observed. Rolling and adhesion in five venules and two arterioles were observed in each mouse.

Mouse Peripheral Blood Cell and Aortic Cell Isolation and Staining

Mouse vasculature was perfused via cardiac puncture with PBS containing 20U/ml of heparin. The aorta was collected and digested as previously described with slight modifications (Koga, 2001; Magoori et al., 2003). Briefly, the entire mouse thoracic and abdominal aorta was isolated from the surrounding fat tissues. Aorta was cut into small pieces and digested with 125U/ml collagenase type XI, 60U/ml hyaluronidase type I, 60U/ml DNase1, and 450U/ml collagenase type I in PBS containing 20mM HEPES at 37°C for 45 minutes. Aortic cell suspension was then washed with Hank's Balanced Salt Solution (HBSS) (HyClone) supplemented with 2% FBS and filtered through a 70μm cell strainer (BD Biosciences). The filtered cell suspension was centrifuged and re-suspended in HBSS containing 2% FBS for antibody staining.

Mouse blood was collected via the inferior vena cava and 100μl of blood was added to a 15-mL tube containing 1mL of PBS with 5μM EDTA. Red blood cells were lysed with 5mL of ACK lysing buffer for 7 minutes at room temperature. The red blood cell lyses was stopped by addition of 7mL of HBSS containing 2% FBS. The cells were centrifuged and re-suspended in HBSS containing 2% FBS for antibody staining.

Blood cells and aortic cells were first stained with the LIVE/DEAD® Fixable Violet Dead Cell Stain Kit (Invitrogen) for 30 minutes at room temperature to exclude dead cells. Then cells were incubated with three monoclonal antibodies, PE-CD11b, APC-Ly6C, and PE-Cy7-F4/80 for 30 minutes at 4°C. After staining, cells were fixed

with 2% PFA for at least 1 hour at room temperature or overnight at 4°C. Cells were analyzed on a LSR II flow cytometer (BD Biosciences).

Flow cytometry data was analyzed by the FlowJo software (Tree Star, Ashland, OR). Forward and side scatter gates were used to select live cell population from clumps and debris, and dead cells were further excluded by the LIVE/DEAD® Fixable Violet Dead Cell Stain. Positive gates were determined by matched IgG controls and single staining controls were used to determine the compensation parameters.

Atherosclerotic Lesion Analysis

Mouse hearts and aortas from the heart to the ileal bifurcation were perfused with PBS, harvested, and fixed overnight with 4% PFA. Fixed tissues were then submerged in 20% sucrose solution. The lower ventricular portion of the mouse heart was removed with a scalpel and the upper cardiac portion was embedded with Optimal Cutting Temperature compound (OCT) (Tissue Tek, Sakura Finetek, DK), and quickly frozen on dry ice. Mouse aortas were transferred to mini-centrifuge tubes containing PBS and stored at 4°C.

Mouse hearts - Serial cross sections of the aortic root were collected on slides; 10μm cryostat sections were taken from where the three aortic valves first appeared to where the aortic valves disappeared, a total of 80 sections were collected on 10 slides. Sections of the aortic sinus were stained with Oil red O and alum hematoxylin. Briefly, fixed sections were rinsed with 60% isopropanol and stained with freshly prepared Oil

red O working solution (0.3% Oil red O in 60% isopropanol) for 18 minutes. Followed with another rinse with 60% isopropanol, the sections were then stained with alum hematoxylin and rinsed with distilled water. The stained sections were then mounted in aqueous mounting medium and stored in room temperature until imaging.

Mouse aortas – Sudan IV was used for *en face* staining of the mouse aorta. Mouse aortas were staining with Sudan IV (5mg/mL in 70% isopropanol) at 37°C for 40 minutes. Then excess staining of the aorta was removed by incubation with 70% isopropanol for 5 minutes. Then a longitudinal cut was made to expose the intimal surface. Stained aortas were pinned on a black silicone tray for imaging.

Images were captured with a Zeiss Axioscope microscope (Carl Zeiss Inc., Thornwood, NY). Atherosclerotic lesion area in the aortic sinus was defined as the red area staining with Oil red O and measured with ImageJ. The percentage of lesion area was calculated by dividing lesion area by the total sinus area and the average value of eight sections on each slide was presented. Percentage of lesion area in the whole aorta was defined as red area staining with Sudan IV divided by the total aorta area.

Lipid Analysis

Whole blood was collected from anesthetized animals via the inferior vena cava in mini-centrifuge tubes coated with EDTA. Plasma was separated by centrifugation. Plasma levels of LDL, HDL, total cholesterol, non-esterified fatty acids, and triglycerides

were measured at the National Mouse Metabolic Phenotyping Center in Yale Medical School (New Haven, CT).

Microarray Analysis

RNA of the aorta from five male ApoE$^{-/-}$ mice and IL-17$^{-/-}$ApoE$^{-/-}$ mice that were fed a Western diet for 3 weeks were isolated with the RNeasy Kit (Qiagen). RNA quantity was determined by the NanoDrop ND-2000 (Thermo Scientific). RNA samples were sent to the Fox Chase Cancer Center Genomic Facility. The RNA integrity was determined by the RNA 28S/18S ratio using the Agilent 2100 Bioanalyzer (Agilent Technologies). Then samples were labeled and hybridized to the Affymetrix Genechip Mouse Gene 2.0ST Arrays following the manufacturer's instructions. Scanned microarray images were analyzed using the Affymetrix Gene Expression Console with Robust Multi-array Average normalization algorithm.

Statistical Analysis

Data are expressed as mean of replicate measurements or mean normalized values of multiple experiments ± Standard error of the mean (SEM). For comparisons between two groups, two-tailed Student t test (α =0.05) was used for evaluation of statistical significance. Comparison across multiple groups, one-way ANOVA was used.

CHAPTER 3

RESULTS

IL-17 in Hyperlipidemia

IL-17-producing Cells and Plasma IL-17 Concentration are Increased in Hyperlipidemia

First, we used ELISA to determine whether there is a difference in the plasma concentrations of IL-17 in WT mice and hyperlipidemic ApoE$^{-/-}$ mice, and ApoE$^{-/-}$ mice fed a Western diet. The IL-17 concentration in WT mice was not detected and the lowest detectable concentration of our ELISA kit was 15.6pg/mL. The plasma IL-17 concentration in ApoE$^{-/-}$ mice was 36.6 ± 6.17pg/mL. Furthermore, we found that after feeding with a Western diet for 8 weeks, the plasma IL-17 concentrations were dramatically increased to 146.0 ± 7.50pg/mL in ApoE$^{-/-}$ mice (Table 2).

In addition, splenocytes were isolated from WT mice and ApoE$^{-/-}$ mice that were fed a normal chow diet, and from WT mice and ApoE$^{-/-}$ mice that were fed a Western diet for 6 weeks to determine whether hyperlipidemia promotes the number of IL-17-producing cells. Splenocytes were primed with cytokines for IL-17 secretion. The cells were stained with conjugated antibodies for CD4, CCR6, and IL-17 expression then analyzed with FACS. The CD4^{+} T cell population was approximately 30% of the live cells within the splenocytes analyzed (Figure 6C). Within the CD4^{+} T cell population, we found that WT mice had 0.63±0.09% and ApoE$^{-/-}$ mice had 1.4±0.27% of CCR6^{+}IL-17^{+} cells which are known as Th17 cells. After feeding with a Western diet, the percentage of

Th17 cells in WT mice and ApoE$^{-/-}$ mice were both increased. WT mice fed a Western diet had 0.95±0.13% of Th17 cells which was statistically significant when compared to WT mice on a normal chow diet. We also found that a Western diet also increased the Th17 population in ApoE$^{-/-}$ mouse splenocytes to 1.7±0.17% (from 1.4±0.27% in normal chow); however this was not of statistical significance when compared to ApoE$^{-/-}$ mice fed a Western diet (Figure 6G).

Since IL-17 is also produced by other cells besides Th17 cells, we also analyzed splenocytes for all cells that produce IL-17. The number of IL-17-producing cells including Th17 cells within the live cells of the spleen was 0.64±0.4% in WT mice and it was increased to 1.02±0.1% in WT mice after feeding with a Western diet. The percentage of IL-17-producing cells in ApoE$^{-/-}$ mice on a normal chow diet was similar to that in WT fed a Western diet (1.06±0.21%) and it was increased to 1.66±0.2% after a Western diet (Figure 6F). Additionally, statistical significance was found when comparing the percentages of Th17 cells or IL-17-producing cells from WT mice fed a Western diet to those from ApoE$^{-/-}$ mice that were also fed a Western diet, but not in those from mice that were fed a normal chow diet.

Table 2. Plasma IL-17 concentrations determined by ELISA

Genotype	IL-17 (pg/mL)
Wild type (n=3)	Not detected
ApoE$^{-/-}$ (n=3)	36.6 ± 6.17
ApoE$^{-/-}$ WD (n=3)	146.0 ± 7.50

Western diet (WD) Fed for 8 weeks.

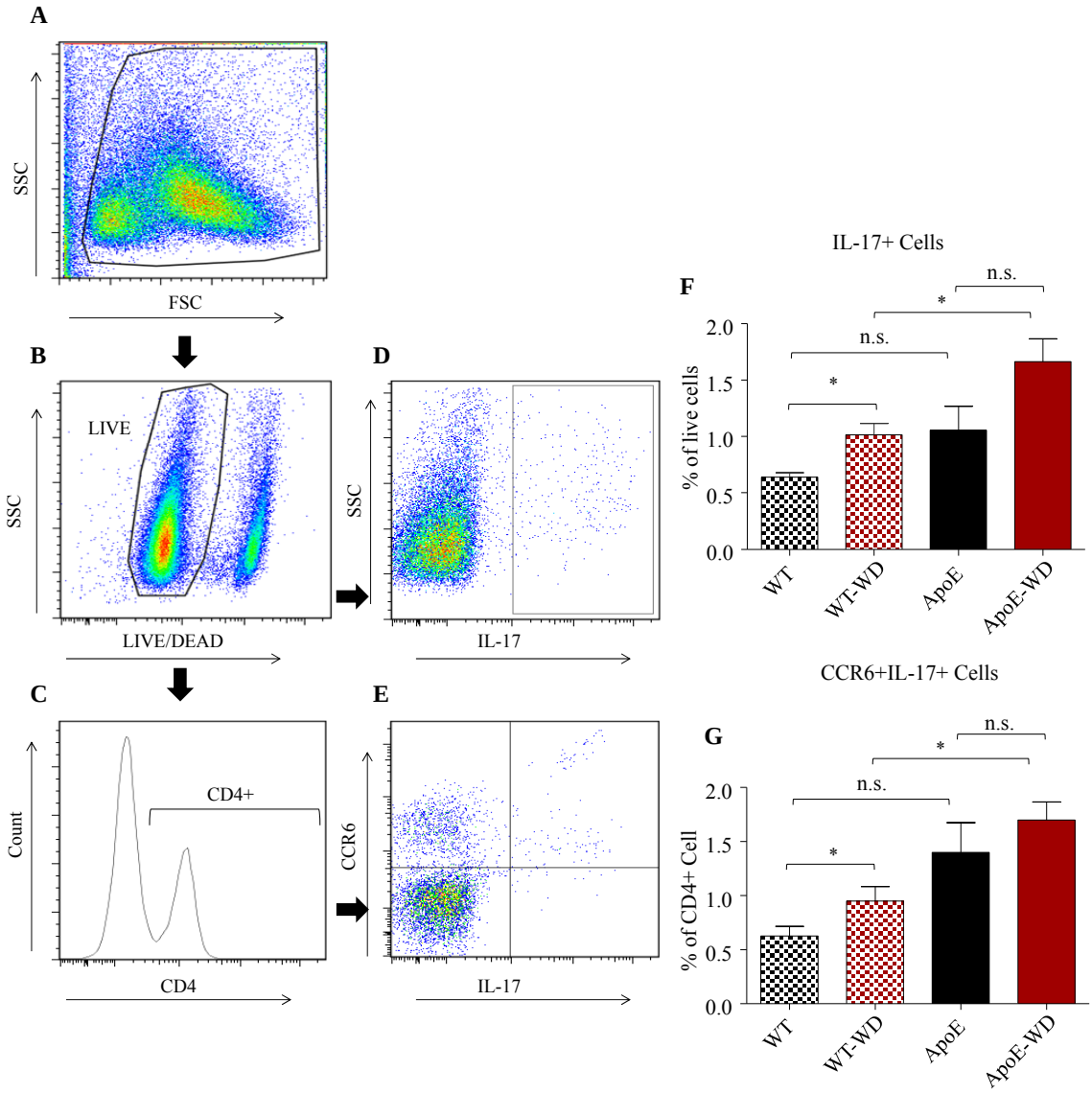

Figure 6. FACS of Th17 and IL-17-producing cells in mouse splenocytes

IL-17-producing cells and Th17 cells from mouse spleen were identified with FACS. Mouse splenocytes from WT mice and ApoE$^{-/-}$ mice that were fed a normal chow diet or Western diet were treated with cytokines that stimulate IL-17 production. Then cells were stained and analyzed with flow cytometry. **A.** Splenocytes were gated from cell debris using the SSC and FSC plot. **B.** Live cells were separated from dead cells with a viability dye. **C & E.** CCR6^{+}IL-17^{+}CD4^{+} T cells (Th17 cells) were gated from the live cell population. **D.** IL-17-producing cells from the live cell population were identified with the IL-17 maker. **F.** IL-17-producing cell percentage of the live cell population. **G.** Th17 cell percentage. Data presented as mean±SEM (n=3), *$p<0.05$; n.s: not significant; WT: wild type; WD: Western diet; ApoE: Apolipoprotein E.

Hyperlipidemia Increases IL-17 Receptor Expression in ECs

IL-17 receptors are shown to be expressed by ECs. To determine whether under hyperlidipidemic conditions, ECs up-regulate the expression of IL-17 receptor in response to the increase of IL-17 within the circulation. We isolated and cultured aortic ECs from WT mice. We used CD31 staining and Dil-ac-LDL uptake in our MAEC culture to ensure the specificity of our cultured ECs (Figure 7). We treated MAECs with OxLDL and used qRT-PCR to determine expression level of L-17ra mRNA transcript. We found that after treatment with OxLDL (50μg/mL) for 24 hours, MAECs increased the expression of the IL-17ra transcript compared to cells that were not treated (Figure 8).

Furthermore, we used FACS to detect IL-17 receptor expression on HAECs after LDL and OxLDL treatment. OxLDL significantly increased the expression of IL-17RA on HAECs after treatment for 24 hours whereas LDL did not induce IL-17RA expression (Figure 9A). LDL and OxLDL both increased the expression of IL-17RC; however, only induction by OxLDL was significant when compared to no treatment control cells (Figure 9B).

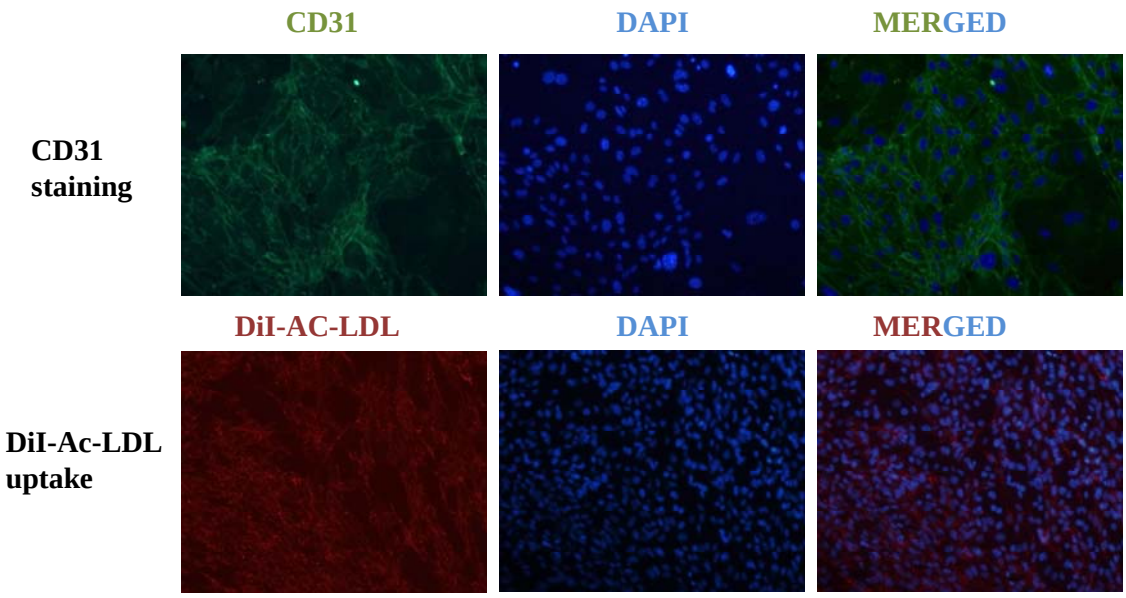

Figure 7. Qualification of MAEC isolation and culture

Qualification of MAEC specificity and function. EC specificity was confirmed with CD31 staining (top panel) and EC function was determined by Dil-AC-LDL uptake (bottom panel).

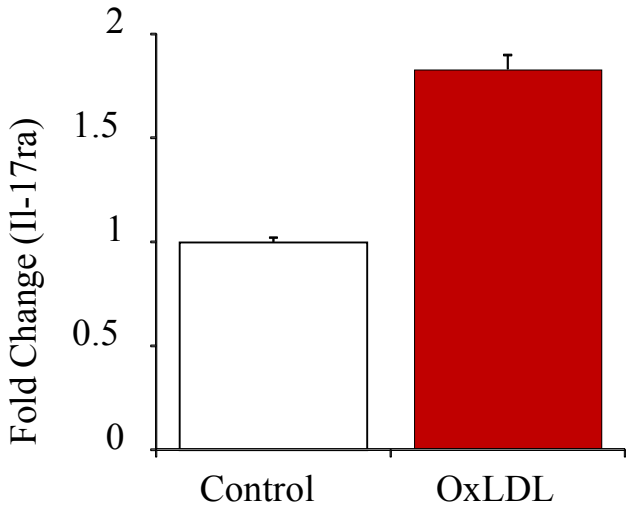

Figure 8. IL-17 receptor mRNA expression in cultured MAECs

IL-17ra mRNA expression in MAECs determined by qRT-PCR. Aortic ECs were isolated from WT mice and cultured until desired confluence was reached. MAECs were treated with OxLDL (50μg/mL) for 24 hours then RNA was isolated. RNA was reverse transcribed to cDNA and cDNA was used in qRT-PCR to determine the expression of IL-17ra. OxLDL treatment increased the expression of IL-17ra mRNA transcript in MAECs when compared to no treatment control cells. Expression of gene was normalized by expression of β-actin.

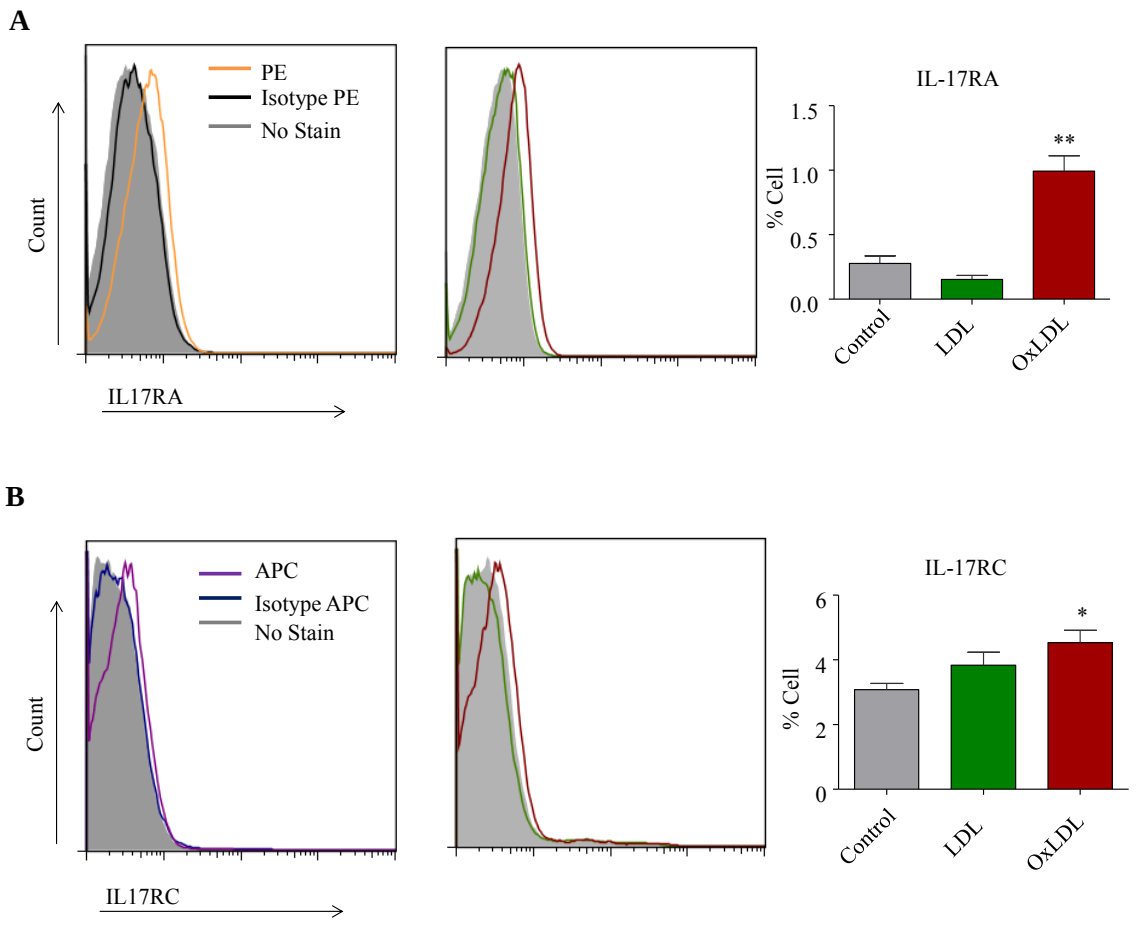

Figure 9. FACS of IL-17 receptor expressions in HAECs

IL-17 receptor A and C expressions in HAECs were quantified by FACS. HAECs grown in 6-well plates were either left untreated or treated with LDL (50µg/mL) or OxLDL (50µg/mL) for 24 hours. Afterwards, cells were stained with IL-17RA and IL-17RC antibodies and fixed with 2% PFA. IL-17 receptor expressions were analyzed with FACS. **A.** IL-17RA expression was increased by OxLDL treatment in HAECs **B.** IL-17RC expression was increased by LDL and OxLDL treatment in HAECs. Data presented as mean±SEM (n=3). *p<0.05, **p<0.01 vs. control untreated cells.

Endothelial Cell Activation

Activation of the endothelium is characterized by a few features which include enhanced pro-inflammatory cytokine and chemokine production, increased adhesion molecule expression, and augmented leukocyte adhesion.

Monocyte Adhesion is Enhanced to IL-17-treated ECs

We utilized the monocyte-EC adhesion assay to investigate whether IL-17 activates ECs and increases monocyte adhesion to ECs. Endothelial monolayer was treated with IL-17 for various time periods *in vitro* and untreated labeled THP-1 cells were allowed to adhere to the monolayers. We found that there was an increase in the number of THP-1 monocytic cells that adhere to the IL-17-treated endothelial monolayer. This effect was first detected in the shortest treatment time of 2 hours. The most dramatic increase in adhesion was seen in the 12-, 24-, and 36-hour treatment periods. After 48 hours of IL-17 treatment, the percentage of adhesion began to return to the level of the control (Figure 10A). Furthermore, to confirm our result seen with the monocytic cell line, we isolated primary human monocytes and allowed them to adhere to ECs that were treated with IL-17 for 24 hours. We found that adhesion of primary human monocytes to IL-17-treated ECs was significantly enhanced when compared to the control group (Figure 10B).

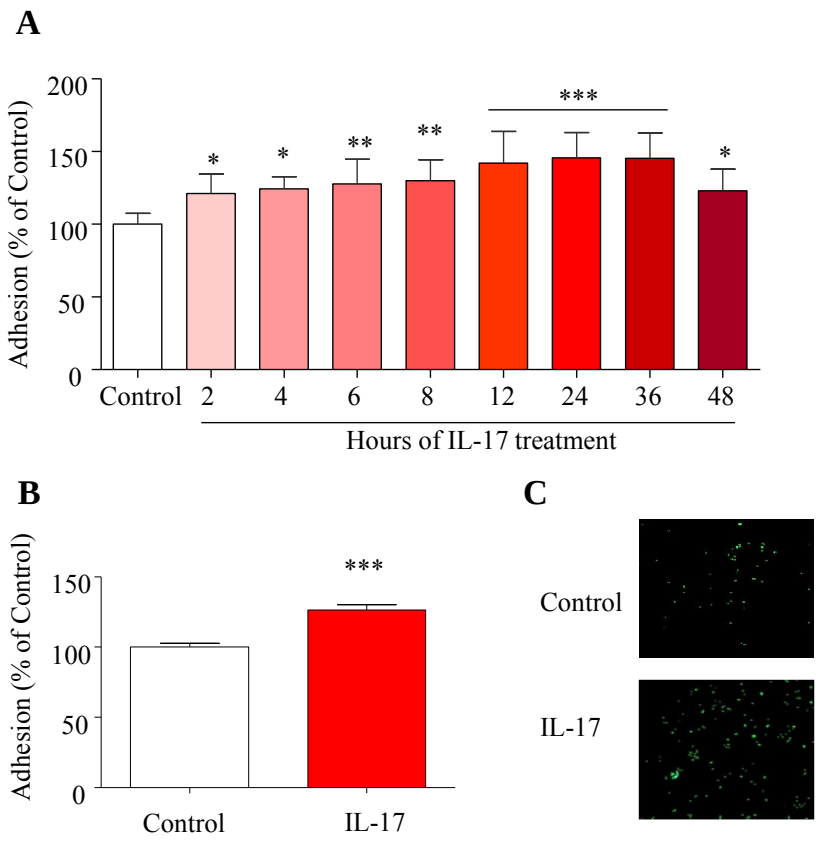

Figure 10. Monocyte adhesion to IL-17-treated ECs

Monocyte-EC adhesion assay with THP-1 cells and primary human monocytes. HAECs grown on 24-well plates were treated with IL-17 for indicated time then untreated labeled monocytes were allow to adhere to the endothelial monolayer. Percentage of cell adhesion was determined by a fluorescence plate reader. **A.** IL-17-activated ECs increased THP-1 monocytic cell adhesion in a time-dependent manner. Adhesion is shown as a percentage of the control group. **B.** Primary human monocyte adhesion to HAECs treated with IL-17 for 24 hours was increased. **C.** Fluorescence microscopic images of labeled primary human monocyte adhered to HAECs. Data presented as mean±SEM (n=3). *p<0.05, **p<0.01, and ***p<0.001 vs. control.

IL-17 Induces Pro-inflammatory Cytokines and Chemokines

We isolated and cultured MAECs to see whether IL-17 induces cytokine and chemokine gene changes. The Mouse Endothelial Cell Biology RT² Profiler™ PCR Array, which profiles the expression of 84 genes related to EC biology was used (Figure 11A). We found that after treatment with IL-17 (100ng/mL) for 24 hours, there were 4 genes which are associated with EC activation that were significantly up-regulated (at least 4 folds) in MAECs (Figure 11B). The 4 genes were pro-inflammatory chemokines and cytokines, Cxcl1, Cxcl2, Il6, and Csf2 (also known as Granulocyte-Macrophage Colony-Stimulating Factor, GM-CSF) (Figure 11C). Furthermore, we used qRT-PCR to determine whether these 4 genes are up-regulated in HAECs after treatment with IL-17. We found that the CXCL1, CXCL2, IL6, and CSF2 mRNA transcripts were also up-regulated in HAECs after treatment with IL-17 for 12 hours. The changes of the 4 genes were significant although the induction in HAECs was not as great as that seen in MAECs (Figure 12).

A

Ace	Adam17	Agt	Agtr1a	Angpt1	Anxa5	Bax	Bcl2	Bcl2l1	Birc1a	Birc2	Blr1
Casp1	Casp3	Casp6	Ccl2	Ccl5	Cdh5	Cflar	Col18a1	Cpb2	Cradd	Csf2	Cx3cl1
Cxcl1	Cxcl2	Cxcl4	Ecgf1	Edn1	Edn2	Ednra	Fas	Fasl	Fgf1	Flt1	Fn1
Icam1	Ifnb1	Il11	Il1b	Il3	Il6	Il7	Itga5	Itgav	Itgb1	Itgb3	Kdr
Kit	Mmp1a	Mmp2	Mmp9	Nos2	Nos3	Nppb	Npr1	Ocln	Pdgfra	Pecam1	Pgf
Plat	Plau	Plg	Ptgis	Rhob	Ripk1	Sele	Sell	Selp	Selplg	Serpine1	Sod1
Tek	Tfpi	Tgfb1	Thbd	Thbs1	Timp1	Tnf	Tnfaip3	Tnfsf10	Vcam1	Vegfa	Vwf
Gusb	Hprt1	Hsp90ab1	Gapdh	Actb	MGDC	RTC	RTC	RTC	PPC	PPC	PPC

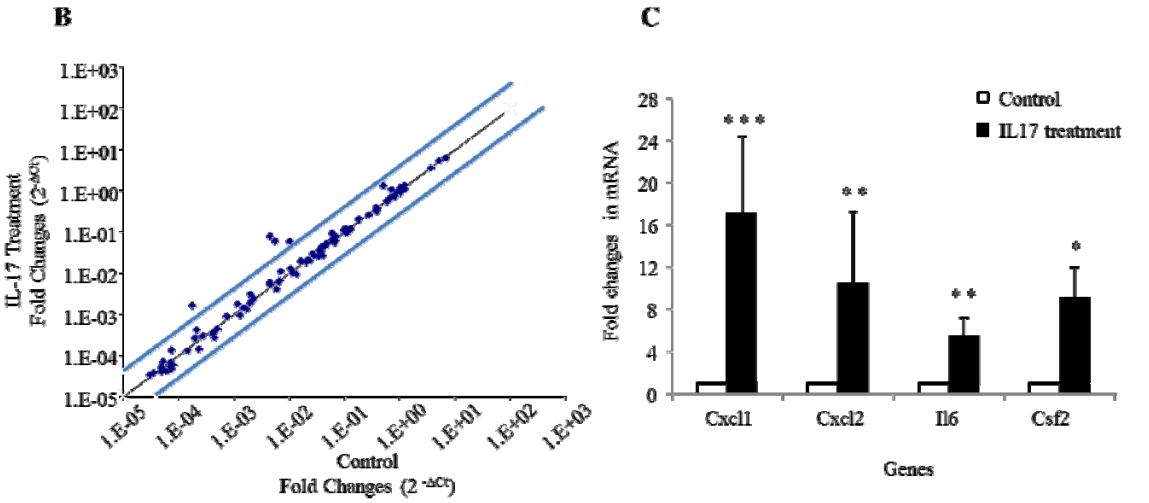

Figure 11. Expression profiles of 84 endothelial biology-related genes in MAECs

Genes related to EC biology profiled by The Mouse Endothelial Cell Biology RT² Profiler™ PCR Array. cDNA from MAECs treated with IL-17 for 24 hours were used in the Mouse Endothelial Cell Biology RT² Profiler™ PCR Array. **A.** 84 genes assessed by the array. **B.** Scatter plot of gene fold changes in MAECs treated with IL-17 compared to MAECs that were untreated. The expressions of 4 genes were dramatically changed by IL-17 treatment; Blue lines indicate fold change of 4. **C.** Four genes found to be up-regulated by IL-17 treatment in MAECs were Cxcl1, Cxcl2, Il6, and Csf2. Data presented as mean±SEM (n=5). *p<0.05, **p<0.01, and ***p<0.001 vs. control.

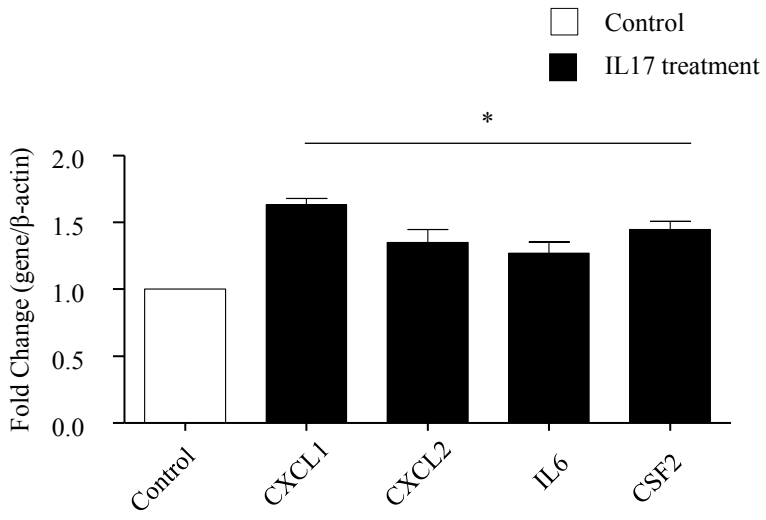

Figure 12. Cytokine and chemokine mRNA expressions in HAECs

mRNA expression of cytokines and chemokines was determined by qRT-PCR. IL-17 treatment significantly enhanced the expression of cytokines and chemokines in HAECs. The gene expression of CXCL1, CXCL2, IL6, and CSF2 in HAECs after treatment with IL-17 (100ng/ml) for 12 hours was assessed with qRT-PCR. Data presented as mean±SEM (n=3), *$p<0.05$ vs. control.

IL-17 Induces Adhesion Molecule E-selectin

With mouse endothelial PCR array, we did not observe significant changes in adhesion molecule transcripts and we wanted to see whether this is also true in HAECs. We treated HAECs with IL-17 for 2, 6, 12, and 24 hours and used qRT-PCR to assess whether the expressions of the transcripts of ICAM-1, VCAM-1, and E-selectin are changed. We found that there was no significant change in the transcript expressions of ICAM-1 and VCAM-1 in all the time points tested (Figure 13A&B). The transcript of E-selectin was found to be up-regulated in HAECs by IL-17. The induction was seen in all the time points assessed. The increase in E-selectin transcript expression was not significant after 2 hours of IL-17 treatment, but it was statistically significant after 6, 12, and 24 hours of IL-17 treatment (Figure 13C).

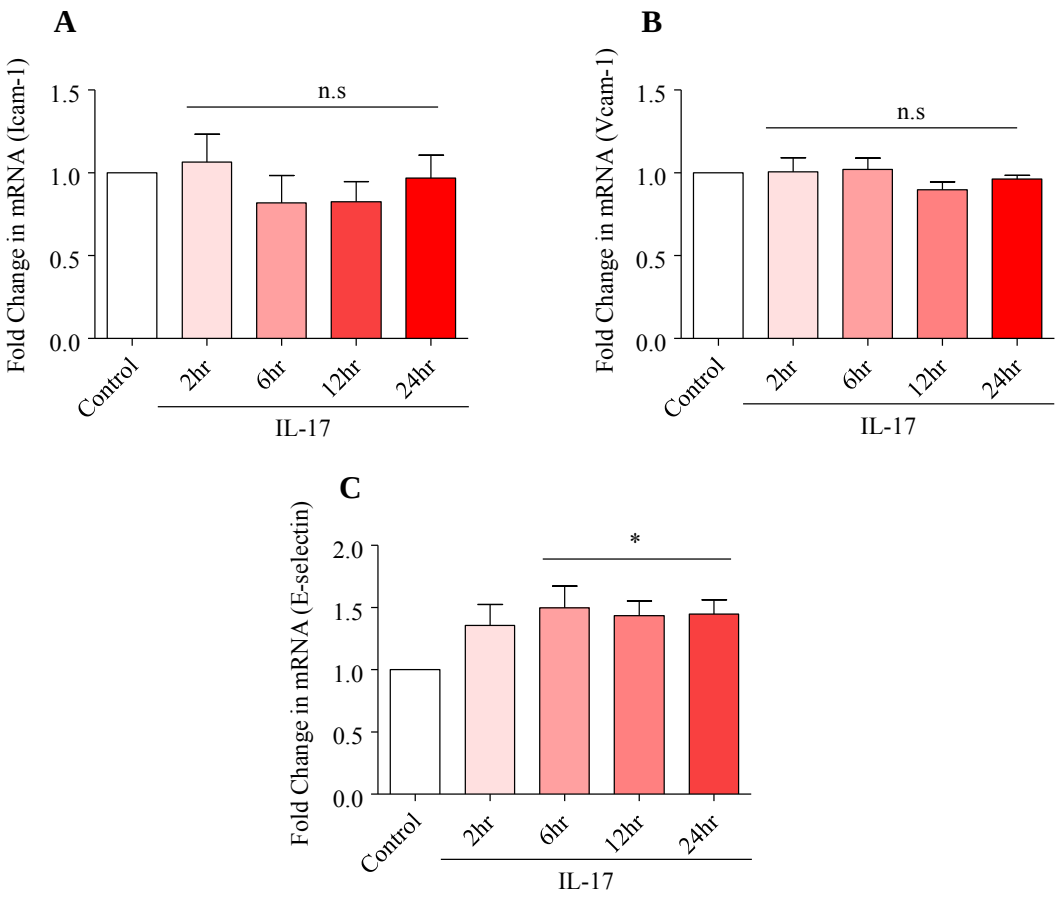

Figure 13. Adhesion molecule mRNA expressions in HAECs

Adhesion molecule expressions in HAECs treated with IL-17 for various time periods was assessed with qRT-PCR. HAECs were treated with IL-17 for the times indicated then RNA was isolated. cDNA from reverse transcription of the RNA isolated was used in qRT-PCR to determine adhesion molecule expressions. **A.** ICAM-1 mRNA expression normalized by β-Actin expression. **B.** VCAM-1 mRNA expression normalized by β-Actin expression. **C.** E-selectin mRNA expression normalized by β-Actin expression. Data presented as mean±SEM (n=5), *$p<0.05$ vs. control. n.s: not significant.

Enhanced Monocyte Adhesion to IL-17-treated ECs is Dependent on Pro-inflammatory Cytokines and Chemokines

We used neutralizing antibodies against CXCL1/2, IL-6, and GM-CSF in our monocyte-EC adhesion assay to determine whether enhanced monocyte adhesion to activated ECs is dependent on these 4 genes up-regulated by IL-17. We found that blocking antibodies against CXCL1/2, IL-6, and GM-CSF abrogated the increased THP-1 monocytic cell adhesion to ECs that were treated with IL-17 for 24 hours. IgG isotype control was used as antibody control and it was ineffective in reducing monocyte adhesion to activated ECs (Figure 14).

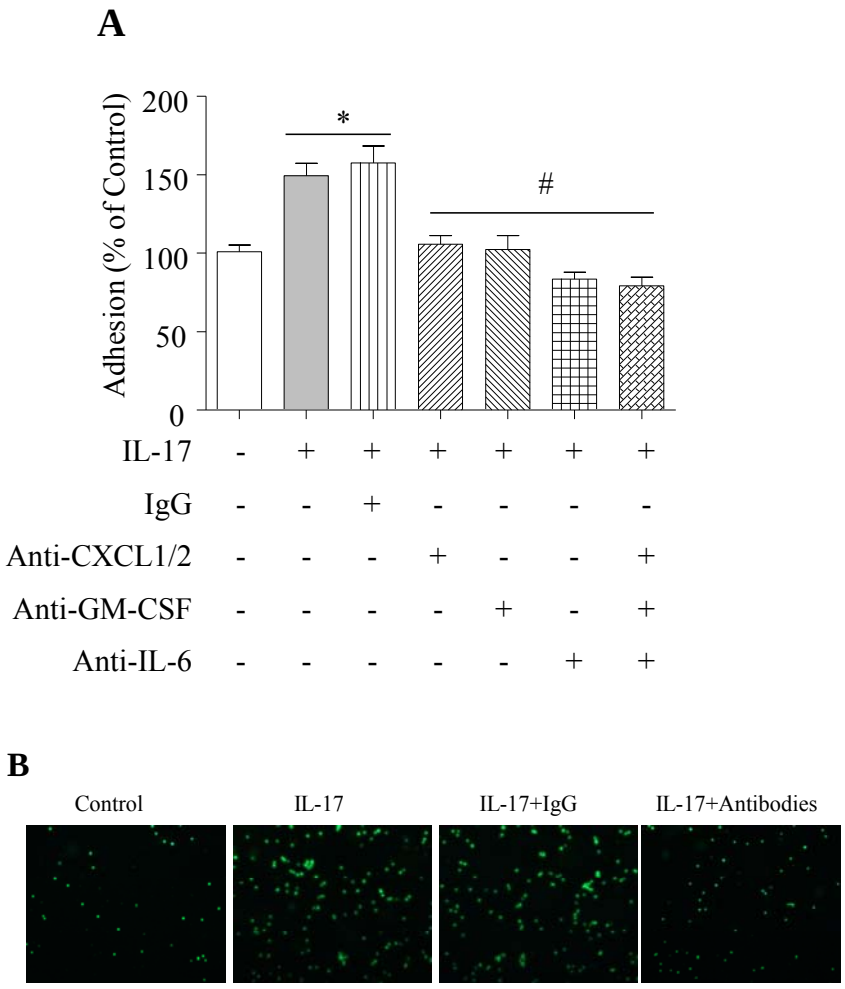

Figure 14. Monocyte adhesion to ECs in the presence of blocking antibodies

THP-1 monocytic cell adhesion to IL-17-activated ECs in the presence of neutralizing antibodies. ECs were treated with IL-17 then blocking antibodies against CXCL1/2, IL-6, and/or GM-CSF were added 30 minutes prior to the adhesion assay. **A.** Antibodies against CXCL1/2, IL-6, and GM-CSF reversed the effect of IL-17 on monocyte adhesion to ECs while IgG control did not. **B.** Fluorescence microscopic image of labeled THP-1 cells adhered ECs. Data presented as mean±SEM (n=3), *$p<0.05$ vs. control, #$p<0.05$ vs. IL-17-treated group.

Generation of IL-17$^{-/-}$ApoE$^{-/-}$ mice

To characterize the function of IL-17 in vascular function and atherogenesis in hyperlipidemia *in vivo*, IL-17$^{-/-}$ mice from Dr. Yoichiro Iwakura's laboratory (Nakae et al., 2002) were crossed with ApoE$^{-/-}$ mice to generate IL-17$^{-/-}$ApoE$^{-/-}$ mice (Figure 15). These mice were viable and fertile. At the age of 8 weeks, male ApoE$^{-/-}$ mice and IL-17$^{-/-}$ ApoE$^{-/-}$ mice were maintained on a normal chow diet (5% fat, Labdiet 5001) or fed with a diet that contains 21% fat by weight, 0.15% by weight cholesterol, and 19.5% by weight casein without sodium cholate (TD. 88137, Harlan Teklad, WI), also known as a Western diet, for 3 or 6 weeks then sacrificed for designated experiments (Figure 16). The body, heart, and spleen weights of mice were not affected by IL-17 gene deletion or a Western diet for 3 weeks (Figure17A-C) or 6 weeks (Figure 17D-E).

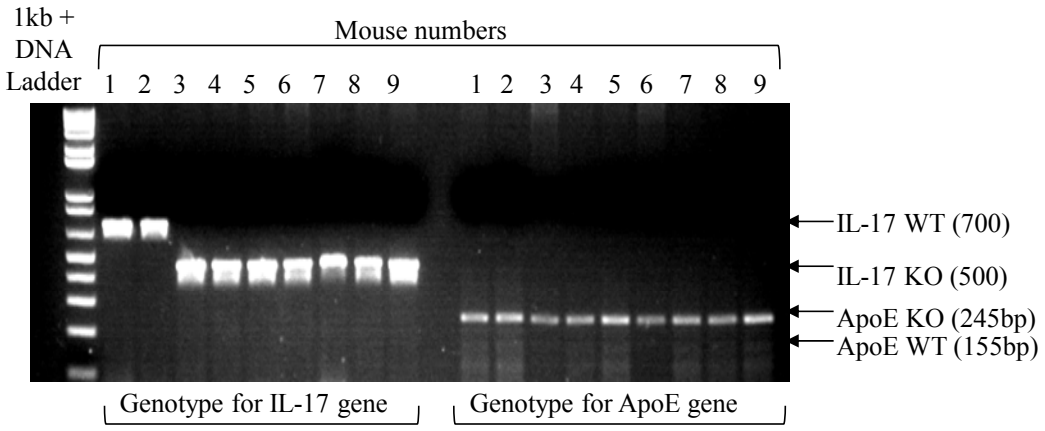

Figure 15. Generation of IL-17$^{-/-}$ApoE$^{-/-}$ mouse

Identification of IL-17$^{-/-}$ApoE$^{-/-}$ mice with PCR of mouse tail DNA followed by agarose gel electrophoresis. Genotype for the IL-17 gene and ApoE gene were realized on a 2% agarose gel. Mice #1 & 2 are homozygous for ApoE deficiency and WT for IL-17 deficiency. Mice #3-9 are homozygous for ApoE and IL-17 deficiency.

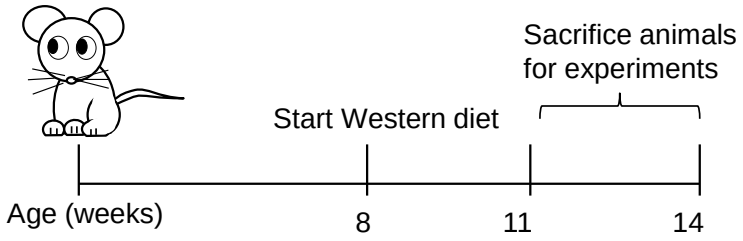

Figure 16. Animal experimental design

The dietary time line of mice used in experiments. Male ApoE$^{-/-}$ mice and IL-17$^{-/-}$ ApoE$^{-/-}$ mice were put on a Western diet or maintain on a regular chow diet at 8 weeks of age. The animals were either fed for 3 or 6 weeks until they were used for designated experiments.

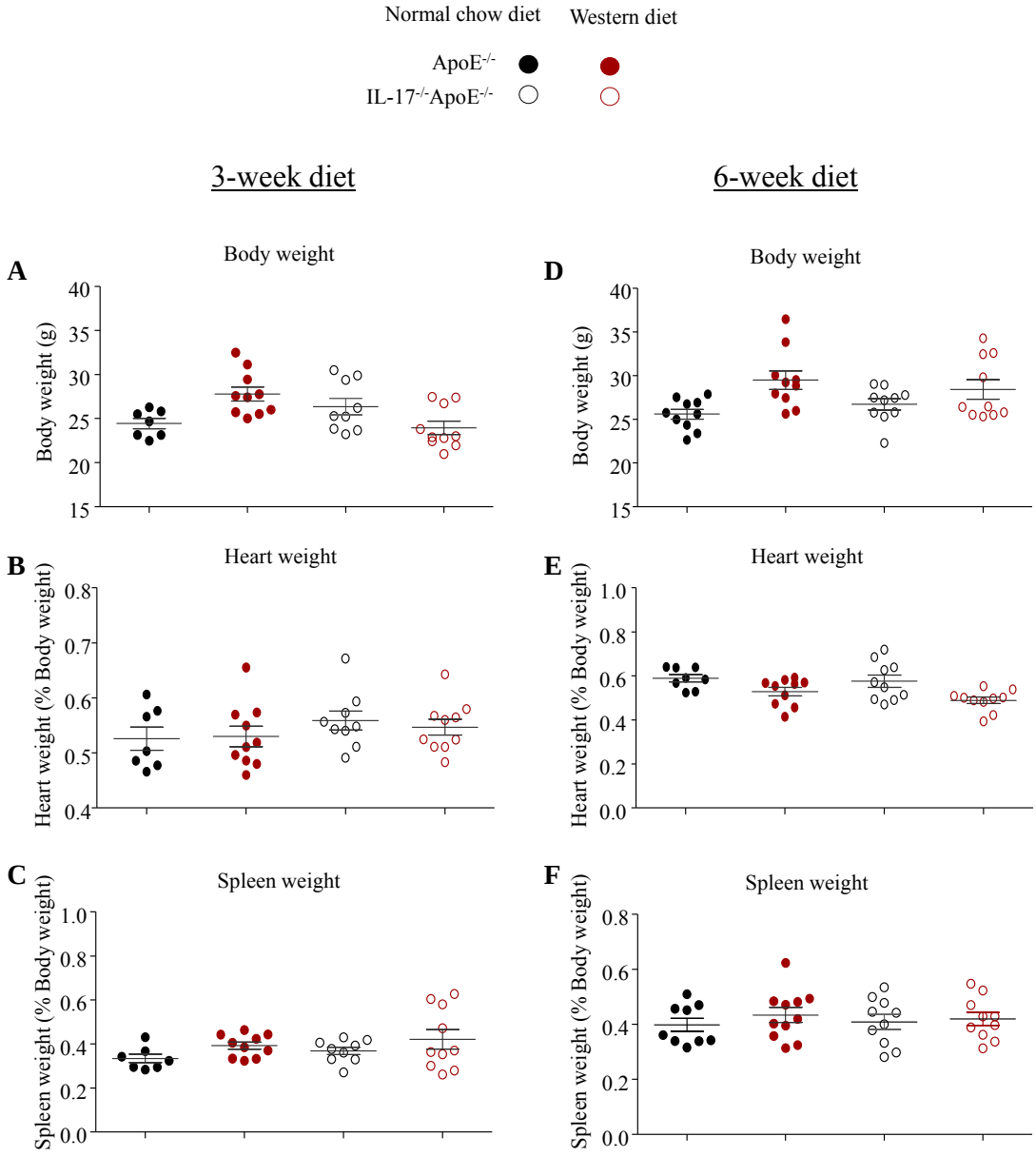

Figure 17. Body and tissue weights of mice on a 3-week or 6-week diet

Body weight, heart weight, and spleen weight of ApoE$^{-/-}$ mice and IL-17$^{-/-}$ApoE$^{-/-}$ mice that were on a normal chow diet or Western diet. A-C. Body, heart, and spleen weights of mice on a 3-week diet. **D-F**. Body, heart, and spleen weights of mice on a 6-week diet. Data presented as mean±SEM (n=7-10).

Role of IL-17 in Vascular Function

To investigate the role of IL-17 in vascular function, we used the Wire Myograph System which allows us to assess the functional responses and vascular reactivity of isolated aortic segments in response to various agonists. We suspect that IL-17 contributes to vascular dysfunction in the aorta of $ApoE^{-/-}$ mice.

Mice on a Regular Chow Diet Retain Normal Vascular Function

Previously, it was summarized that $ApoE^{-/-}$ mice that were fed a normal chow diet did not exhibit vascular dysfunction of the aorta until they were well advanced in their age (Meyrelles, Peotta, Pereira, & Vasquez, 2011). To confirm others' previous findings as well as to ensure that our Wire Myograph System is functional and reliable, we assessed whether vascular function in young $ApoE^{-/-}$ mice that are on a regular chow diet is sustained. We compared the vascular function of 11-week old $ApoE^{-/-}$ mice and $IL\text{-}17^{-/-}$ $ApoE^{-/-}$ mice to their age-matched WT mice. We found that depolarization-induced vessel contraction and α-adrenoceptor-induced contraction responses to KCl and PE, respectively, were similar in all three genotypes (Figure 18A&B). Next, we assessed endothelium-dependent relaxation to ACh and endothelium-independent vessel relaxation to SNP and found that these two parameters were not different in the three genotypes (Figure 18C&D). This result confirms the reliability of our experimental system.

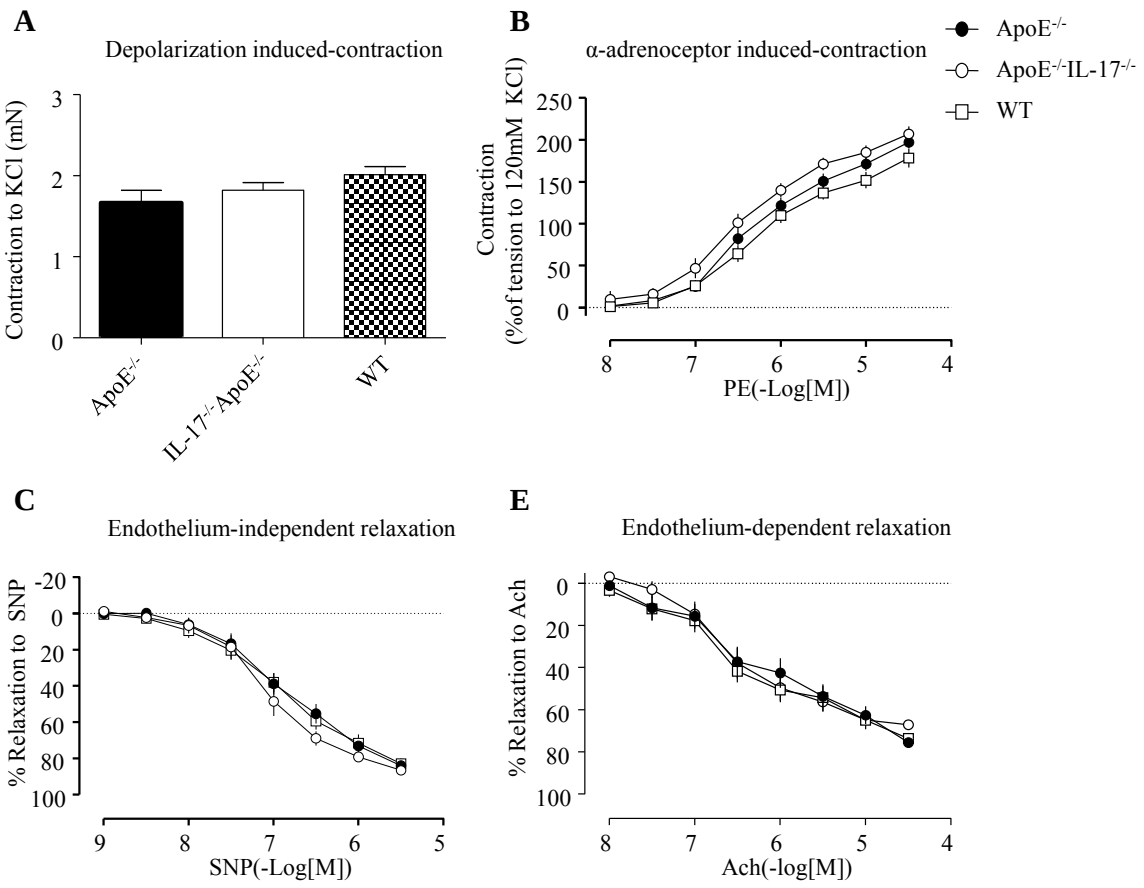

Figure 18. Vascular function of mice on a normal chow diet

Vascular responses of aortic segments from mice fed a normal chow diet. A. Depolarization induced-contraction by 120mM KCl. **B.** α-adrenoceptor induced-contraction by cumulative doses of PE. **C.** Endothelium-independent relaxation to cumulative doses of SNP in vessel segments pre-contracted with PE. **D.** Endothelium-dependent relaxation to cumulative doses of ACh in vessel segments pre-contracted with PE. Data presented as mean±SEM (n=5-6, two aortic segments per mouse).

No Change in Vascular Contractile Responses in Western Diet Fed Mouse Aorta

To test whether vascular function of the aorta in Western diet fed mice are changed, we measured vascular responses in $ApoE^{-/-}$ mice and $IL\text{-}17^{-/-}ApoE^{-/-}$ mice that were fed a Western diet for 3 weeks or 6 weeks, respectively. First, we tested the vascular contractile responses. As it was done in the regular chow diet mouse aortas, a single dose of KCl (120mM) was used to determine depolarization-induced vessel contraction and cumulative doses of PE (10nM-33μM) were used to assess α-adrenoceptor-induced contraction in the Western diet fed mouse aortas. Contraction responses to KCl and PE were similar in aorta segments from $IL\text{-}17^{-/-}ApoE^{-/-}$ mice and $ApoE^{-/-}$ mice that were either fed a Western diet for 3 weeks (Figure 19A&C) or 6 weeks (Figure 20A&B). This result shows that IL-17 deficiency does not affect contractile response changes in Western diet fed mouse aortas in $ApoE^{-/-}$ mice induced by KCl and PE.

IL-17 Impairs Endothelium-dependent Relaxation in Western Diet Fed Mouse Aorta

Endothelial dysfunction is a critical event to the inception of atherosclerosis development. We examined endothelial dysfunction in $ApoE^{-/-}$ mice fed a Western diet for 3 weeks or 6 weeks, respectively, by assessing the endothelium–dependent relaxation to ACh in the aortas. Endothelium-dependent relaxation was examined by the cumulative dose response to ACh (10nM-33μM) in aortas pre-contracted with PE.

Dose-dependent relaxation produced by ACh was significantly impaired in the aortas of $ApoE^{-/-}$ mice compared to $IL\text{-}17^{-/-}ApoE^{-/-}$ mice in the 3-week Western diet

groups (48.8% relaxation in ApoE$^{-/-}$ mice vs. 73.5% in IL-17$^{-/-}$ApoE$^{-/-}$ mice) (Figure 19D). Endothelium-dependent relaxation in 3-week Western diet fed IL-17$^{-/-}$ApoE$^{-/-}$ mouse aortas was normal as it was similar to that in WT mice on a regular chow diet (73.7% relaxation) (Figure 19E), which was also the same as those in ApoE$^{-/-}$ mice and IL-17$^{-/-}$ApoE$^{-/-}$ mice that were on a normal chow (Figure 18E). In ApoE$^{-/-}$ mice and IL-17$^{-/-}$ApoE$^{-/-}$ mice that were fed a 6-week Western diet, endothelium-dependent relaxation in the aortas was impaired compared to the aortas of regular chow fed WT mice (

Figure 20E). Endothelium-dependent relaxation seemed more impaired in the aortas of ApoE$^{-/-}$ mice than in those of of IL-17$^{-/-}$ApoE$^{-/-}$ mice, although there is no statistical difference between the two (

Figure 20D).

Endothelium-independent Relaxation is Not Affected in Mouse Aorta by IL-17 Deficiency

In addition to assessing endothelium-dependent relaxation, we tested the endothelium-independent relaxation in the aortas of ApoE$^{-/-}$ mice and IL-17$^{-/-}$ApoE$^{-/-}$ mice that were fed a Western diet for 3 weeks or 6 weeks, respectively. Endothelium-independent vascular relaxation response was assessed using responses to cumulative doses of SNP, an NO donor, which directly relaxes VSMCs. Relaxation responses to SNP were similar between ApoE$^{-/-}$ mice and IL-17$^{-/-}$ApoE$^{-/-}$ mice in the 3-week and 6-week Western diet groups (Figure 19C & Figure 20C).

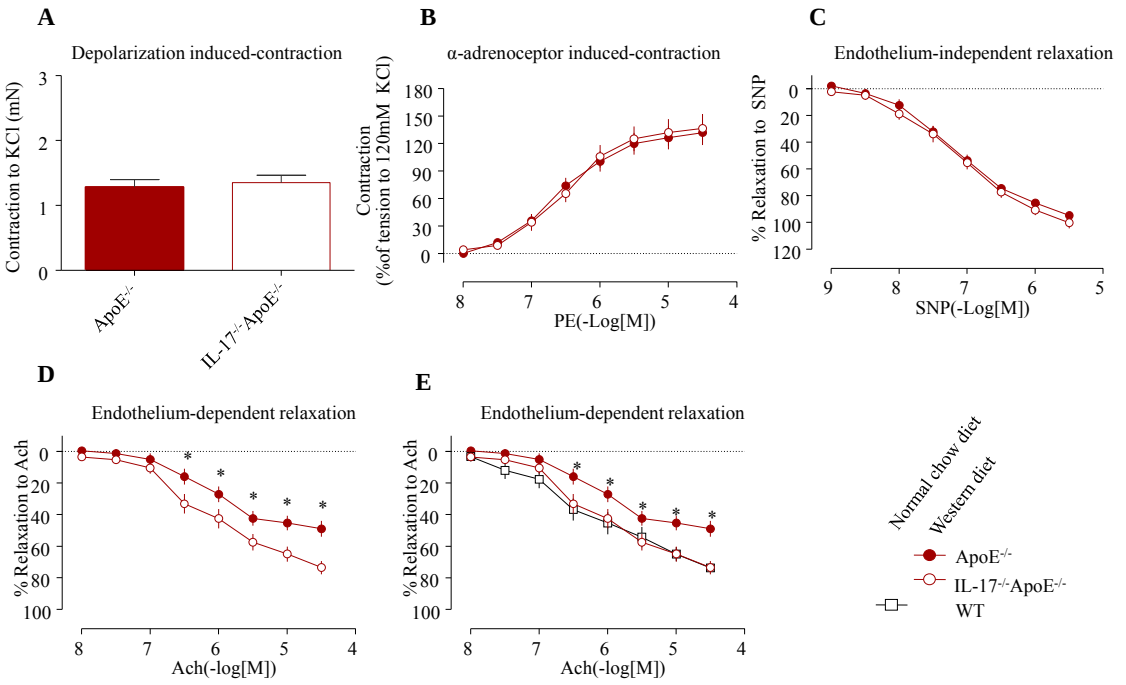

Figure 19. Vascular function of mice on a 3-week Western diet

Vascular responses of aortic segments from ApoE$^{-/-}$ mice and IL-17$^{-/-}$ApoE$^{-/-}$ mice fed a Western diet for 3 weeks. A. Depolarization induced-contraction by 120mM KCl. **B.** α-adrenoceptor induced-contraction by cumulative doses of PE. **C.** Endothelium-independent relaxation to cumulative doses of SNP in vessel segments pre-contracted with PE. **D.** Endothelium-dependent relaxation to cumulative doses of ACh in vessel segments pre-contracted with PE. **E.** Endothelium-dependent relaxation in aortic segments from ApoE$^{-/-}$ mice and IL-17$^{-/-}$ApoE$^{-/-}$ mice compared to aortic segments from WT mice fed a normal chow diet. Data presented as mean±SEM, *$p<0.05$ ApoE$^{-/-}$ mice vs. IL-17$^{-/-}$ApoE$^{-/-}$ mice or WT mice (Western diet n=10; normal chow diet n=6, two aortic segments per mouse).

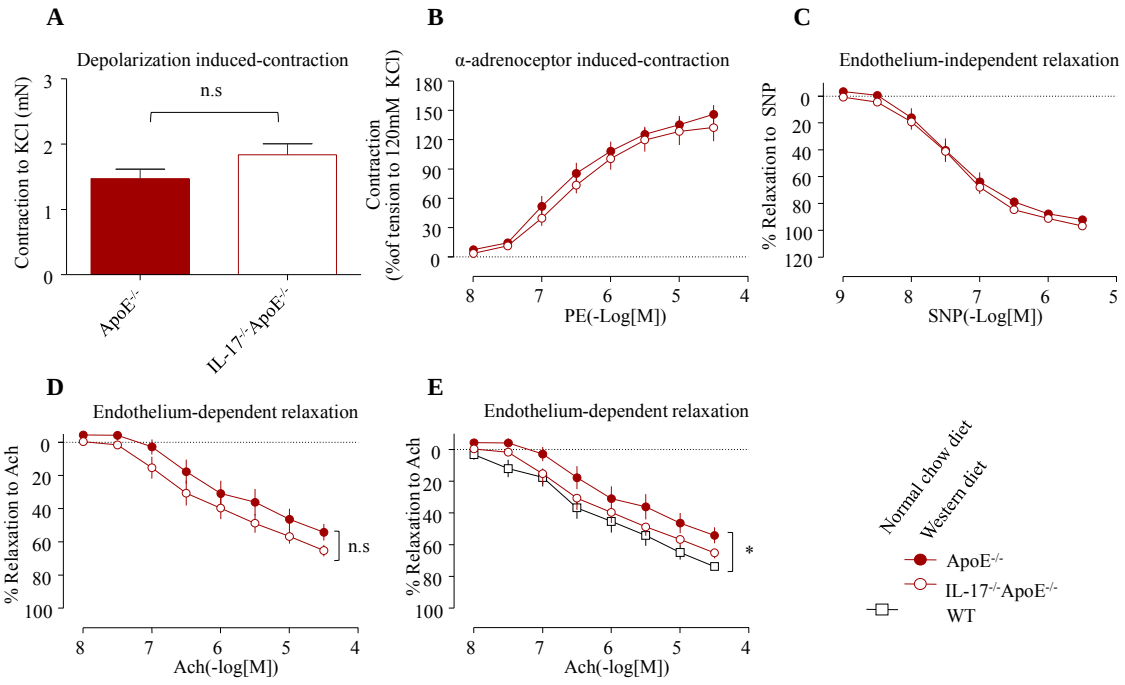

Figure 20. Vascular function of mice on a 6-week Western diet

Vascular responses of aortic segments from ApoE$^{-/-}$ mice and IL-17$^{-/-}$ApoE$^{-/-}$ mice fed a Western diet for 6 weeks. A. Depolarization induced-contraction by 120mM KCl. **B.** α-adrenoceptor induced-contraction by cumulative doses of PE. **C.** Endothelium-independent relaxation to cumulative doses of SNP in vessel segments pre-contracted with PE. **D.** Endothelium-dependent relaxation to cumulative doses of ACh in vessel segments pre-contracted with PE. **E.** Endothelium-dependent relaxation in aortic segments from ApoE$^{-/-}$ mice and IL-17$^{-/-}$ApoE$^{-/-}$ mice compared to aortic segments from WT mice fed a normal chow diet. Data presented as mean±SEM, *$p<0.05$ ApoE$^{-/-}$ mice vs. WT mice (n=6, two aortic segments per mouse).

Expression of pP38 is Specifically Decreased in Aortic Tissues of IL-17$^{-/-}$ApoE$^{-/-}$ Mice

To explore the possible mechanisms that lead to impairment of endothelium-dependent relaxation in our 3-week Western diet fed mice, we used western blot to see whether the protein expressions of phosphorylated- eNOS and MAPK are changed in the aorta. The phosphorylations of eNOS at two sites (ser1177 and thr495) were determined. There was a trend to have more phosphorylated eNOS ser1177 expression and less phosphorylated eNOS thr495 expression in the aortas of IL-17$^{-/-}$ApoE$^{-/-}$ mice; however, there was no statistical significance in these changes (Figure 21B&C). We found that the phosphorylation of JNK was relatively the same in the two mouse groups (Figure 21D). Next, we looked at the phosphorylation of P38 and found that IL-17$^{-/-}$ApoE$^{-/-}$ mice had a significant lower expression of pP38 in the aortas, suggesting that P38 may be an important mediator in our vessel function phenotype (Figure 21E).

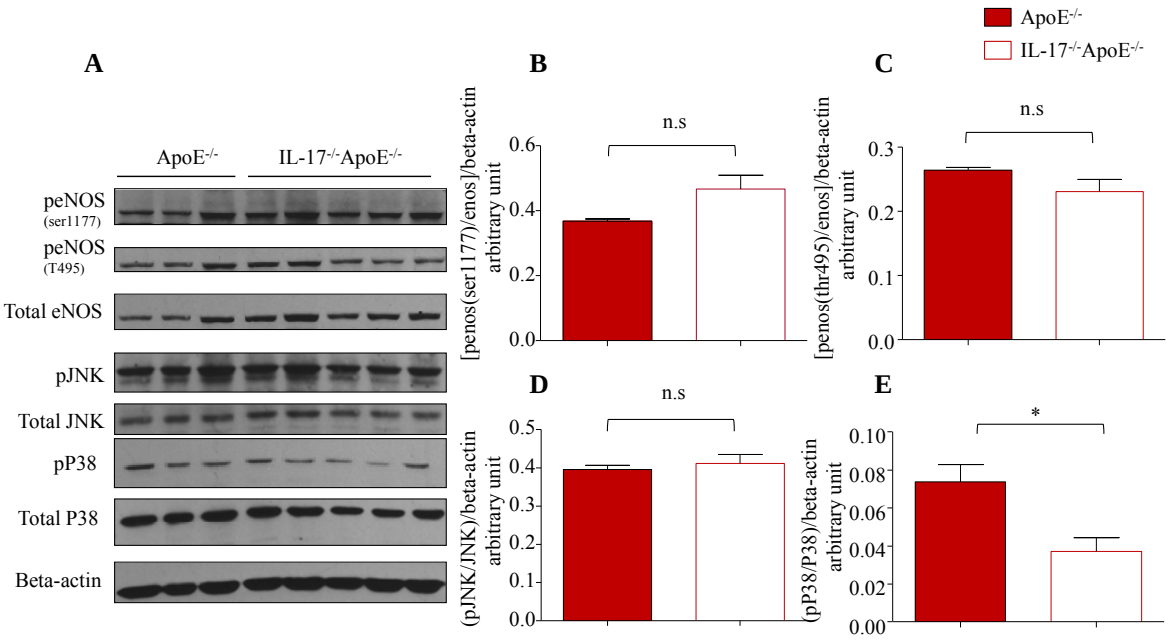

Figure 21. Expression of phosphorylated- eNOS and MAPK in mouse aorta

Phosphorylated- eNOS and MAPK expressions in mouse aortas were assessed with western blot. A. Representative western blots of phosphorylated and total eNOS, JNK, and P38 expressions and beta-actin expression in mouse aorta protein. **B.** Quantification of phosphorylated-eNOS (ser1177). **C.** Quantification of phosphorylated-eNOS (thr495). **D.** Quantification of phosphorylated-JNK. **E.** Quantification of phosphorylated-P38. Quantification shown as phosphorylated protein expression divided by total protein expression normalized by beta-actin. Data presented as mean±SEM, *p<0.05; n.s: not significant.

Leukocyte Rolling and Adhesion *In Vivo*

In the vascular function assays, we found that the 3-week Western diet mouse group had a significant phenotype in the endothelium-dependent vascular response, thus we want to assess whether there is a difference in *in vivo* leukocyte rolling and adhesion to the endothelium between $ApoE^{-/-}$ mice and $IL\text{-}17^{-/-}ApoE^{-/-}$ mice that are on a 3-week Western diet. To visualize *in vivo* leukocyte rolling and adhesion to the endothelium, we used intravital microscopy to look at vessels of the cremaster muscle. We were not able to detect any leukocyte rolling or adhesion in the arterioles of the cremaster muscle due to the rapid movement of cells within these vessels. In the venules, we were able to assess leukocyte rolling and adhesion on the endothelium. There was no difference in the detected total numbers of leukocyte rolling on the endothelium of the cremaster muscle venules between $ApoE^{-/-}$ mice and $IL\text{-}17^{-/-}ApoE^{-/-}$ mice (Figure 22B). However, we did find that there was an increase in the numbers of leukocytes adhered to the endothelium of the $ApoE^{-/-}$ mice compared to that of $IL\text{-}17^{-/-}ApoE^{-/-}$ mice and this increase in leukocyte adhesion was statistically significant (Figure 22C).

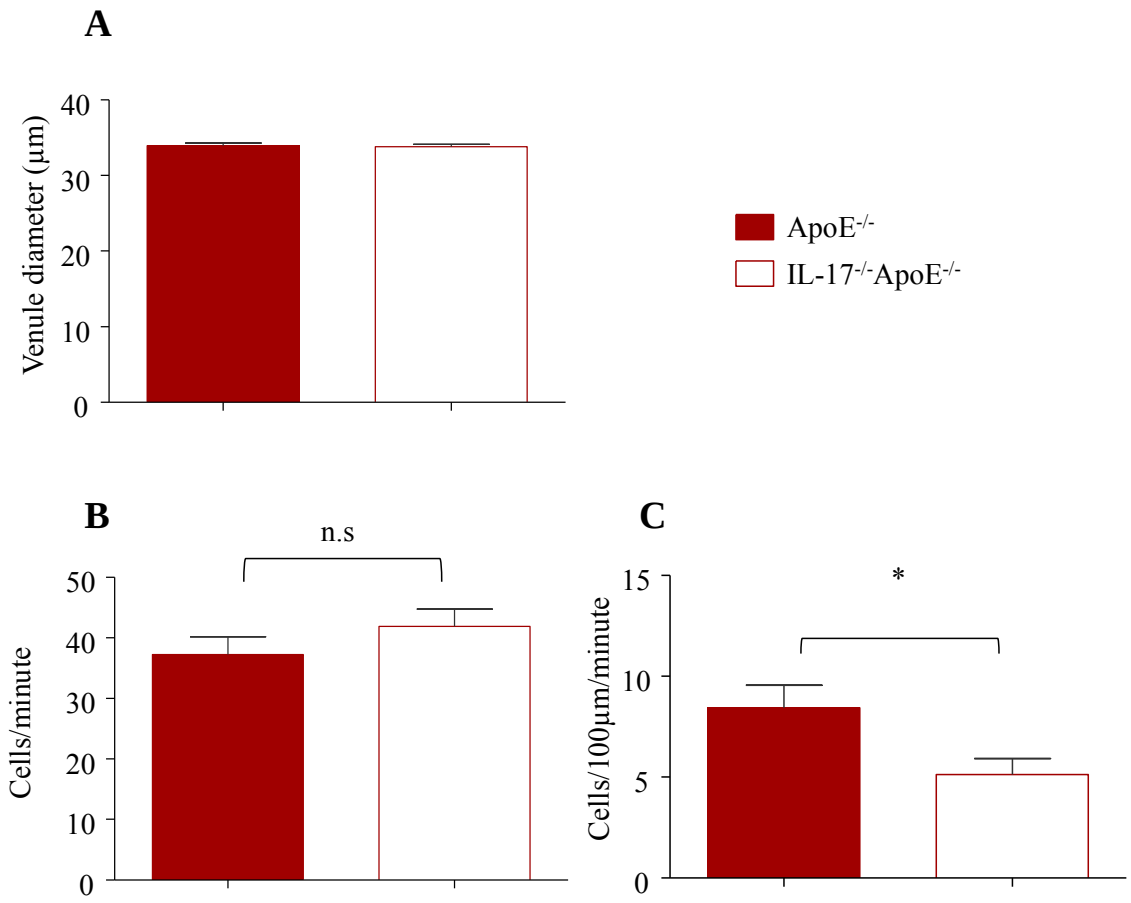

Figure 22. Intravital microscopy of *in vivo* leukocyte rolling and adhesion

***In vivo* leukocyte rolling on and adhesion to mouse cremaster endothelium was determined by intravital microscopy. A.** Mean vessel diameter of venules used in study. **B.** Number of cells that rolled pass an imaginary line that was perpendicular to the vessels during a 1 minute period observed. **C.** Number of cells adhered to the endothelium for 1 minute, 100um length observed. Data presented as mean±SEM (n=7-8, five vessels per mouse were recorded), *p<0.05; n.s: not significant.

Peripheral Blood and Aortic Single Cell Suspension

Monocyte transendothelial migration and subsequent differentiation into macrophage are key events that lead to foam cell formation and atherogenesis. We want to see whether there is a change in the number of mononuclear cells and monocytes that are in the circulation when the IL-17 gene is knock-out in $ApoE^{-/-}$ mice. Additionally, we want to determine whether there are less monocyte infiltrated and macrophage located in the aortas of $IL\text{-}17^{-/-}ApoE^{-/-}$ mice when compared to those of $ApoE^{-/-}$ mice. To realize these issues, we used cellular staining and flow cytometry of single cell preparation from the peripheral blood and the aortas of $IL\text{-}17^{-/-}ApoE^{-/-}$ mice and $ApoE^{-/-}$ mice that were fed a Western diet for 3 weeks.

Based on the measurements of the side-scattered (SSC) and forward-scattered (FSC) which correlate with cell granularity and size, respectively, we gated on the mononuclear cell (MNC) population of the peripheral blood (Figure 23A). In the MNC population, we used the cell marker CD11b to identify monocytes (Figure 23B). Furthermore, we used the Ly6C marker to characterize the different subsets of the monocytes within the MNC population in the peripheral blood (Figure 23C). There was no difference in the number of MNCs in the peripheral blood of $IL\text{-}17^{-/-}ApoE^{-/-}$ mice and $ApoE^{-/-}$ mice fed a Western diet for 3 week (Figure 23D). There was statistically higher numbers of $CD11b^{+}$ monocytes in $IL\text{-}17^{-/-}ApoE^{-/-}$ mice (Figure 23E); however, when we further characterize the $CD11b^{+}$ monocyte population into subsets, we did not find any difference in the subsets of monocytes within the two mouse groups (Figure 23F).

An enzyme cocktail was used to prepare a single cell suspension of the whole aorta for staining of monocytes and macrophages. Enzymatic digestion of the aorta induces cell death, and dead cells may non-specifically bind to FACS antibodies thus we first used a cell viability dye to stain the aortic single cell suspension. We then stained the aorta cells with CD11b, Ly6C, and F4/80 markers. After gating out the dead cells (Figure 24B), we defined monocytes as $CD11b^{+}Ly6C^{+}$ cells and macrophages as $CD11b^{+}F4/80^{+}$ cells (Figure 24C&D). The percentages of monocytes and macrophages tend to be lower in the $IL\text{-}17^{-/-}ApoE^{-/-}$ mouse group than in the $ApoE^{-/-}$ mouse group, however, there was no statistical significance (Figure 24E&F).

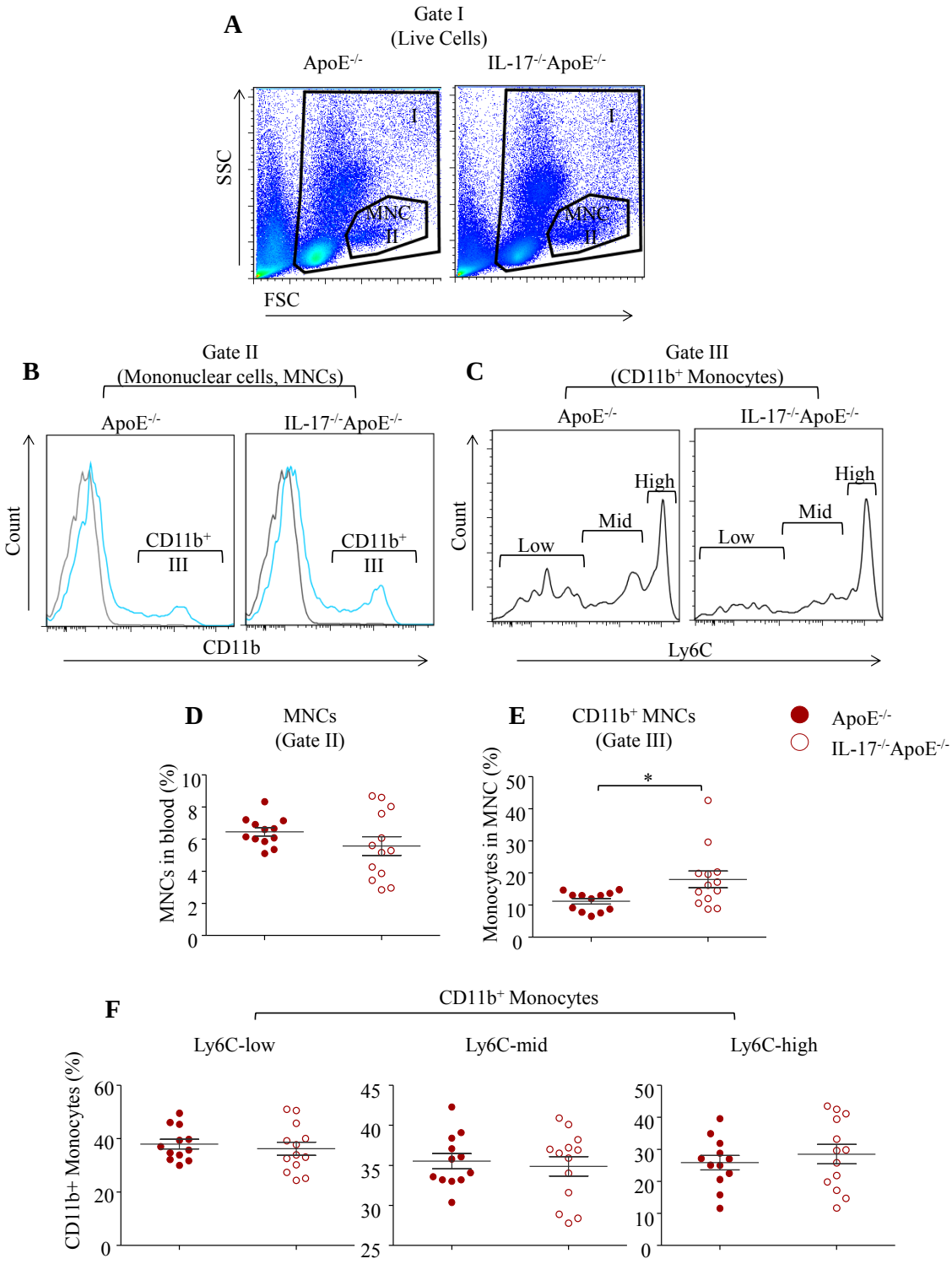

Figure 23. Peripheral blood MNC and monocyte identification

Peripheral blood mononuclear cells and monocytes were assessed by FACS. A. MNCs were gated from within the live cells of the FSC and SSC plot (Gate I). **B**. $CD11b^{+}$ monocytes were selected from the MNC population (Gate II). **C.** Characterization of monocyte subsets from the $CD11b^{+}$ monocyte population (Gate III). **D.** Quantification of MNC percentage in $ApoE^{-/-}$ mice and $IL\text{-}17^{-/-}ApoE^{-/-}$ mice. **E.** Quantification of $CD11b^{+}$ monocyte percentage. **F.** Quantification of monocyte subset percentages. Data presented as mean±SEM (n=12-13), *$p<0.05$.

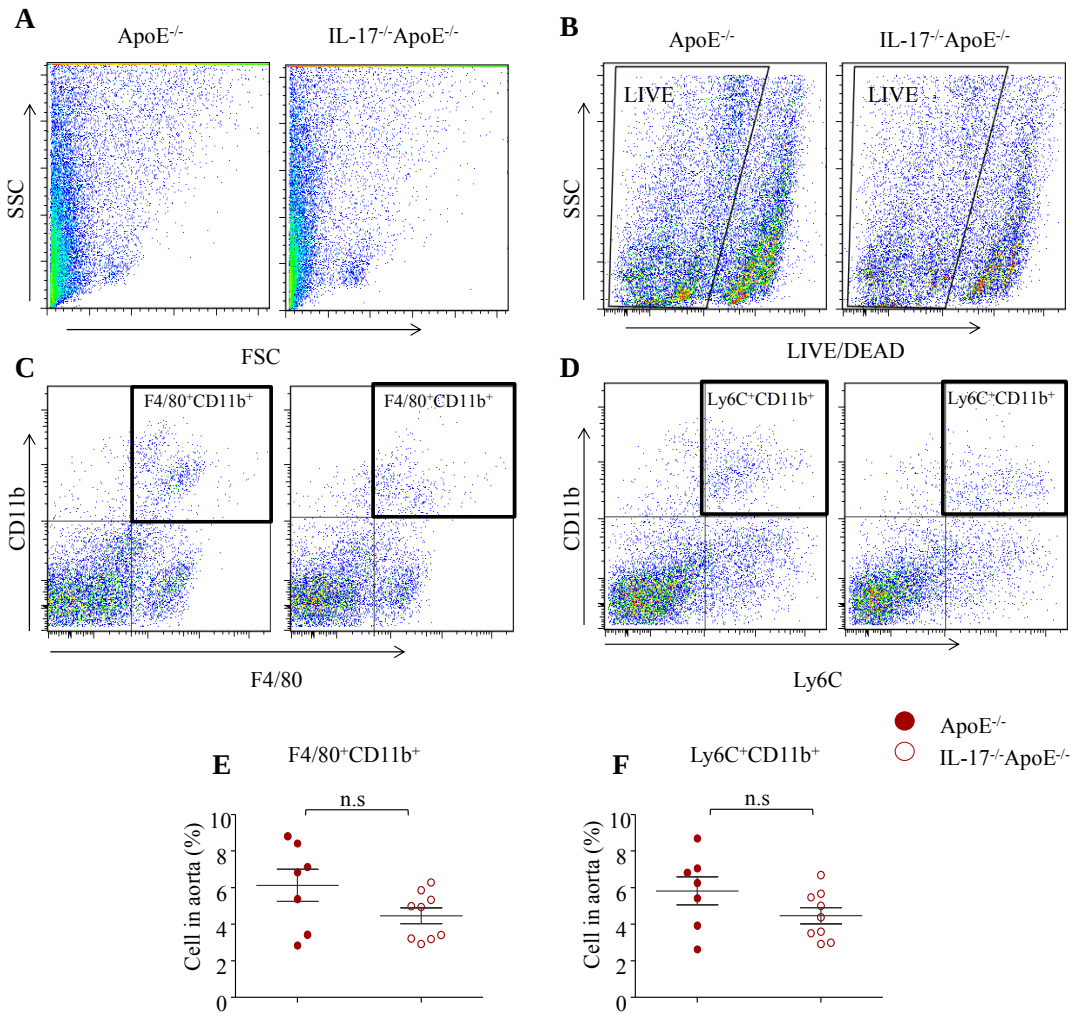

Figure 24. Monocyte and macrophage populations of aortic tissues

Aortic tissue monocyte and macrophage populations were determined by FACS. A. Representative FSC and SSC plots of cells within the aortas of ApoE$^{-/-}$ mice and IL-17$^{-/-}$ ApoE$^{-/-}$ mice. **B.** Selection of live cells. **C.** Identification of CD11b^{+}F4/80^{+} macrophages. **D.** Identification of CD11b^{+}Ly6C^{+} monocytes. **E.** Quantification of CD11b^{+}F4/80^{+} macrophages. **F.** Quantification of CD11b^{+}Ly6C^{+} monocytes. Data presented as mean±SEM (n=7-9).

Atherosclerotic Lesion Quantification

We used two approaches to quantify atherosclerotic lesion in our mice; we stained the lipids in the whole aorta with Sudan IV and aortic sinus sections with Oil red O. The atherosclerotic plaque formation was evaluated in 3-week and 6-week Western diet fed $ApoE^{-/-}$ mice and $IL\text{-}17^{-/-}ApoE^{-/-}$ mice as well as in their respective regular chow diet littermates.

IL-17 Deficiency Does Not Affect Atherosclerotic Plaque Buildup in the Whole Aorta

A Western diet significantly increased the percentages of atherosclerotic lesion found in $ApoE^{-/-}$ mice and $IL\text{-}17^{-/-}ApoE^{-/-}$ mice when compared to mice of the same age and genotype on a regular chow diet. Of both the 3-week and 6-week feeding groups, there was a trend of a smaller lesion area percentage in the $IL\text{-}17^{-/-}ApoE^{-/-}$ mouse group than in the $ApoE^{-/-}$ mouse group when the mice were maintained on a regular diet, but there was no statistical significance in this trend (Figure 25). After feeding with a Western diet, there was a tendency in the $IL\text{-}17^{-/-}ApoE^{-/-}$ mouse group to have a slight higher percentage of lesion area, but this trend was not significant when compared to the $ApoE^{-/-}$ mouse group.

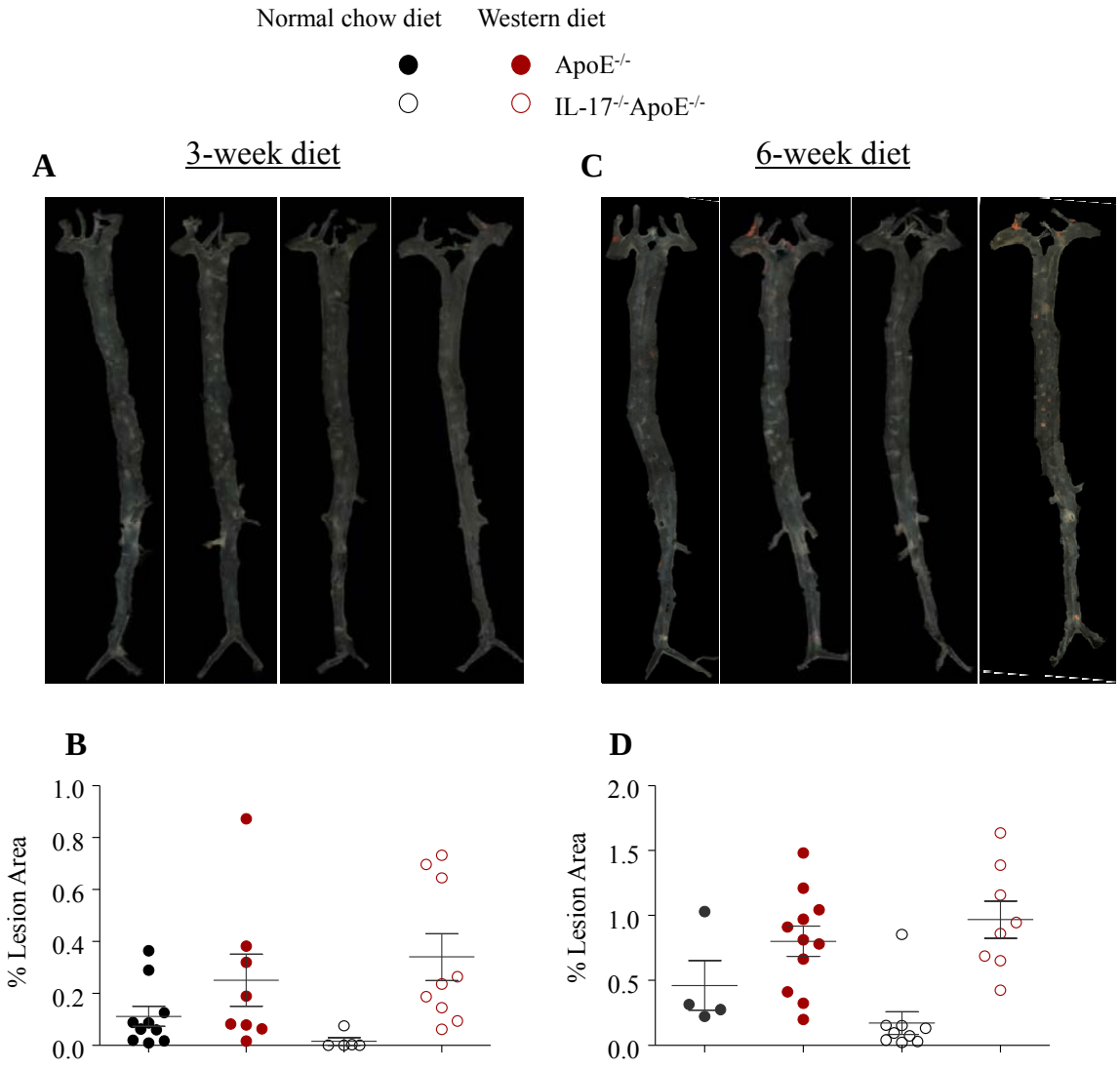

Figure 25. ***En face*** **staining of atherosclerotic lesions in the whole aorta**

Atherosclerotic plaque formation in the whole aorta was assessed with Sudan IV staining. A. Representative images of 3-week diet mouse group aortas stained with Sudan IV. **B.** Quantification of atherosclerotic area percentage in the whole aorta of 3-week diet mouse group. **C.** Representative images of 6-week diet mouse group aortas stained with Sudan IV. **D.** Quantification of atherosclerotic area percentage in the whole aorta of 6-week diet mouse group. Data presented as mean±SEM (n=4-11).

IL-17 Deficiency Does Not Affect Atherosclerotic Lesion Formation in the Aortic Sinus

In agreement with results found in the *en face* staining, a Western diet significantly increased the percentage of atherosclerotic lesion in the aortic sinus of our mice when compared to their normal chow controls. In the 3-week diet group, the percentages of lesion were similar in the $ApoE^{-/-}$ mouse group and $IL\text{-}17^{-/-}ApoE^{-/-}$ mouse group that were on a normal diet; however, when the mice were put on a Western diet, there was a slight increase, although not significant, in lesion formation in $IL\text{-}17^{-/-}ApoE^{-/-}$ mice when compared to the $ApoE^{-/-}$ mouse group. In the 6-week diet group, the percentages of lesion were similar in $ApoE^{-/-}$ mice and $IL\text{-}17^{-/-}ApoE^{-/-}$ mice when compared in their respective diet groups (Figure 26).

Overall, the two methods used to quantify atherosclerotic plaques in the mice yielded similar results; there was no statistical difference in atherosclerosis development between the two mouse groups either on a regular chow or a Western diet for 3 weeks or 6 weeks.

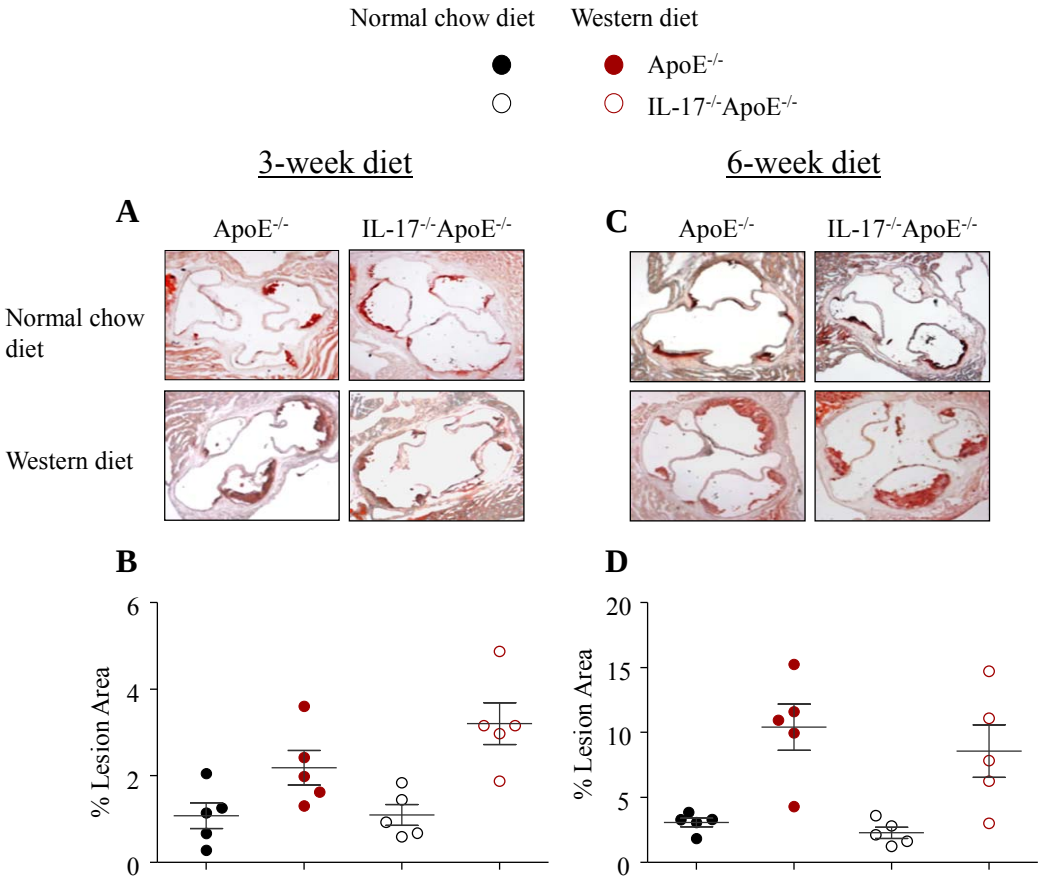

Figure 26. Oil red O staining of atherosclerotic plaques in the aortic sinus

Atherosclerotic plaque in aortic sinus was determined by Oil red O staining of aortic cross sections. A. Representative images of 3-week diet mouse group aortic sinus cross sections stained with Oil red O. **B.** Quantification of atherosclerotic area percentage in the aortic sinus of 3-week diet mouse group. **C.** Representative images of 6-week diet mouse group aortic sinus cross sections stained with Oil red O. **D.** Quantification of atherosclerotic area percentage in the aortic sinus of 6-week diet mouse group. Data presented as mean±SEM (n=5).

Lipid Profile

We analyzed the concentrations of HDL, LDL, triglyceride, non-esterified fatty acid, and total cholesterol in the plasma of our mice. The lipid profiles of ApoE$^{-/-}$ mice and IL-17$^{-/-}$ApoE$^{-/-}$ mice either on a 3-week or 6-week diet were analyzed at the MMPC in Yale University.

A 3-week Western Diet Induces Changes in the Total Cholesterol, LDL, and HDL Levels

ApoE$^{-/-}$ mice and IL-17$^{-/-}$ApoE$^{-/-}$ mice that were on a 3-week Western diet did not display changes in their triglyceride and non-esterified free fatty acid levels when compared to each other as well as to their respective normal diet controls (Figure 27C&D). The total cholesterol levels in ApoE$^{-/-}$ mice and IL-17$^{-/-}$ApoE$^{-/-}$ mice were dramatically increased by a 3-week Western diet when compared to their respective regular chow counterparts (Figure 27E). Similarly, the change in total cholesterol levels correlates with the change in the LDL levels in the mice; a Western diet significantly increased the LDL levels in mice when compared to their normal diet controls (Figure 27A). Moreover, we found that in the normal diet groups, the LDL levels in ApoE$^{-/-}$ mice were significantly higher than that in IL-17$^{-/-}$ApoE$^{-/-}$ mice (37.86± 1.58 mg/dL vs. 26.33±2.93 mg/dL). In addition, a Western diet significantly decreased the levels of HDL in IL-17$^{-/-}$ApoE$^{-/-}$ mice when compared to their normal chow controls (9.89±1.48 mg/dL vs 21.71±1.38 mg/dL). The decrease in the HDL levels in IL-17$^{-/-}$ApoE$^{-/-}$ mice was also statistically different from that in ApoE$^{-/-}$ mice that were fed the same diet (9.89±1.48 mg/dL vs. 18.82±1.67 mg/dL) (Figure 27B).

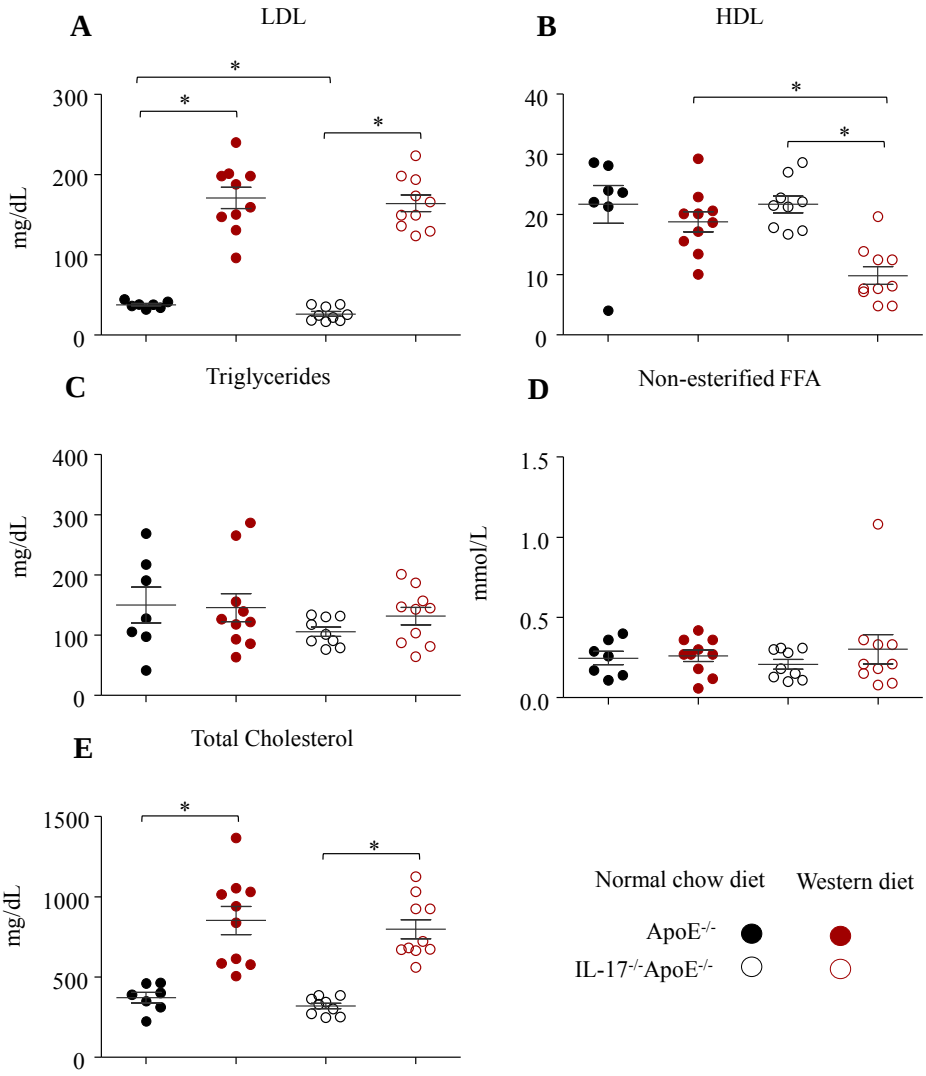

Figure 27. Lipid profiles of mice on a 3-week diet

The plasma lipid profiles of mice that were fed a 3-week diet. A. LDL levels. **B.** HDL levels. **C.** Triglyceride levels. **D.** Non-esterified free fatty acid (FFA) levels. **E.** Total cholesterol levels. Data presented as mean±SEM (n=7-10), *p<0.05.

A 6-week Western Diet Induces Changes in the Total Cholesterol, LDL, Triglyceride, and Non-esterified Free Fatty Acid Levels

After a Western diet for 6 weeks, there were dramatically elevations in the total cholesterol, LDL, triglyceride, and non-esterified free fatty acid levels in $ApoE^{-/-}$ mice and $IL\text{-}17^{-/-}ApoE^{-/-}$ mice when compared to their respective normal chow controls (Figure 28 A, C, D, & E). In mice that were fed a normal chow diet, the difference between the two genotypes in LDL levels seen in the 3-week diet group was no longer detected in the 6-week group (Figure 27A & Figure 28A). Moreover, the discrepancy in HDL levels found in the 3-week diet groups was resolved in the 6-week diet group (Figure 27B & Figure 28B). The HDL levels in $IL\text{-}17^{-/-}ApoE^{-/-}$ mice after a 6-week Western diet were similar compared to their normal chow control as well as to $ApoE^{-/-}$ mice that were on the same Western diet. Overall, the HDL levels were similar in all the mice of the 6-week diet group regardless of the genotype or the dietary manipulation (Figure 28B).

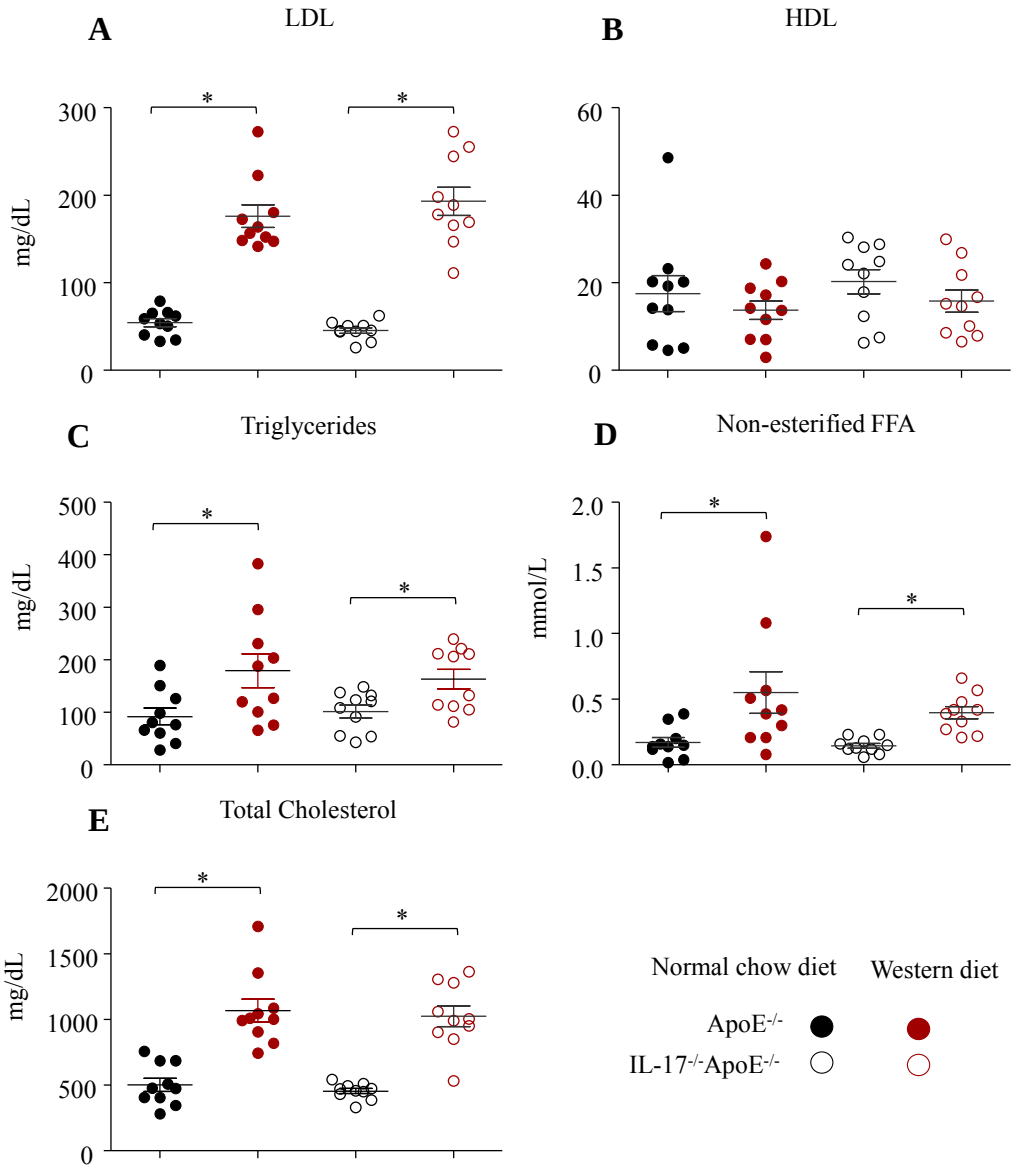

Figure 28. Lipid profiles of mice on a 6-week diet

The plasma lipid profiles of mice that were fed a 6-week diet. A. LDL levels. **B.** HDL levels. **C.** Triglyceride levels. **D.** Non-esterified free fatty acid (FFA) levels. **E.** Total cholesterol levels. Data presented as mean±SEM (n=10), $p<0.05$.

Microarray

Altered gene expression levels may contribute to phenotypes in our mouse studies. To investigate which molecular pathways may affect the outcomes of our *in vivo* and *ex vivo* studies, we performed microarray analysis of aortic tissues to identify differentially expressed genes in $ApoE^{-/-}$ mice and $IL\text{-}17^{-/-}ApoE^{-/-}$ mice that were fed a Western diet for 3 weeks. The Affymetrix Genechip Mouse Gene 2.0ST Arrays covers 35,240 RefSeq transcripts found in The Reference Sequence (RefSeq) database of the National Center for Biotechnology Information. The microarray data was analyzed by using the Limma package and the R environment for statistical computing.

Systemic deficiency of IL-17 has a widespread effect on gene expressions. There were a lot of transcripts which were modified by IL-17 knock-out in the $ApoE^{-/-}$ mouse (Figure 29). We analyzed our array data with the focus on genes that may be associated with our *in vitro* and *in vivo* phenotypes to further clarify the role of IL-17 on EC activation and vascular function. We first analyzed whether IL-17 signaling molecule transcripts are changed in $IL\text{-}17^{-/-}ApoE^{-/-}$ mice. Our array analysis showed that IL-17ra transcript was significantly decreased in $IL\text{-}17^{-/-}ApoE^{-/-}$ mice while transcripts for adaptor molecules, including Traf3ip2, Traf2, Traf5, and Traf6, of the IL-17 receptor signaling cascade were not affected (Figure 30). Next, we analyzed the transcript expressions of EC-associated adhesion molecules and found that a number of adhesion molecule transcripts were significantly lower in $IL\text{-}17^{-/-}ApoE^{-/-}$ mice than in $ApoE^{-/-}$ mice. The adhesion molecule transcripts that were significantly down-regulated in IL-17-deficient

ApoE$^{-/-}$ mice were Esam, Icam1, Icam2, Pecam1, Jam2, Itgal, and F11r. Itgb3and Itga5 were up-regulated with significance in IL-17$^{-/-}$ApoE$^{-/-}$ mice (Figure 31). Additionally, we focused on several genes which are associated with vascular function and found that Agtr1a, Nos3, Ednra, and Npr1 were transcripts with significant changes in ApoE$^{-/-}$ mice that were deficient of IL-17 (Figure 32). Since P38 MAPK may contribute to improved vessel function in IL-17$^{-/-}$ApoE$^{-/-}$ mice, we analyzed the transcripts of kinases that are involved in the P38 MAPK pathway. We found that a few kinases in this pathway were significantly changed by IL-17 deficiency. The kinases included Map3k1, Map3k11, Mapk11, Mapk12, Rps6ka4, Mknk1, and Mknk2, and all of them were down-regulated in IL-17$^{-/-}$ApoE$^{-/-}$ mice when compared to ApoE$^{-/-}$ mice (Figure 33). In addition, we found that several genes involved in lipoprotein signaling and cholesterol metabolism were significantly changed in IL-17$^{-/-}$ApoE$^{-/-}$ mice when compared to ApoE$^{-/-}$ mice (Figure 34).

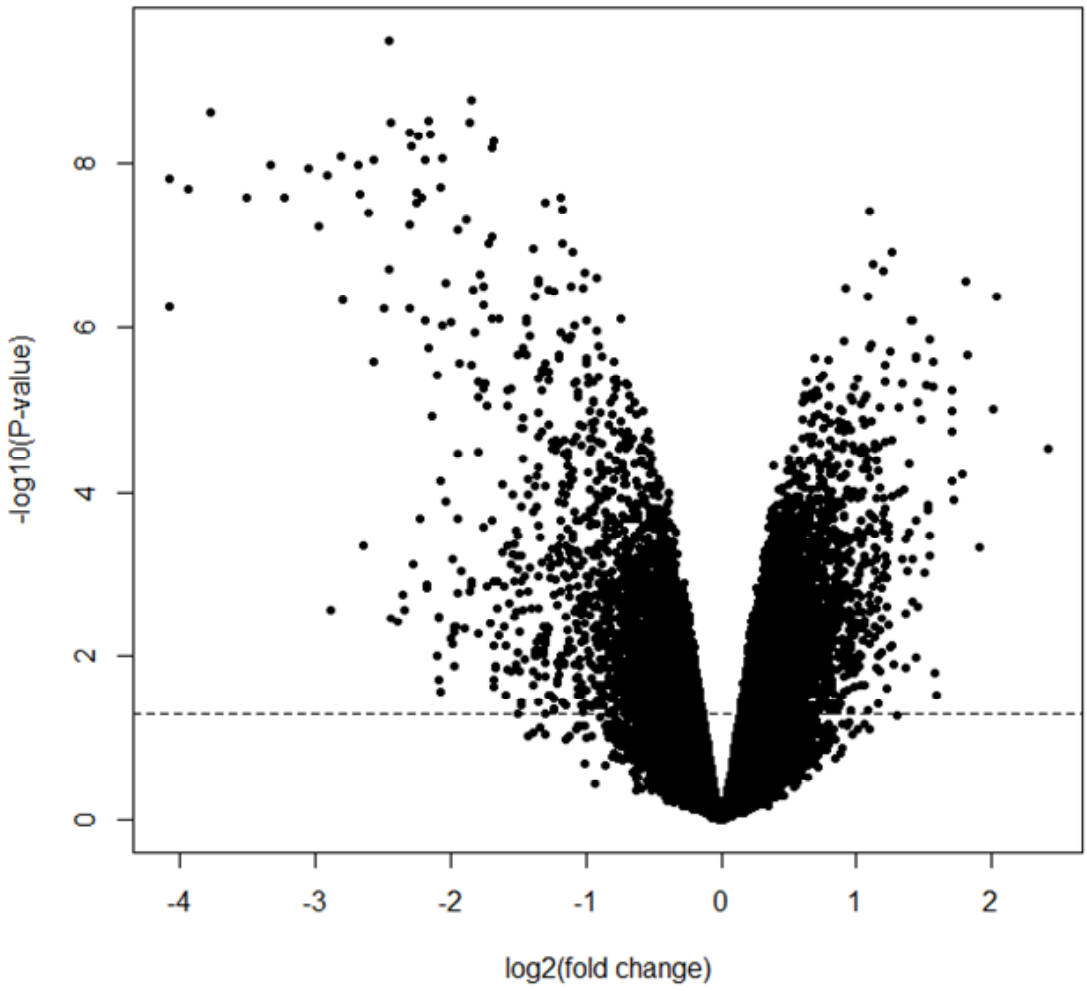

Figure 29. Scatter plot of all transcript changes determined by microarray

Scatter plot of fold change versus P value for all tanscripts determined by the The Affymetrix Genechip Mouse Gene 2.0ST Arrays. Scatter plots shows there are numerous genes that were modified with statistical significance in IL-17$^{-/-}$ApoE$^{-/-}$ mice when compared to ApoE$^{-/-}$ mice.

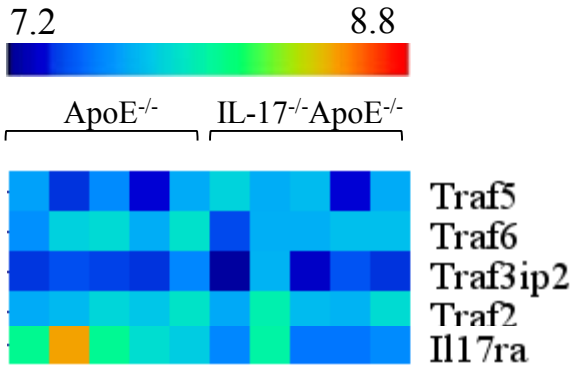

Gene	Fold Change	P Value
Il17ra	0.754	0.016
Traf3ip2	0.989	0.872
Traf2	1.005	0.937
Traf5	1.091	0.276
Traf6	0.928	0.257

Figure 30. Heat map and fold changes of IL-17 receptor signaling genes

IL-17 receptor signaling gene expression determined by microarray. Heat map representation of microarray data showing the expressions of IL-17 receptor signaling genes in the aorta tissues of ApoE$^{-/-}$ mice and IL-17$^{-/-}$ApoE$^{-/-}$ mice that were fed a Western diet for 3 weeks. Fold changes of genes are shown as expressions in IL-17$^{-/-}$ ApoE$^{-/-}$ mice compared to expressions in ApoE$^{-/-}$ mice.

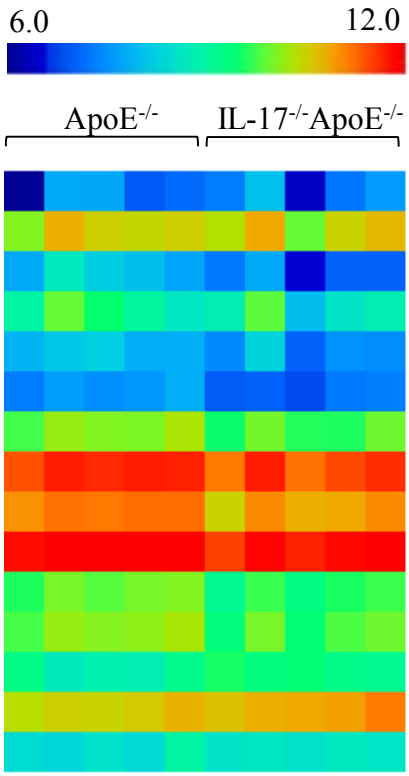

Gene	Fold Change	P Value
Sele	1.138	0.622
Selp	0.999	0.995
Esam	0.772	0.029
Icam1	0.753	0.012
Icam2	0.720	0.003
Pecam1	0.861	0.048
Jam2	0.794	0.013
Jam3	1.048	0.564
Itgal	0.513	0.002
Itgam	0.739	0.055
Itgb2	0.761	0.254
Itgb3	1.281	0.013
Itga5	1.254	0.010
F11r	0.792	0.027
Cdh5	0.870	0.119

Figure 31. Heat map and fold changes of endothelial adhesion molecule genes

Endothelial adhesion molecule gene expression determined by microarray. Heat map representation of microarray data showing the expressions of endothelial adhesion molecule genes in the aorta tissues of ApoE$^{-/-}$ mice and IL-17$^{-/-}$ApoE$^{-/-}$ mice that were fed a Western diet for 3 weeks. Fold changes of genes are shown as expressions in IL-17$^{-/-}$ApoE$^{-/-}$ mice compared to expressions in ApoE$^{-/-}$ mice.

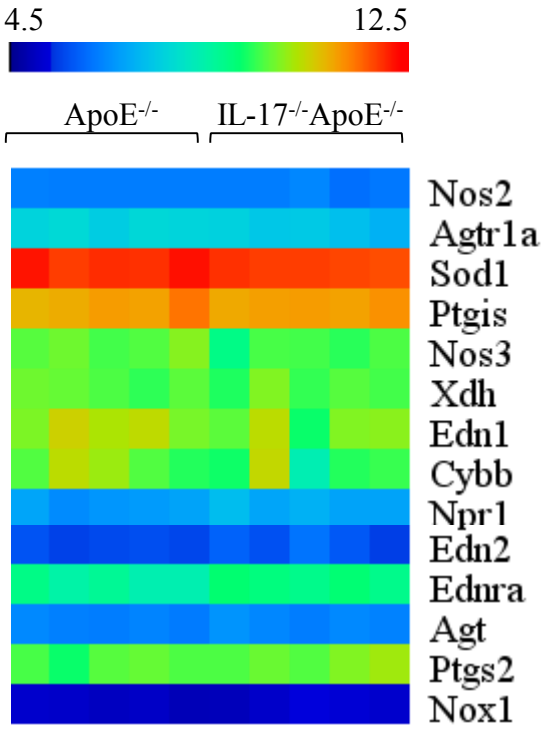

Gene	Fold Change	P Value
Agt	1.052	0.371
Agtr1a	0.807	0.017
Nos2	0.980	0.697
Nos3	0.788	0.037
Ptgis	1.001	0.989
Ptgs2	1.206	0.074
Ednra	1.335	0.006
Edn1	0.777	0.116
Edn2	1.134	0.138
Npr1	1.237	0.006
Cybb	0.725	0.203
Xdh	0.955	0.604
Nox1	1.071	0.264
Sod1	0.877	0.050

Figure 32. Heat map and fold changes of vascular function genes

Expression of vascular function related genes determined by microarray. Heat map representation of microarray data showing the expressions of vascular function related genes in the aorta tissues of ApoE$^{-/-}$ mice and IL-17$^{-/-}$ApoE$^{-/-}$ mice that were fed a Western diet for 3 weeks. Fold changes of genes are shown as expressions in IL-17$^{-/-}$ ApoE$^{-/-}$ mice compared to expressions in ApoE$^{-/-}$ mice.

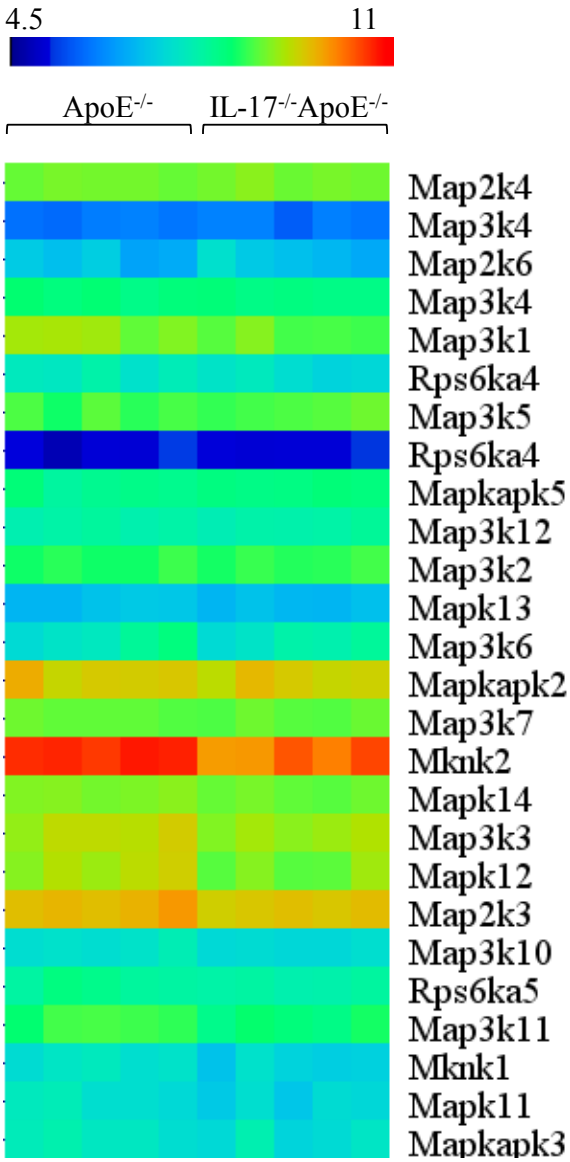

Gene	Fold Change	P Value
Map3k12	1.003	0.957
Map3k1	0.799	0.011
Map3k2	1.049	0.388
Map3k3	0.869	0.060
Map3k4	0.951	0.332
Map3k10	0.891	0.072
Map3k11	0.792	0.006
Map3k5	1.065	0.365
Map3k6	0.968	0.816
Map3k7	0.988	0.800
Map2k3	0.891	0.056
Map2k6	1.080	0.517
Map2k4	1.030	0.529
Mapk11	0.823	0.032
Mapk12	0.781	0.011
Mapk13	0.950	0.401
Mapk14	0.906	0.055
Mapkapk3	0.887	0.174
Mapkapk5	1.088	0.167
Mapkapk2	0.950	0.451
Rps6ka5	0.885	0.062
Rps6ka4	0.839	0.035
Mknk1	0.809	0.010
Mknk2	0.699	0.001

Figure 33. Heat map and fold changes of P38 MAPK pathway genes

Expression of P38 MAPK pathway genes determined by microarray. Heat map representation of microarray data showing the expressions of P38 MAPK pathway genes in the aorta tissues of ApoE$^{-/-}$ mice and IL-17$^{-/-}$ApoE$^{-/-}$ mice that were fed a Western diet for 3 weeks. Fold changes of genes are shown as expressions in IL-17$^{-/-}$ApoE$^{-/-}$ mice compared to expressions in ApoE$^{-/-}$ mice.

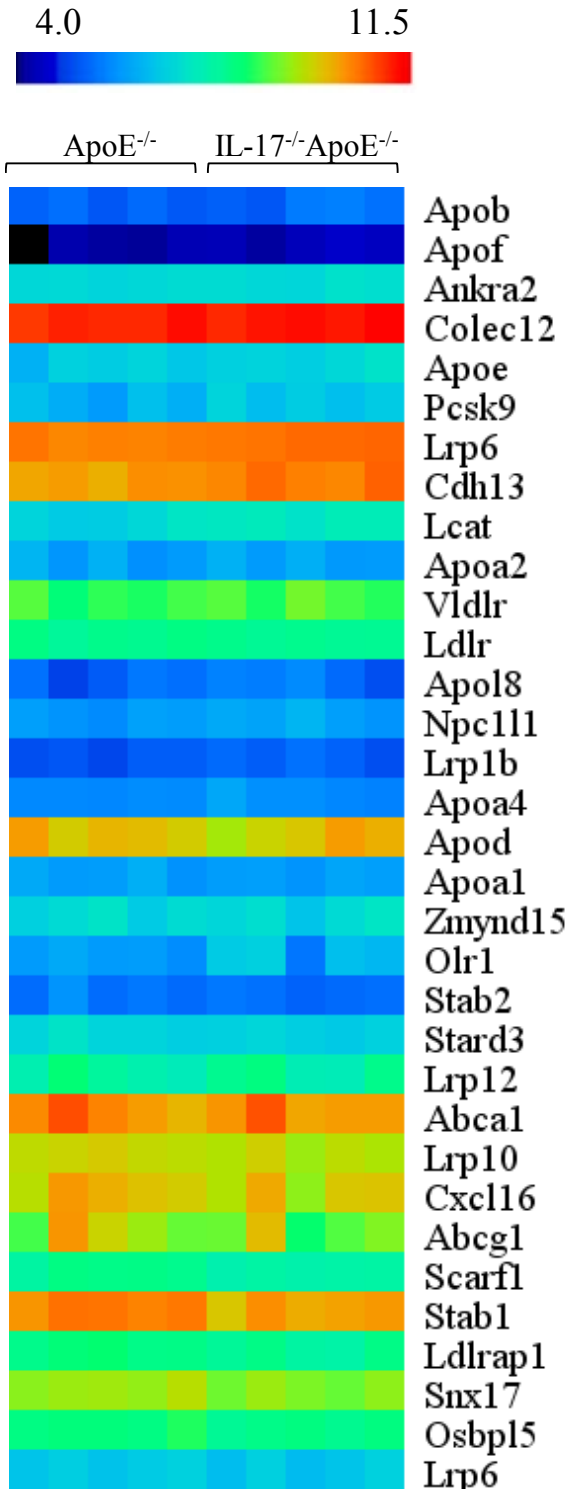

Gene	Fold Change	P Value
Cxcl16	0.873	0.301
Ldlr	0.964	0.492
Lrp10	0.901	0.130
Lrp12	1.052	0.688
Lrp1b	1.113	0.123
Lrp6	0.959	0.556
Olr1	1.314	0.091
Stab1	0.785	0.008
Stab2	0.930	0.353
Vldlr	1.098	0.335
Zmynd15	1.015	0.874
Ldlrap1	0.843	0.035
Pcsk9	1.275	0.017
Snx17	0.873	0.065
Ankra2	1.047	0.364
Apoa4	1.064	0.364
Cdh13	1.234	0.007
Colec12	1.083	0.195
Scarf1	0.801	0.003
Apoa1	0.975	0.695
Apod	0.922	0.478
Apof	1.162	0.042
Apol8	1.135	0.282
Abca1	0.973	0.820
Abcg1	0.794	0.325
Apoe	1.178	0.085
Stard3	0.917	0.200
Apoa2	1.009	0.920
Lcat	1.357	0.002
Apob	1.091	0.286
Npc1l1	1.112	0.153
Osbpl5	0.875	0.060

Figure 34. Heat map and fold changes of lipid metabolism genes

Lipoprotein signaling and cholesterol metabolism gene expressions determined by microarray. Heat map representation of microarray data showing the expressions of lipid metabolism genes in the aorta tissues of $ApoE^{-/-}$ mice and $IL\text{-}17^{-/-}ApoE^{-/-}$ mice that were fed a Western diet for 3 weeks. Fold changes of genes are shown as expressions in $IL\text{-}17^{-/-}ApoE^{-/-}$ mice compared to expressions in $ApoE^{-/-}$ mice.

CHAPTER 4

DISCUSSION

CVDs are the leading cause of mortality globally; it accounts for 30% of all deaths. Heart disease and stroke are the main cause of death of those who died from CVDs. Heart attack and stroke are usually due to an obstruction that stops blood from flowing to the heart or brain, and the most common reason for blockage of blood flow is atherosclerosis. Atherosclerosis is a disease in which fatty plaques build up in the arteries leading to the narrowing and hardening of the blood vessels. Atherosclerosis is not solely a disease that involves lipids; it is well-established that it is a chronic inflammatory disease that involves various risk factors such as pro-inflammatory cytokines. There are many cell types that are involved in the progression of the disease, including cells of the innate and adaptive immune systems.

As cells that line the inner surface of blood vessels, ECs are the first to be exposed to various pro-inflammatory factors in the blood. Exposure to pro-inflammatory stimuli can lead to EC activation. Activation of ECs from a quiescent state to one that is involved in immune responses is associated with the initiation of atherosclerosis. In this current study, we investigate the role of IL-17, a pro-inflammatory cytokine, in EC activation and atherosclerosis. In our study we utilized cell culture of mouse aortic ECs and human primary aortic ECs for *in vitro* studies of IL-17's effects on EC biology. In addition, we used IL-17-deficient mice on an ApoE background to determine the role of IL-17 in vascular function and early atherosclerosis development *in vivo*.

Primary Cell Culture

In the *in vitro* studies, we used ECs that are of aortic origin from mouse and human. ECs are routinely used in our laboratory (Jiang et al., 2005). MAECs isolated and cultured are used during the first passage thus we avoided any potential phenotype changes that may occur with prolonged culture. Moreover, we also routinely perform quality control of our MAEC culture with CD31 staining and labeled LDL uptake assay. These two methods ensure that our isolated MAEC are endothelial specific and that the ECs maintain their function after being cultured *in vitro*. For ECs of human origin, we used commercially available HAECs. These primary cells have been extensively used in *in vitro* studies by others as well as our lab. For our studies, we used cells that are passage 9, which have been shown to have the same morphology and functions as earlier passages. Thus, cells that we used in our *in vitro* studies are pathophysiological relevant as our primary cells in culture retain their *in vivo* phenotype and morphology.

Up-regulation of IL-17 in Hyperlipidemia

IL-17 is a pro-inflammatory cytokine that serves a host-defensive role in numerous infectious diseases. More importantly, IL-17 is up-regulated in various autoimmune conditions and has been shown to play a central role in these autoimmune diseases, including EAE, psoriasis, rheumatoid arthritis, and inflammatory bowel disease. Hypercholesterolemia, a form of hyperlipidemia, is a well-established risk factor for atherosclerosis. Thus, we determined if IL-17 is up-regulated during hyperlipidemia. First, we found that the plasma concentrations of IL-17 in hyperlipidemic $ApoE^{-/-}$ mice

were higher than in WT mice. Additionally, a Western diet which significantly enhances the total cholesterol levels in ApoE$^{-/-}$ mice dramatically increased the plasma IL-17 levels in ApoE$^{-/-}$ mice. Furthermore, we used FACS and determined that hyperlipidemia induced by a Western diet also increased the number of IL-17-producing cells, including Th17 cells which are the major producers of IL-17, in splenocytes that were isolated from WT mice and ApoE$^{-/-}$ mice.

ECs express IL-17 receptors thus can respond to IL-17 stimulation (Moseley, Haudenschild, Rose, & Reddi, 2003). To determine whether ECs are more responsive to IL-17 stimulation during hyperlipidemia, we used OxLDL, an *in vitro* model of hyperlipidemia, to treat ECs and see whether IL-17 receptor expressions are up-regulated. We treated isolated MAECs and determined that the mRNA transcript of IL-17ra was up-regulated with OxLDL treatment. Also, we used FACS and found that OxLDL stimulation of HAECs also increased the cell surface expressions of IL-17 receptors A and C. For our study in MAECs, we were interested in IL-17ra because it is the only receptor that has been shown to mediate IL-17 signaling in the mouse. In HAECs, IL-17 receptors A and C were of interest because these two receptors have been found to facilitate IL-17 signaling in humans (Kuestner et al., 2007).

Our results suggest that hyperlipidemia increases the amount of IL-17 in the circulation which can activate ECs and promote vascular inflammation and atherosclerosis. In the presence of hyperlipidemia, ECs also enhance the expression of IL-17 receptors to augment the responses to elevated IL-17 levels in circulation.

IL-17 Activates ECs

The results from the previous mentioned studies show that IL-17 signaling is enhanced during hyperlipidemia; elevated plasma IL-17 levels, increased number of IL-17-producing cells, and up-regulated expression of IL-17 receptors in ECs. To confirm that ECs are in fact the cells that respond to IL-17 stimulation, we carried out a set of *in vitro* assays to determine whether IL-17 activates ECs. EC activation is judged by adhesion molecule expression, cytokine and chemokine secretion, and leukocyte-endothelium interaction. Adhesion molecule E-selectin was found to be increased in HAECs treated with IL-17. Endothelial expression of E-selectin has been shown to be important in inflammation; it mediates the interaction with leukocytes (Ley, 2003). Also, we found that IL-17 up-regulated the expression of pro-inflammatory chemokines and cytokines, including CXCL1, CXCL2, IL-6, and GM-CSF in MAECs and HAECs. These four cytokines and chemokines have been implicated in atherosclerosis.

Chemokines play a critical role in directing leukocyte migration into injury sites and activating residential vascular cells (Schober, 2008). CXCL1 is up-regulated in atherosclerotic lesions and it also has been found to play a central role in macrophage accumulation (Boisvert et al., 2006), monocyte arrest on the endothelium (Huo et al., 2001), and lesion development (Boisvert et al., 2006). CXCL2 is also up-regulated in atherosclerotic aortic lesions in $ApoE^{-/-}$ mice (Lutgens et al., 2005). Moreover, CXCL1 and CXCL2 are significantly elevated in hypercholesterolemic mice (Murphy et al., 2002), and they are also listed as serum inflammatory markers for predicting

atherosclerosis (Tabibiazar, Wagner, Deng, Tsao, & Quertermous, 2006). Deficiency of IL-6 in the $ApoE^{-/-}$ mouse has been shown to reduce inflammatory cell recruitment to the atherosclerotic lesion (Galkina & Ley, 2009; Schieffer et al., 2004; Song & Schindler, 2004). Elevated IL-6 level is also one of the identified risk factors for human heart disease (Song & Schindler, 2004). IL-6 has been shown to have a critical role in monocyte recruitment during acute and chronic inflammations (Gabay, 2006; Kaplanski, Marin, Montero-Julian, Mantovani, & Farnarier, 2003). GM-CSF is an important factor for the production of monocytes as well as other cells important in immunity. GM-CSF expression is found in atherosclerotic lesions (Ditiatkovski, Toh, & Bobik, 2006). GM-CSF deficiency in $LDLR^{-/-}$ mice attenuated atherosclerosis (Shaposhnik, Wang, Weinstein, Bennett, & Lusis, 2007) but in $ApoE^{-/-}$ mice GM-CSF deficiency yielded different results (Ditiatkovski et al., 2006).

In addition, we found that IL-17-treated ECs had enhanced interaction with monocytes as seen in our monocyte-EC adhesion assay with monocytic THP-1 cell line and human primary monocytes. After treatment with IL-17, there was an increase in monocyte adhesion to activated ECs. More importantly, higher number of monocytes adhered to ECs was dependent on the four cytokines and chemokines, CXCL1, CXCL2, IL-6, and GM-CSF, up-regulated by IL-17. Neutralization of the four cytokines and chemokine with blocking antibodies attenuated the effect of IL-17 on enhancing monocyte adhesion to ECs. Our results show the functions of the pro-inflammatory cytokines and chemokines up-regulated by IL-17 in our *in vitro* study are in line with the previous published results by other groups. More importantly, we show that IL-17 treated

ECs have increased adhesion molecule, cytokine, and chemokine expressions, and enhanced monocyte interactions. Thus, IL-17 activates ECs, an important step to the initiation of atherosclerosis.

Mouse Models

For atherosclerosis study with mouse models, the limitation of extrapolating murine data to human studies includes difference in lipid profile, cholesterol metabolism, and plaque pathology. In humans, polymorphism, and sometimes rare occurrences of mutation and deficiency of ApoE are associated with Type III hyperlipoproteinemia which is an uncommon condition manifested with elevated concentrations of both plasma cholesterol and triglycerides (Plump & Breslow, 1995; Schaefer et al., 1986). In $ApoE^{-/-}$ mice, the marked increase of triglycerides are not detected. In addition, homozygous deficiency of the LDLR is rare in humans with one case out of a million people. However, LDLR deficiency in humans is detrimental; it leads to marked hypercholesterolemia which cause myocardial infarction in early childhood (Goldstein & Brown, 2009) whereas in mice, LDLR deficiency in the absence of a modified diet, atherosclerosis is not observed. More importantly, these mouse models are not helpful in the studies of plaque rupture and thrombotic occlusion due to the lack of these events in mice. Despite these shortcomings, experimental mouse models such as $ApoE^{-/-}$ mice and $LDLR^{-/-}$ mice are still very important in the study of the initiation and early progression of atherosclerosis.

For our study, we chose to use the ApoE$^{-/-}$ mouse, a model that has been used for over 20 years and studied extensively for the development of atherosclerosis (Meir & Leitersdorf, 2004). The ApoE$^{-/-}$ mouse has been bred with numerous specific gene knock-out mice to illuminate the roles of these various genes in atherosclerosis development. We also chose the ApoE$^{-/-}$ mouse for this model does not require a special diet to induce atherosclerosis as seen with the LDLR$^{-/-}$ mice. ApoE$^{-/-}$ mice also have dramatic elevation in total plasma cholesterol levels. More importantly, these mice are readily available through commercial laboratories and they are easily bred and maintained. In determining the role of our interested gene in atherosclerosis development, we cross bred IL-17$^{-/-}$ mice with ApoE$^{-/-}$ mice to obtain mice that were deficient of both IL-17 and ApoE genes.

Diet and Atherosclerosis

Although, ApoE$^{-/-}$ mice development spontaneous atherosclerosis in the absence of diet intervention, in our study, we fed mice with a special diet. For our study, we fed mice with a diet that has been modified to have 21% fat by weight, 0.15% cholesterol by weight, and 19.5% casein by weight without sodium cholate. This diet is commonly known in literatures as the "Western" Diet, which has been used extensively by others for atherosclerosis studies. Moreover, a Western diet in humans has been shown to increase the incidence of chronic illness and healthy issues such as CVDs (Cordain et al., 2005). We utilized a modified diet so we can enhance the baseline of our studies to amplify any phenotype that may be too subtle for measurement. And feeding our mice a Western diet

is extremely important in studying the impact of hyperlipidemia in vascular function and atherosclerosis development.

Endothelial Dysfunction in ApoE$^{-/-}$ Mice

The wire myograph is a technique used to assess the vascular functional responses and reactivity of isolated arteries *ex vivo*. This system is routinely used in our laboratory to assess the vascular function of the mesenteric arteries and aortas from mice (Cheng et al., 2011). Endothelial dysfunction in the ApoE$^{-/-}$ mouse was reviewed extensively (Meyrelles et al., 2011). Aortas of young and adult ApoE$^{-/-}$ mice on a regular chow diet were shown to have normal response to ACh. Young mice were defined as approximately 15 weeks old and adult mice were ones that are about 20-35 weeks of age. It was found that aged mice, which were defined as older than 50 weeks, on a normal chow diet were shown to have impaired endothelium-dependent and independent relaxations in response to agonists. When fed a Western diet, young ApoE$^{-/-}$ mice were found to have impaired endothelium-dependent relaxation in response to ACh but endothelium-independent relaxation to NO donor was preserved.

In our vessel function studies, we used young mice that were either 11 weeks or 14 weeks old. First, vascular function of 11-week old ApoE$^{-/-}$ mice and IL-17$^{-/-}$ApoE$^{-/-}$ mice that were on a normal chow diet were assessed. Endothelium- dependent and independent functions were preserved in these mice. This result confirms the findings of others and it shows that our wire myograph system and method are reliable. Moreover,

the result shows vascular function in the aorta of young ApoE$^{-/-}$ mice fed a regular chow diet are not affected by IL-17-deficiency.

Impaired vascular function was found in ApoE$^{-/-}$ mice that were fed a Western diet (Meyrelles et al., 2011), we then proceeded to see whether IL-17 deficiency rescues vascular function in ApoE$^{-/-}$ mice. After a 3-week Western diet, vascular function in IL-17$^{-/-}$ApoE$^{-/-}$ mice was similar to WT mice that were on a regular chow diet, whereas in ApoE$^{-/-}$ mice, endothelium-dependent relaxation to ACh was impaired. Our results confirm what was previous found by others. Moreover, our results also show that IL-17 deficiency rescues vascular function in Western diet fed young ApoE$^{-/-}$ mice. Furthermore, to investigate whether IL-17-deficient ApoE$^{-/-}$ mice that were fed a longer Western diet maintain normal vascular function, we fed mice with a 6-week Western diet. ApoE$^{-/-}$ mice and IL-17$^{-/-}$ApoE$^{-/-}$ mice that were fed a 6-week Western diet had impaired endothelium-dependent relaxation to ACh. Meanwhile, endothelium-independent relaxation to SNP was preserved in both mouse groups. The endothelium-dependent relaxation was more impaired in ApoE$^{-/-}$ mice than IL-17$^{-/-}$ApoE$^{-/-}$ mice when compared to WT mice, suggesting that IL-17's beneficial effect on vascular function was still present after a 6-week Western diet. Taken together, these results suggest that IL-17 deficiency in ApoE$^{-/-}$ mice delays the onset of vascular dysfunction induced by a Western diet.

To elucidate the possible molecular mechanisms that contribute to our vascular function phenotype, aortic proteins from ApoE$^{-/-}$ mice and IL-17$^{-/-}$ApoE mice fed a 3-

week Western diet were blotted for eNOS, MAPK P38, and JNK. NO is an important signaling molecule used by the endothelium to relax surrounding VSMCs, which leads to vasodilation. NO in the blood vessel is generated by eNOS. eNOS can be activated by phosphorylation at Ser1177 and dephosphorylation at Thr495 by multiple protein kinases and phosphatases (Forstermann & Munzel, 2006). JNK and P38 MAPK pathway are strongly linked with vascular inflammation (Zarubin & Han, 2005). More importantly, some of the inflammatory effects of IL-17 were found to be mediated via the P38 MAPK pathway (Roussel et al., 2010). There was no significant difference in eNOS phosphorylation or JNK phosphorylation between $ApoE^{-/-}$ mice and $IL\text{-}17^{-/-}ApoE^{-/-}$ mice; however, P38 phosphorylation was significantly decreased in $IL\text{-}17^{-/-}ApoE^{-/-}$ mice. This result suggests that the P38 MAPK pathway may contribute to the effects of IL-17 on vascular function in $ApoE^{-/-}$ mice. However, P38 MAPK is not only present in ECs; it is also found in other vascular cells. In an attempt to verify and specify the role of P38 on vascular function, we used a P38 MAPK inhibitor (SB203580) to see whether vascular dysfunction in $ApoE^{-/-}$ mice may be rescued. However, we were not able to carry out our vascular function assay with this inhibitor due to the fact that it completely blunted the effect of PE (data not shown). Since we could not induce vessel contraction with PE in the presence of SB203580, we were not able to test endothelium-dependent and independent relaxations to ACh and SNP, respectively. A different inhibitor that does not affect PE-induced contraction in the aortas is needed for future experiment to clarify the role of P38 in vascular function in $IL\text{-}17^{-/-}ApoE^{-/-}$ mice.

Monocyte-EC Interaction *In Vivo*

The result found in our *in vitro* experiment shows that IL-17 activates ECs and enhances monocyte adhesion to activated ECs. We followed these results with a set of experiment to determine whether there is less monocyte infiltration into the aorta and whether there is less leukocyte adhesion on the endothelium of the IL-17$^{-/-}$ApoE$^{-/-}$ mouse. We used FACS analysis and intravital microscopy to realize these issues.

In our FACS analysis of the mouse peripheral blood cells, there was a higher percentage of CD11b^{+} monocyte in IL-17$^{-/-}$ApoE$^{-/-}$ mice than in ApoE$^{-/-}$ mice that were fed a 3-week Western diet (Figure 23E), which suggest that there are more circulating monocytes in IL-17$^{-/-}$ApoE$^{-/-}$ mice. Monocytes in the circulation are an important component of the innate immune system; they are part of the mononuclear phagocyte system. Circulating monocytes can migrate out of the circulation and into tissues where they differentiate into macrophages and carry out phagocytic activities within these tissues. Increased circulating monocyte counts may be due to increased production in the bone marrow or decreased migration out of the circulation. A set of experiments are needed in order to determine whether monocyte production is increased in the bone marrow. However, we believe the increase in CD11b^{+} monocyte in the peripheral blood of IL-17$^{-/-}$ApoE$^{-/-}$ mice is due to decreased extravasation of monocyte out of the blood vessels. There was a trend, although not of statistical significance, of lower numbers of CD11b^{+}F4/80^{+} macrophages and CD11b^{+}Ly6C^{+} monocytes present in the aortic tissues from IL-17$^{-/-}$ApoE$^{-/-}$ mice (Figure 24E &F). These results suggest that there are less

monocyte infiltrations in the aorta of IL-17$^{-/-}$ApoE$^{-/-}$ mice thus fewer turnovers of monocytes into macrophages within the aorta. In addition, in our intravital microscopy study of leukocyte rolling and adhesion to the cremaster vascular, we found that there was less leukocyte adhesion to the endothelium of IL-17$^{-/-}$ApoE$^{-/-}$ mice (Figure 22). Previously, a study by Dr. Eriksson showed that venules in atherosclerosis serve as major entry ways for leukocytes to migrate into lesions (Eriksson, 2011) thus leukocyte rolling and adhesion in the microvasculature especially on the venules are important in atherogenesis. These results suggest that there is less vascular inflammation in IL-17$^{-/-}$ ApoE$^{-/-}$ mice which contributes to decreased leukocyte adhesion on the endothelium, decreased monocyte transmigrations into the aorta, and increased monocyte numbers in the peripheral blood of IL-17$^{-/-}$ApoE$^{-/-}$mice.

Atherosclerosis in IL-17$^{-/-}$ApoE$^{-/-}$ Mice

With the results found with the wire myograph vessel function assay, peripheral blood and aortic single cell suspension FACS analysis, and intravital microscopy of *in vivo* leukocyte rolling and adhesion, and the established role of IL-17 as a pro-inflammatory cytokine, we expected IL-17$^{-/-}$ApoE$^{-/-}$ mice would have decrease in atherosclerotic lesion formation. Previous atherosclerosis studies that used neutralizing antibodies against IL-17 or disruption of IL-17 receptor produced a significant reduction in atherosclerotic plaque in the ApoE$^{-/-}$ mouse (Erbel et al., 2009; Gao et al., 2010; Smith et al., 2010). To further understand the role of IL-17 in atherosclerosis, the IL-17$^{-/-}$ApoE$^{-/-}$ mouse was generated in our lab as well as in others'.

To date, there are four major articles that have used the IL-17$^{-/-}$ApoE$^{-/-}$ mouse model and addressed the issue of atherosclerosis (Butcher et al., 2012; Danzaki et al., 2012; Madhur et al., 2011; Usui et al., 2012). The results from these studies did not reach a consensus on the role of IL-17 in atherosclerosis. IL-17 deficiency in ApoE$^{-/-}$ mice was shown to attenuate atherosclerosis by two groups (Butcher et al., 2012; Usui et al., 2012). IL-17 deficiency was found to accelerate atherosclerotic plaque formation by one group (Danzaki et al., 2012). Another group concluded that IL-17 did not alter atherosclerotic plaque formation in ApoE$^{-/-}$ mice (Madhur et al., 2011). Similar to this last group, we did not find a statically significant difference in atherosclerotic lesion formation in IL-17$^{-/-}$ ApoE$^{-/-}$ mice when compared to ApoE$^{-/-}$ mice, but we did see a trend that shows a slight increase in the lesion area percentage in IL-17$^{-/-}$ApoE$^{-/-}$ mice when they were fed a Western diet.

The duration of diet intervention and the age of the mice at the beginning of the diet intervention are two important differences seen in these studies and in our experiment, and these differences may contribute to the different results. For the most part, the four studies fed mice for a longer period than we did in our study. Usui et al. and Madhur et al. fed their mice for exactly 12 weeks. The Usui group fed the mice when they were 8 weeks old whereas Madhur et al. started diet intervention when mice were between 8 and 11 weeks old. The other two studies used two feeding periods; for 8 or 16 weeks, feeding started at 6 or 8 weeks of age (Danzaki et al., 2012) and for 12 or 15 weeks, feeding started at 6 weeks of age (Butcher et al., 2012). In our study, we fed mice for 3 or 6 weeks starting at the age of 8 weeks at which they are considered to be adults.

The diet intervention of our study was relatively short compared to those of others. We have chosen to observe atherosclerosis development with a shorter diet at an earlier age because we are interested in early atherogenesis. Also, we believe that phenotypes that occur during early atherosclerosis may be blunted by other factors as the disease progresses and become more complicated.

Another distinction among these studies and ours is the diet that was used. It is possible the different phenotypes seen in these studies are due to the variation in the diet used. It was shown that in the $LDLR^{-/-}$ mouse, a Paigen diet (high fat, high cholesterol with cholate) induced a significant greater amount of atherosclerotic plaques than a Western diet (high fat with moderate level of cholesterol) (Lichtman et al., 1999). In $ApoE^{-/-}$ mice, it was shown that a regular diet supplemented with fats from different sources have different effects on atherosclerotic lesion development. And the authors concluded some of the differences observed may be due to changes in the plasma lipid levels (Calleja et al., 1999). Usui et al. fed mice with either a Western diet or a Paigen diet, and they found that a Paigen diet did not influence atherosclerotic lesion development in $ApoE^{-/-}$ mice and IL-$17^{-/-}ApoE^{-/-}$ mice. However, in their Western diet fed mice, atherosclerotic lesion was found to be decreased in IL-$17^{-/-}ApoE^{-/-}$ mice. In the work by Madhur et al., a Paigen diet was used and it was found that there was no difference in atherosclerosis in the mice which correlates with the data of the Paigen diet found by Usui et al. In the studies by Butcher et al. and Danzaki et al. the same diet (Western diet) was used and the phenotypes from these two studies opposed each other. Butcher et al. showed a decrease in atherosclerosis in IL-$17^{-/-}ApoE^{-/-}$ mice and Danzaki et

al. found increased lesions in IL-17$^{-/-}$ApoE$^{-/-}$ mice. The difference in these two experiments may be due to the duration of the feed and the age of the start of the feed rather than the type of diet used. Moreover, the methodologies used by these two laboratories may also contribute to the differences noted. Similar to these two studies, we used the Western diet and our results did not agreed with either study thus perhaps the duration of diet and age of diet intervention are important parameters for atherosclerosis development.

Lipid Profiles

The four studies that used the IL-17$^{-/-}$ApoE$^{-/-}$ mouse mentioned in the previous section did not highlight any difference in the lipid profiles of the mice. Madhur et al. was the only one to note that the total cholesterol and triglyceride levels were not different in ApoE$^{-/-}$ mice and IL-17$^{-/-}$ApoE$^{-/-}$ mice that were fed a Paigen diet. This piece of data correlates well with the lipid profiles of our mice that were on a 6-week diet (Figure 28). A 6-week Western diet induced elevations in LDL, triglyceride, non-esterified FFA, and total cholesterol levels in ApoE$^{-/-}$ mice and IL-17$^{-/-}$ApoE$^{-/-}$ mice when compared to their respective normal chow diet counterparts. However, we did not find any difference in the LDL, HDL, triglyceride, non-esterified FFA, and total cholesterol levels between the two genotypes that were on a normal chow diet or Western diet. This piece of data suggests that IL-17 may not modify lipid levels in ApoE$^{-/-}$ mice but it can also be an implication that the effects of IL-17 on lipid levels may be overpowered by other factors during this later stage of atherosclerosis. Thus, we sought to determine the

lipid profiles of younger mice that were on a diet for a shorter period. It is our belief that phenotypes that occur during early atherosclerosis may not be present during the later stages of the disease for other factors may take on a more important role as the disease progress.

We found that in our 3-week diet group, there was a significant difference in the LDL levels of mice that were on a normal chow diet. $ApoE^{-/-}$ mice were found to have higher LDL levels when compared to IL-$17^{-/-}$$ApoE^{-/-}$ mice. This difference was resolved when the mice were put on a Western diet. However, after a Western diet, there were dramatic changes in the HDL levels in the mice. The HDL levels in $ApoE^{-/-}$ mice were not significantly affected by a Western diet (21.71±3.124 mg/dL on a normal diet vs. 18.82±1.67 mg/dL on a Western diet). A Western diet in IL-$17^{-/-}$$ApoE^{-/-}$ mice reduced the HDL levels by more than 50%. More importantly, there was no difference in the total cholesterol levels in $ApoE^{-/-}$ mice and IL-$17^{-/-}$$ApoE^{-/-}$ mice that were on the same diet. These data suggest that IL-17 plays an important role in lipid modification during early atherosclerosis. The effects of IL-17 on lipid levels are blunted as the disease progresses because this lipid phenotype is only presented in the 3-week diet group and not in the 6-week diet group. Moreover, IL-17's role in modifying the HDL and LDL, but not total cholesterol levels may be an explanation for atherosclerosis lesion formation in the mice.

As seen in the lipid profiles, the levels LDL and HDL, two important cholesterols that have been implicated in CVDs, are significantly modified in the IL-$17^{-/-}$$ApoE^{-/-}$ mouse. High plasma levels of LDL are a main contributor to the initiation and

progression of atherosclerosis. LDL is pro-atherogenic in that it readily crosses the endothelium and becomes trapped in the sub-endothelium. LDL crosses the endothelium via modification of the endothelium permeability. High LDL levels have been shown to increase the endothelium permeability and decrease basement membrane associated heparan sulfate proteoglycan (Guretzki, Gerbitz, Olgemoller, & Schleicher, 1994). Exposure to elevated levels of LDL is shown to reduce NO bioavailability suggesting that one of the mechanisms of LDL in promoting atherosclerosis is the induction of endothelial dysfunction (Vidal, Colome, Martinez-Gonzalez, & Badimon, 1998). LDL is also one of the major components that make up the atherosclerotic lesion. Retention of LDL in the sub-endothelium is essential for uptake by macrophages and sequential foam cell formation. Interactions of the ApoB protein on LDL with extracellular matrix proteoglycans of the sub-endothelium are important for the retention of LDL (Gustafsson et al., 2007). However, retention of native LDL in the sub-endothelium is not sufficient to induce fatty streak formation for cellular uptake of lipids, a highly regulated event. As previously mentioned, cells that internalize exogenous lipid have cellular mechanism to decrease lipid receptor expression and prevent lipid overload thus it is not native LDL that induces the formation of foam cells but rather OxLDL. LDL that is retained in the sub-endothelial space is modified to become OxLDL and internalized by macrophage for foam cell formation. OxLDL has been shown to activate PPARγ-dependent induction of scavenger receptor expression and scavenger receptor-mediated cellular uptake of OxLDL (Nagy, Tontonoz, Alvarez, Chen, & Evans, 1998). In the mice that were fed a 3-week normal chow diet, we can see that the percentages of atherosclerotic lesion of the

whole aorta in IL-17$^{-/-}$ApoE$^{-/-}$ mice were lower than those in ApoE$^{-/-}$ mice (0.11±0.038 vs. 0.02±0.02%), but it was not of statistical significance. Moreover, this trend was not observed in the aortic sinus cross section staining; the percentages of lesion in the aortic sinus of ApoE$^{-/-}$ mice and IL-17$^{-/-}$ApoE$^{-/-}$ mice were similar (1.08±0.30% vs. 1.10±0.24%). In addition, in the 6-week normal diet group, the percentages of lesions determined by *en face* of the whole aorta and Oil red O of the aorta sinus were decreased in IL-17$^{-/-}$ApoE$^{-/-}$ mice when compared to ApoE$^{-/-}$ mice. Although these changes were not statistically significant, these results suggest that the effect of IL-17 on LDL levels in normal chow diet fed animals may modify atherosclerotic lesion formation.

HDL is an important regulator of cellular cholesterol homeostasis. HDL reduces the lipid load of non-hepatic cells and decreases the plasma cholesterol concentrations via reverse cholesterol transport. HDL has been shown to have anti-atherogenic properties and epidemiological studies have shown that the levels of HDL in the plasma is negatively correlated with cardiovascular risks (Assmann & Gotto, 2004). HDL is the universal plasma acceptor for cholesterol and it promotes the efflux of excess cholesterol from cells via ABCA1. HDL transfers excessive cholesterol to liver by reverse cholesterol transport via SR-B1. In the 3-week diet group, a Western diet dramatically reduced the HDL levels in IL-17$^{-/-}$ApoE$^{-/-}$ mice when compared to ApoE$^{-/-}$ mice on the same diet and IL-17$^{-/-}$ApoE$^{-/-}$ mice on a normal chow diet. However, after being fed a 6-week Western diet, the HDL levels in IL-17$^{-/-}$ApoE$^{-/-}$ mice are increased when compared to the 3-week Western diet group. The fluctuation in the HDL levels correlates with the changes in atherosclerosis lesion formation in the 3-week and 6-week Western diet

groups. In the 3-week Western diet group, IL-17$^{-/-}$ApoE$^{-/-}$ mice have a slightly higher percentage of lesion area than ApoE$^{-/-}$ mice whereas in the 6-week group, the lesion area in the ApoE$^{-/-}$ mice is slightly greater in the aortic sinus (10.41±1.77% vs. 8.58± 2.01%) (Figure 26). These results suggest the HDL levels in our mice may contribute to the atherosclerotic phenotype observed. It is important to note that although epidemiologic studies have shown a link of HDL with cardiovascular risk, clinical studies that aim to elevate HDL levels have yet to produce a positive outcome in cardiovascular events (Vickers & Remaley, 2014). This fact demonstrates that elevated HDL levels may not be equivalent to better HDL function. Recently, it was found that apolipoprotein A-I (ApoAI), a major structural protein of the HDL, may be extensively oxidized by myeloperoxidase (MPO) which impairs HDL's cholesterol acceptor function and lead to HDL dysfunction (Huang et al., 2014). Overall, our results suggest that the modification of lipid levels in ApoE$^{-/-}$ mice by IL-17 may influence atherosclerosis lesion development and contribute to vascular function.

Microarray

The Affymetrix Genechip Mouse Gene 2.0ST Array contains probes that measure mRNA as well non-coding RNA transcripts was used to determine the gene changes in the total RNA isolated from the aortas of IL-17$^{-/-}$ApoE$^{-/-}$ mice and ApoE$^{-/-}$ mice (Figure 29). Since IL-17-deficiency in the ApoE$^{-/-}$ mouse has an extensive effect on gene expressions, we analyzed the array data with a focus on a set of genes that may be related to our *in vitro* and *in vivo* phenotypes. IL-17ra transcript expression was reduced when

IL-17 was knocked out suggesting that the activation of the IL-17 signaling pathway may be decreased in the absences of IL-17 (Figure 30). Although IL-17 is the main ligand for IL-17ra, IL-17ra also forms complexes with other IL-17 receptors for signaling by other IL-17 cytokine family members (Kawaguchi, Kokubu, Fujita, Huang, & Hizawa, 2009; Rickel et al., 2008). This may also explain why the adaptor molecules, Traf3ip2, Traf2, Traf5, and Traf6 involved in IL-17 signaling were not significantly changed. Besides utilization by other members of the IL-17 cytokine family, these adaptors are also involved in CD40 (Qian, Zhao, Jiang, & Li, 2002), IL-1β (H. J. Lee, Jang, Kim, Yoon, & Chung, 2012) , and TNF signaling cascades (Yoon et al., 2008).

Transcript expressions of EC-related adhesion molecules including Esam, Icam1, Icam2, Pecam1, Jam2, Itgal, and F11r were decreased when IL-17 was knocked out suggesting that there is less EC activation in IL-17$^{-/-}$ApoE$^{-/-}$ mice. These molecules are involved in leukocyte adhesion and migration thus this data suggest that there may be less leukocyte-EC interactions in the absence of IL-17. Although expressions of the majority of adhesion molecules analyzed were decreased, Itgb3and Itga5 were found to be up-regulated (Figure 31). Itgb3 and Itgb5 code for integrin β3 and integrin β5, respectively. Integrins are a superfamily of transmembrane αβ heterodimeric cell adhesion receptors that bind to extracellular matrix ligands, cell-surface ligands, and soluble ligands. The two main functions of integrins are attachment to extracellular matrix and activation of intracellular signaling pathways when activated by matrix binding (Takada, Ye, & Simon, 2007). The increased in Itgb3 and Itgb5 transcript expressions may indicate enhanced interaction between cells with extracellular matrix since IL-17 have been

shown to promote matrix metalloproteinase expressions (Li et al., 2011; Shen & Gaffen, 2008).

Then we analyzed the array for genes that may regulate vascular functions, we examined genes involved in the angiotensin system: Agt and Agtr1a; NO System: Nos2 and Nos3; vasoconstriction: Edn1, Edn2; prostacyclin system: Ptgis and Ptgs2; and blood pressure regulation: Ednra and Npr1. The mRNA transcript expression of Agtrla which codes for angiotensin II receptor type 1a was significantly decreased in the absences of IL-17 (Figure 32). Endra which codes for endothelin receptor type A and Npr1 which codes for atrionatriuretic peptide receptor A were significantly increased when IL-17 was knocked out. Nos3 which encodes eNOS was significantly decreased in IL-17$^{-/-}$ApoE$^{-/-}$ mice. Decrease in the transcript of Agtrla and increase in Npr1 expression suggest that IL-17-deficient ApoE$^{-/-}$ mice may have improve vascular function with lowered blood pressure. However, the increase in Endra transcript expression suggests that IL-17 deficiency may increase the blood pressure because endothelin receptor type A mediates vasoconstriction. Previously, it was found that IL-17 promotes angiotensin II-mediated hypertension thus the role of IL-17 in regulating blood pressure needs further clarification. Moreover, the expression of Nos3, which encodes eNOS, was significantly decreased in IL-17$^{-/-}$ApoE$^{-/-}$ mice. eNOS is important in the generation of NO by endothelial cells which leads to the relaxation of smooth muscle cells and vasodilation. This piece of data correlates well with results previously found by others; IL-17 increased the expression of eNOS by human ECs (Liu, Lee, McManus, & Choy, 2012). However, induction of eNOS does not necessarily lead to enhanced function of eNOS since proper

function eNOS is regulated by various factors including phosphorylation, association with caveolae (Bernatchez et al., 2005), and eNOs coupling (Rabelink & van Zonneveld, 2006).

Next, we examined the transcript expressions of kinases that are involved in the P38 MAPK pathway. We found that all the transcripts that we examined were either unchanged or reduced in IL-17$^{-/-}$ApoE$^{-/-}$ mice. Expressions of Map3k1, Map3k11, Mapk11, Mapk12, Rps6ka4, Mknk1, and Mknk2 were found to be significantly decreased when compared to ApoE$^{-/-}$ mice (Figure 33). Map3k1 and Map3k11 code for MEKK1 and MLK3, respectively. MEKK1 and MLK3 are upstream kinases of P38 that phosphorylate and activate kinases that lead to P38 activation. Mapk11 and Mapk12 encode P38β and P38γ MAPK, respectively. Rps6ka4, Mknk1, and Mknk2 code for MSK2, Mnk1, and Mnk2, respectively. These three kinases are downstream of and activated by P38 MAPK (Zarubin & Han, 2005). Besides its role in various cellular functions including cell cycle, cell death, development, and cell differentiation, the P38 MAPK pathway is also important in mediating inflammation. The decrease expressions of kinases in the P38 MAPK pathway in the absence of IL-17 suggest that IL-17 is one of the important activators of the P38 MAPK pathway and this pathway may be critical for IL-17-mediated vascular dysfunction in ApoE$^{-/-}$ mice.

Furthermore, we found that a few genes involved in lipoprotein signaling and cholesterol metabolism were significantly changed in IL-17$^{-/-}$ApoE$^{-/-}$ mice when compared to ApoE$^{-/-}$ mice. Stab1, Ldlrap1, and Pcsk9 code for proteins that are

associated with the LDLR. Cdh13 and Scarf1 encode proteins that are associated with LDL. Apof is associated with HDL. Lcat is important in cholesterol transport (Figure 34).

Stab1 codes for stabilin-1, a scavenger receptor with numerous functions. Stabilin expressed by Chinese Hamster Ovary cells were shown to mediate the uptake of acetylated LDL (Kzhyshkowska et al., 2006b). The expression of Stabilin on macrophages and endothelial cells was induced during chronic inflammation and tumorigenesis (Kzhyshkowska, Gratchev, & Goerdt, 2006a). Stab1 expression was significantly down-regulated in IL-17$^{-/-}$ApoE$^{-/-}$ mice which suggest a decrease inflammatory profile in these mice. The Ldlrap1 gene (also known as ARH) codes for low-density lipoprotein receptor adapter protein 1. Association of the Ldlrap1 protein with the LDLR is important for receptor function. Mutations in the Ldlrap1 genes lead to LDLR malfunction and cause the disorder autosomal recessive hypercholesterolemia in humans (He et al., 2002). Ldlrap1 was significantly down-regulated in IL-17$^{-/-}$ApoE$^{-/-}$ mice which suggest that LDL levels in these mice would be increased. LDL levels in IL-17$^{-/-}$ApoE$^{-/-}$ mice that were fed a 3-week Western diet were not different from ApoE$^{-/-}$ mice on the same diet. However, there was a difference in the LDL levels when the animals were fed a normal chow thus Ldlrap1 may be important in negating this difference in the Western diet fed mice. Pcsk9 codes for proprotein convertase subtilisin/kexin type 9. Pcsk9 regulates LDL cholesterol level via down regulation of the LDLR thus Pcsk9 is important in modulating plasma LDL levels (Dong et al., 2010). Pcsk9 was significantly increased in the absence of IL-17 in ApoE$^{-/-}$ mice suggesting that

it may be important regulator of LDL levels and contributes to the changes in the lipid profiles.

Cdh13 codes for T-cadherin, a member of a superfamily of adhesion molecules called cadherins. LDL had been shown to bind to T-cadherin and induced L929 cell (murine aneuploid fibrosarcoma cell line) migration which suggest that binding of LDL to T-cadherin can induce intracellular signaling and functional responses. T-cadherin may play an important role in vascular remodeling during atherosclerosis such as mediating VSMC migration and proliferation (Rubina et al., 2005). Scarf1 encodes a scavenger receptor (SERC-1) that is expressed by ECs. SERC-1 on ECs was shown to bind and uptake carbamylated LDL, an atherogenic modified LDL. SERC-1 has atherogenic properties thus down-regulation of Scarf1 suggests that IL-17 deficiency is athero-protective.

Apof codes for apolipoprotein F, a protein component of lipoproteins including HDL. Apof transcript expression was significantly increased in IL-17$^{-/-}$ApoE$^{-/-}$ mice. It was shown that the overexpression of ApoF in mice significantly reduced the HDL cholesterol levels via accelerated plasma clearance of HDL cholesteryl esters (Lagor et al., 2009). The increase Apof expression may contribute to the lower HDL levels found in our lipid profiles of IL-17$^{-/-}$ApoE$^{-/-}$ mice on a 3-week Western diet. Lcat which codes for lecithin—cholesterol acyltransferase is important for HDL synthesis, was also significantly increased when IL-17 was knocked out. Lcat converts free cholesterol into cholesterol ester which is then packed into the HDL core for the maturation of HDL

(Lewis & Rader, 2005). Lcat expression was significantly increased in IL-17$^{-/-}$ApoE$^{-/-}$ mice. An increase in Lcat suggests that there would be higher levels of HDL; however, we know this is not true based on our lipid profile data of mice that were on a 3-week diet. Thus, the increase in Lcat may be a systemic compensatory effect to increase the HDL levels. As seen from the lipid profiles of mice on a 6-week diet, the HDL levels in IL-17$^{-/-}$ApoE$^{-/-}$ fed a Western diet recovered to the levels of ApoE$^{-/-}$ mice on the same diet and IL-17$^{-/-}$ApoE$^{-/-}$ mice on a normal chow diet. These data suggest that Apof and Lcat may be important in contributing to the changes in HDL levels found in IL-17$^{-/-}$ ApoE$^{-/-}$ mice.

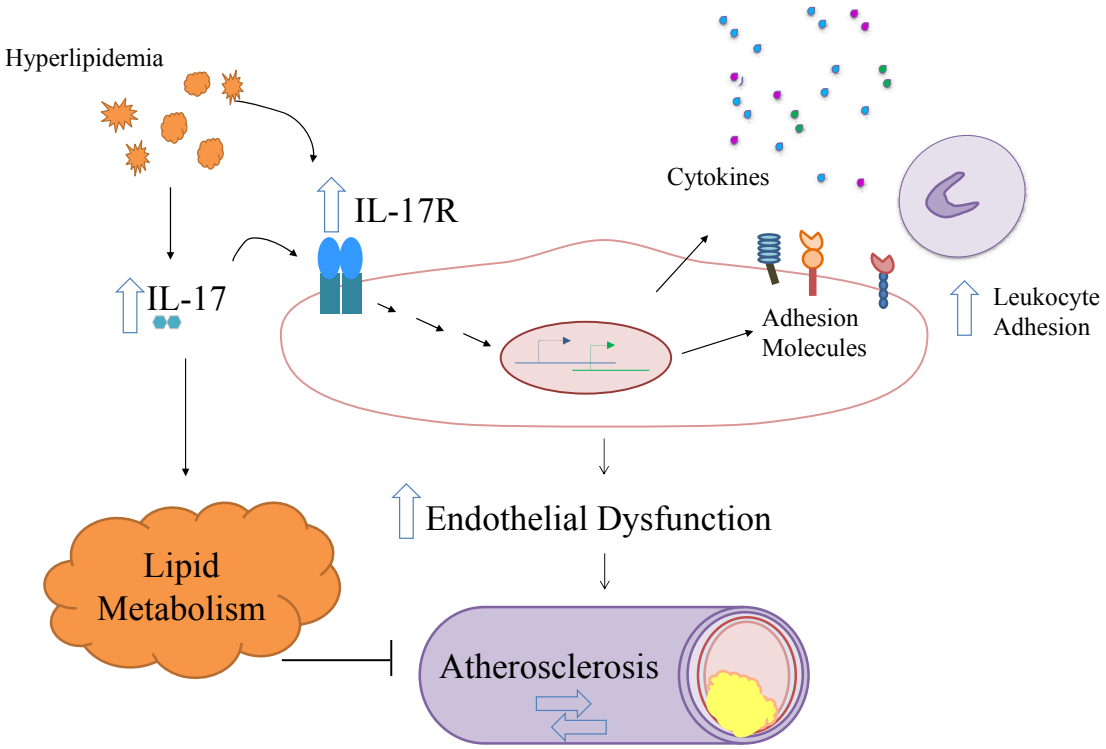

Figure 35. Work Model

Schematic of the effects of IL-17 on EC activation, endothelial dysfunction, and early atherosclerosis development. IL-17 activates ECs to produce pro-inflammatory cytokines and chemokines, and adhesion molecules. The pro-inflammatory cytokines and chemokines enhance the adhesion of leukocytes such as monocytes to the endothelium. IL-17 potentiates impaired endothelial function in $ApoE^{-/-}$ mice induced by a Western diet. The role of IL-17 in lipid metabolism may counteract the pro-atherogenic potential of IL-17 seen in ECs thus atherosclerotic lesion formation is not affected by IL-17 deficiency in $ApoE^{-/-}$ mice.

Summary and Future Directions

In our current study, we found that IL-17 is up-regulated in hyperlipidemia and its receptor expression is increased with pro-atherogenic OxLDL treatment in mouse and human aortic ECs. Future studies are needed to define other cells besides Th17 that contribute to the increase IL-17 levels observed in mice that are fed a Western diet. It has been published that IL-17 enhances the expression of pro-inflammatory cytokines and chemokines in various cell types either via up-regulating the gene expression or pro-longing the mRNA half-life of the targeted genes. It is very likely that these two mechanisms are also involved in EC activation by IL-17 in our study.

IL-17 deficiency in $ApoE^{-/-}$ mice was found to delay the onset of vascular dysfunction when mice were fed with a Western diet. Our data suggest that the P38 MAPK pathway may be important in mediating this. Further study is needed to clarify the role of P38 MAPK in vascular dysfunction in our mouse model. A P38 MAPK inhibitor that we used completely reduced the PE-induced contraction in the aorta thus another inhibitor is needed. Moreover, it is possible that the inhibitor dose and incubation time may play a role in this phenotype thus modulating these two parameters may be essential if another suitable inhibitor is not available.

Our atherosclerotic lesion study did not show a difference in lesion area between the two mouse models; however, it is of interest to determine the cellular makeup of the lesions to determine whether the cells present in the lesions are influence by IL-17. It is

also of interest to determine the lipid content within the atherosclerotic plaque since there were transient changes in the lipid profiles in the mice. LDL and HDL are two cholesterols that were found to be affected by IL-17 deficiency in $ApoE^{-/-}$ mice. For future studies, it is of interest to assess whether IL-17 affects the production of these two cholesterols. Moreover, the functions of LDL and HDL from the mice may be assessed to determine whether their functions are influenced by IL-17.

Furthermore, in our microarray analysis, we found numerous genes that are regulated by IL-17, thus these genes serve as important targets for future studies. In addition, a new mouse model that is EC-specific for IL-17R deficiency may be important to clarify and cast off any doubts in the phenotypes that were found with the intravital microscopy study with leukocytes and peripheral blood study with monocytes. An EC-specific IL-17R knock-out mouse model would secure the argument that our phenotypes are due to the effects of IL-17 on EC rather than on other cells. Alternatively, adoptive transfer of leukocytes or monocytes from $ApoE^{-/-}$ mice into $IL\text{-}17^{-/-}ApoE^{-/-}$ mice may also be useful to solidify our findings as ones that are attributed to IL-17's effects on ECs.

Our current work has shed lights onto the role of IL-17 on EC biology and has provided insights into the effects of IL-17 on aortic EC activation, vascular function, lipid modification, and atherosclerosis development. Our study shows that IL-17 is important in promoting vascular dysfunction and modifying lipid levels in mice thus therapy that target these two problems may bring beneficial effects and improve vascular function in hyperlipidemia.

REFERENCES CITED

Anthony, R. M., Rutitzky, L. I., Urban, J. F., Jr., Stadecker, M. J., & Gause, W. C. (2007). Protective immune mechanisms in helminth infection. *Nat Rev Immunol, 7*(12), 975-987.

Applebaum-Bowden, D., Haffner, S. M., Hartsook, E., Luk, K. H., Albers, J. J., & Hazzard, W. R. (1984). Down-regulation of the low-density lipoprotein receptor by dietary cholesterol. [Research Support, Non-U.S. Gov't]. *Am J Clin Nutr, 39*(3), 360-367.

Arca, M., Quagliarini, F., Pigna, G., Catalano, C., & Napoli, A. (2011). Severe coronary and extracoronary atherosclerosis in autosomal recessive hypercholesterolemia detected by whole-body computed tomography angiography. [Case Reports Letter]. *Intern Emerg Med, 6*(6), 571-573.

Assmann, G., & Gotto, A. M., Jr. (2004). HDL cholesterol and protective factors in atherosclerosis. [Review]. *Circulation, 109*(23 Suppl 1), III8-14.

Bazzoni, G., & Dejana, E. (2004). Endothelial cell-to-cell junctions: molecular organization and role in vascular homeostasis. *Physiol Rev, 84*(3), 869-901.

Bernatchez, P. N., Bauer, P. M., Yu, J., Prendergast, J. S., He, P., & Sessa, W. C. (2005). Dissecting the molecular control of endothelial NO synthase by caveolin-1 using cell-permeable peptides. [Research Support, Non-U.S. Gov't Research Support, U.S. Gov't, P.H.S.]. *Proc Natl Acad Sci U S A, 102*(3), 761-766.

Boden, W. E. (2000). High-density lipoprotein cholesterol as an independent risk factor in cardiovascular disease: assessing the data from Framingham to the Veterans Affairs High--Density Lipoprotein Intervention Trial. [Review]. *Am J Cardiol, 86*(12A), 19L-22L.

Boisvert, W. A., Rose, D. M., Johnson, K. A., Fuentes, M. E., Lira, S. A., Curtiss, L. K., et al. (2006). Up-regulated expression of the CXCR2 ligand KC/GRO-alpha in atherosclerotic lesions plays a central role in macrophage accumulation and lesion progression. *Am J Pathol, 168*(4), 1385-1395.

Bonecchi, R., Bianchi, G., Bordignon, P. P., D'Ambrosio, D., Lang, R., Borsatti, A., et al. (1998). Differential expression of chemokine receptors and chemotactic responsiveness of type 1 T helper cells (Th1s) and Th2s. *J Exp Med, 187*(1), 129-134.

Boullier, A., Bird, D. A., Chang, M. K., Dennis, E. A., Friedman, P., Gillotre-Taylor, K., et al. (2001). Scavenger receptors, oxidized LDL, and atherosclerosis. [Research Support, Non-U.S. Gov't Research Support, U.S. Gov't, P.H.S. Review]. *Ann N Y Acad Sci, 947*, 214-222; discussion 222-213.

Buono, C., Binder, C. J., Stavrakis, G., Witztum, J. L., Glimcher, L. H., & Lichtman, A. H. (2005). T-bet deficiency reduces atherosclerosis and alters plaque antigen-specific immune responses. [Research Support, U.S. Gov't, P.H.S.]. *Proc Natl Acad Sci U S A, 102*(5), 1596-1601.

Butcher, M. J., Gjurich, B. N., Phillips, T., & Galkina, E. V. (2012). The IL-17A/IL-17RA Axis Plays a Proatherogenic Role via the Regulation of Aortic Myeloid Cell Recruitment. *Circ Res, 110*(5), 675-687.

Caligiuri, G., Rudling, M., Ollivier, V., Jacob, M. P., Michel, J. B., Hansson, G. K., et al. (2003). Interleukin-10 deficiency increases atherosclerosis, thrombosis, and low-density lipoproteins in apolipoprotein E knockout mice. [Research Support, Non-U.S. Gov't]. *Mol Med, 9*(1-2), 10-17.

Calleja, L., Paris, M. A., Paul, A., Vilella, E., Joven, J., Jimenez, A., et al. (1999). Low-cholesterol and high-fat diets reduce atherosclerotic lesion development in ApoE-knockout mice. [Comparative Study Research Support, Non-U.S. Gov't]. *Arterioscler Thromb Vasc Biol, 19*(10), 2368-2375.

Chen, Z., Laurence, A., Kanno, Y., Pacher-Zavisin, M., Zhu, B. M., Tato, C., et al. (2006). Selective regulatory function of Socs3 in the formation of IL-17-secreting T cells. *Proc Natl Acad Sci U S A, 103*(21), 8137-8142.

Cheng, Z., Jiang, X., Kruger, W. D., Pratico, D., Gupta, S., Mallilankaraman, K., et al. (2011). Hyperhomocysteinemia impairs endothelium-derived hyperpolarizing factor-mediated vasorelaxation in transgenic cystathionine beta synthase-deficient mice. [Research Support, N.I.H., Extramural]. *Blood, 118*(7), 1998-2006.

Cines, D. B., Pollak, E. S., Buck, C. A., Loscalzo, J., Zimmerman, G. A., McEver, R. P., et al. (1998). Endothelial cells in physiology and in the pathophysiology of vascular disorders. *Blood, 91*(10), 3527-3561.

Cordain, L., Eaton, S. B., Sebastian, A., Mann, N., Lindeberg, S., Watkins, B. A., et al. (2005). Origins and evolution of the Western diet: health implications for the 21st century. [Review]. *Am J Clin Nutr, 81*(2), 341-354.

Cox, R. A., & Garcia-Palmieri, M. R. (1990). Cholesterol, Triglycerides, and Associated Lipoproteins. In H. K. Walker, W. D. Hall & J. W. Hurst (Eds.), *Clinical Methods: The History, Physical, and Laboratory Examinations* (3rd ed.). Boston.

Cua, D. J., Sherlock, J., Chen, Y., Murphy, C. A., Joyce, B., Seymour, B., et al. (2003). Interleukin-23 rather than interleukin-12 is the critical cytokine for autoimmune inflammation of the brain. *Nature, 421*(6924), 744-748.

Curtis, M. M., & Way, S. S. (2009). Interleukin-17 in host defence against bacterial, mycobacterial and fungal pathogens. *Immunology, 126*(2), 177-185.

Danzaki, K., Matsui, Y., Ikesue, M., Ohta, D., Ito, K., Kanayama, M., et al. (2012). Interleukin-17A deficiency accelerates unstable atherosclerotic plaque formation in apolipoprotein E-deficient mice. [Research Support, Non-U.S. Gov't]. *Arterioscler Thromb Vasc Biol, 32*(2), 273-280.

Daugherty, A., Rateri, D. L., & King, V. L. (2004). IL-5 links adaptive and natural immunity in reducing atherosclerotic disease. [Comment Review]. *J Clin Invest, 114*(3), 317-319.

Davenport, P., & Tipping, P. G. (2003). The role of interleukin-4 and interleukin-12 in the progression of atherosclerosis in apolipoprotein E-deficient mice. [Research Support, Non-U.S. Gov't]. *Am J Pathol, 163*(3), 1117-1125.

Davidson, S. M. (2010). Endothelial mitochondria and heart disease. *Cardiovasc Res, 88*(1), 58-66.

de Boer, O. J., van der Meer, J. J., Teeling, P., van der Loos, C. M., Idu, M. M., van Maldegem, F., et al. (2010). Differential expression of interleukin-17 family cytokines in intact and complicated human atherosclerotic plaques. *J Pathol, 220*(4), 499-508.

De Caterina, R., Libby, P., Peng, H. B., Thannickal, V. J., Rajavashisth, T. B., Gimbrone, M. A., Jr., et al. (1995). Nitric oxide decreases cytokine-induced endothelial activation. Nitric oxide selectively reduces endothelial expression of adhesion molecules and proinflammatory cytokines. *J Clin Invest, 96*(1), 60-68.

Dervisoglu, E., Turgut, T., & Yilmaz, A. (2007). Analbuminemia presenting with severe hypercholesterolemia: a risk for atherosclerosis? [Case Reports Letter]. *Acta Clin Belg, 62*(1), 68-69.

Ditiatkovski, M., Toh, B. H., & Bobik, A. (2006). GM-CSF deficiency reduces macrophage PPAR-gamma expression and aggravates atherosclerosis in ApoE-deficient mice. *Arterioscler Thromb Vasc Biol, 26*(10), 2337-2344.

Dong, B., Wu, M., Li, H., Kraemer, F. B., Adeli, K., Seidah, N. G., et al. (2010). Strong induction of PCSK9 gene expression through HNF1alpha and SREBP2: mechanism for the resistance to LDL-cholesterol lowering effect of statins in dyslipidemic hamsters. [Research Support, N.I.H., Extramural Research Support, U.S. Gov't, Non-P.H.S.]. *J Lipid Res, 51*(6), 1486-1495.

Eid, R. E., Rao, D. A., Zhou, J., Lo, S. F., Ranjbaran, H., Gallo, A., et al. (2009). Interleukin-17 and interferon-gamma are produced concomitantly by human coronary artery-infiltrating T cells and act synergistically on vascular smooth muscle cells. *Circulation, 119*(10), 1424-1432.

Elhage, R., Jawien, J., Rudling, M., Ljunggren, H. G., Takeda, K., Akira, S., et al. (2003). Reduced atherosclerosis in interleukin-18 deficient apolipoprotein E-knockout mice. [Research Support, Non-U.S. Gov't]. *Cardiovasc Res, 59*(1), 234-240.

Erbel, C., Chen, L., Bea, F., Wangler, S., Celik, S., Lasitschka, F., et al. (2009). Inhibition of IL-17A attenuates atherosclerotic lesion development in apoE-deficient mice. *J Immunol, 183*(12), 8167-8175.

Eriksson, E. E. (2011). Intravital microscopy on atherosclerosis in apolipoprotein e-deficient mice establishes microvessels as major entry pathways for leukocytes to advanced lesions. [Research Support, Non-U.S. Gov't]. *Circulation, 124*(19), 2129-2138.

Forstermann, U., & Munzel, T. (2006). Endothelial nitric oxide synthase in vascular disease: from marvel to menace. [Review]. *Circulation, 113*(13), 1708-1714.

Gabay, C. (2006). Interleukin-6 and chronic inflammation. *Arthritis Res Ther, 8 Suppl 2*, S3.

Galkina, E., & Ley, K. (2009). Immune and inflammatory mechanisms of atherosclerosis (*). *Annu Rev Immunol, 27*, 165-197.

Gao, Q., Jiang, Y., Ma, T., Zhu, F., Gao, F., Zhang, P., et al. (2010). A critical function of Th17 proinflammatory cells in the development of atherosclerotic plaque in mice. [Research Support, N.I.H., Intramural Research Support, Non-U.S. Gov't]. *J Immunol, 185*(10), 5820-5827.

Glass, C. K., & Witztum, J. L. (2001). Atherosclerosis. the road ahead. *Cell, 104*(4), 503-516.

Goldstein, J. L., & Brown, M. S. (2009). The LDL receptor. [Historical Article Portraits Research Support, N.I.H., Extramural Research Support, Non-U.S. Gov't Review]. *Arterioscler Thromb Vasc Biol, 29*(4), 431-438.

Goldstein, J. L., Ho, Y. K., Basu, S. K., & Brown, M. S. (1979). Binding site on macrophages that mediates uptake and degradation of acetylated low density lipoprotein, producing massive cholesterol deposition. *Proc Natl Acad Sci U S A, 76*(1), 333-337.

Gonzalez-Navarro, H., Vila-Caballer, M., Pastor, M. F., Vinue, A., White, M. F., Burks, D., et al. (2007). Plasma insulin levels predict the development of atherosclerosis when IRS2 deficiency is combined with severe hypercholesterolemia in apolipoprotein E-null mice. [Research Support, Non-U.S. Gov't]. *Front Biosci, 12*, 2291-2298.

Griffin, G. K., Newton, G., Tarrio, M. L., Bu, D. X., Maganto-Garcia, E., Azcutia, V., et al. (2012). IL-17 and TNF-alpha sustain neutrophil recruitment during inflammation through synergistic effects on endothelial activation. [Research Support, N.I.H., Extramural Research Support, Non-U.S. Gov't]. *J Immunol, 188*(12), 6287-6299.

Gupta, S., Pablo, A. M., Jiang, X., Wang, N., Tall, A. R., & Schindler, C. (1997). IFN-gamma potentiates atherosclerosis in ApoE knock-out mice. [Research Support, Non-U.S. Gov't Research Support, U.S. Gov't, P.H.S.]. *J Clin Invest, 99*(11), 2752-2761.

Guretzki, H. J., Gerbitz, K. D., Olgemoller, B., & Schleicher, E. (1994). Atherogenic levels of low density lipoprotein alter the permeability and composition of the endothelial barrier. [Research Support, Non-U.S. Gov't]. *Atherosclerosis, 107*(1), 15-24.

Gustafsson, M., Levin, M., Skalen, K., Perman, J., Friden, V., Jirholt, P., et al. (2007). Retention of low-density lipoprotein in atherosclerotic lesions of the mouse: evidence for a role of lipoprotein lipase. [Comparative Study Research Support, N.I.H., Extramural Research Support, Non-U.S. Gov't]. *Circ Res, 101*(8), 777-783.

Hansson, G. K., Robertson, A. K., & Soderberg-Naucler, C. (2006). Inflammation and atherosclerosis. [Research Support, N.I.H., Extramural Research Support, Non-U.S. Gov't Review]. *Annu Rev Pathol, 1*, 297-329.

Harrington, L. E., Hatton, R. D., Mangan, P. R., Turner, H., Murphy, T. L., Murphy, K. M., et al. (2005). Interleukin 17-producing CD4+ effector T cells develop via a lineage distinct from the T helper type 1 and 2 lineages. [Research Support, N.I.H., Extramural Research Support, Non-U.S. Gov't Research Support, U.S. Gov't, P.H.S.]. *Nat Immunol, 6*(11), 1123-1132.

Hasty, A. H., Shimano, H., Osuga, J., Namatame, I., Takahashi, A., Yahagi, N., et al. (2001). Severe hypercholesterolemia, hypertriglyceridemia, and atherosclerosis in mice lacking both leptin and the low density lipoprotein receptor. [Research Support, Non-U.S. Gov't]. *J Biol Chem, 276*(40), 37402-37408.

He, G., Gupta, S., Yi, M., Michaely, P., Hobbs, H. H., & Cohen, J. C. (2002). ARH is a modular adaptor protein that interacts with the LDL receptor, clathrin, and AP-2. [Research Support, Non-U.S. Gov't Research Support, U.S. Gov't, P.H.S.]. *J Biol Chem, 277*(46), 44044-44049.

Hofstetter, H. H., Ibrahim, S. M., Koczan, D., Kruse, N., Weishaupt, A., Toyka, K. V., et al. (2005). Therapeutic efficacy of IL-17 neutralization in murine experimental autoimmune encephalomyelitis. *Cell Immunol, 237*(2), 123-130.

Huang, Y., Didonato, J. A., Levison, B. S., Schmitt, D., Li, L., Wu, Y., et al. (2014). An abundant dysfunctional apolipoprotein A1 in human atheroma. *Nat Med, 20*(2), 193-203.

Huo, Y., Weber, C., Forlow, S. B., Sperandio, M., Thatte, J., Mack, M., et al. (2001). The chemokine KC, but not monocyte chemoattractant protein-1, triggers monocyte arrest on early atherosclerotic endothelium. *J Clin Invest, 108*(9), 1307-1314.

Huppert, J., Closhen, D., Croxford, A., White, R., Kulig, P., Pietrowski, E., et al. (2010). Cellular mechanisms of IL-17-induced blood-brain barrier disruption. [Research Support, Non-U.S. Gov't]. *FASEB J, 24*(4), 1023-1034.

Ikonen, E. (2008). Cellular cholesterol trafficking and compartmentalization. [Review]. *Nat Rev Mol Cell Biol, 9*(2), 125-138.

Ishibashi, S., Brown, M. S., Goldstein, J. L., Gerard, R. D., Hammer, R. E., & Herz, J. (1993). Hypercholesterolemia in low density lipoprotein receptor knockout mice and its reversal by adenovirus-mediated gene delivery. *J Clin Invest, 92*(2), 883-893.

Ishibashi, S., Goldstein, J. L., Brown, M. S., Herz, J., & Burns, D. K. (1994). Massive xanthomatosis and atherosclerosis in cholesterol-fed low density lipoprotein receptor-negative mice. [Research Support, Non-U.S. Gov't Research Support, U.S. Gov't, P.H.S.]. *J Clin Invest, 93*(5), 1885-1893.

Jiang, X., Yang, F., Tan, H., Liao, D., Bryan, R. M., Jr., Randhawa, J. K., et al. (2005). Hyperhomocystinemia impairs endothelial function and eNOS activity via PKC activation. [Research Support, N.I.H., Extramural]. *Arterioscler Thromb Vasc Biol, 25*(12), 2515-2521.

Jovanovic, D. V., Di Battista, J. A., Martel-Pelletier, J., Jolicoeur, F. C., He, Y., Zhang, M., et al. (1998). IL-17 stimulates the production and expression of proinflammatory cytokines, IL-beta and TNF-alpha, by human macrophages. *J Immunol, 160*(7), 3513-3521.

Kaplanski, G., Marin, V., Montero-Julian, F., Mantovani, A., & Farnarier, C. (2003). IL-6: a regulator of the transition from neutrophil to monocyte recruitment during inflammation. *Trends Immunol, 24*(1), 25-29.

Kato, R., Mori, C., Kitazato, K., Arata, S., Obama, T., Mori, M., et al. (2009). Transient increase in plasma oxidized LDL during the progression of atherosclerosis in apolipoprotein E knockout mice. *Arterioscler Thromb Vasc Biol, 29*(1), 33-39.

Kawaguchi, M., Kokubu, F., Fujita, J., Huang, S. K., & Hizawa, N. (2009). Role of interleukin-17F in asthma. [Research Support, N.I.H., Extramural Research Support, Non-U.S. Gov't Review]. *Inflamm Allergy Drug Targets, 8*(5), 383-389.

King, V. L., Cassis, L. A., & Daugherty, A. (2007). Interleukin-4 does not influence development of hypercholesterolemia or angiotensin II-induced atherosclerotic lesions in mice. [Research Support, N.I.H., Extramural Research Support, Non-U.S. Gov't]. *Am J Pathol, 171*(6), 2040-2047.

King, V. L., Szilvassy, S. J., & Daugherty, A. (2002). Interleukin-4 deficiency decreases atherosclerotic lesion formation in a site-specific manner in female LDL receptor$^{-/-}$ mice. [Research Support, U.S. Gov't, P.H.S.]. *Arterioscler Thromb Vasc Biol, 22*(3), 456-461.

Koga, N. (2001). Effects of low-density lipoprotein apheresis on coronary and carotid atherosclerosis and diabetic scleredema in patients with severe hypercholesterolemia. [Review]. *Ther Apher, 5*(4), 244-251.

Komiyama, Y., Nakae, S., Matsuki, T., Nambu, A., Ishigame, H., Kakuta, S., et al. (2006). IL-17 plays an important role in the development of experimental autoimmune encephalomyelitis. [Comparative Study Research Support, Non-U.S. Gov't]. *J Immunol, 177*(1), 566-573.

Korn, T., Oukka, M., Kuchroo, V., & Bettelli, E. (2007). Th17 cells: effector T cells with inflammatory properties. *Semin Immunol, 19*(6), 362-371.

Krakowski, M., & Owens, T. (1996). Interferon-gamma confers resistance to experimental allergic encephalomyelitis. *Eur J Immunol, 26*(7), 1641-1646.

Kuestner, R. E., Taft, D. W., Haran, A., Brandt, C. S., Brender, T., Lum, K., et al. (2007). Identification of the IL-17 receptor related molecule IL-17RC as the receptor for IL-17F. *J Immunol, 179*(8), 5462-5473.

Kzhyshkowska, J., Gratchev, A., & Goerdt, S. (2006a). Stabilin-1, a homeostatic scavenger receptor with multiple functions. [Research Support, Non-U.S. Gov't Review]. *J Cell Mol Med, 10*(3), 635-649.

Kzhyshkowska, J., Workman, G., Cardo-Vila, M., Arap, W., Pasqualini, R., Gratchev, A., et al. (2006b). Novel function of alternatively activated macrophages: stabilin-1-mediated clearance of SPARC. [Research Support, N.I.H., Extramural Research Support, Non-U.S. Gov't]. *J Immunol, 176*(10), 5825-5832.

Lagor, W. R., Brown, R. J., Toh, S. A., Millar, J. S., Fuki, I. V., de la Llera-Moya, M., et al. (2009). Overexpression of apolipoprotein F reduces HDL cholesterol levels in vivo. [Research Support, N.I.H., Extramural]. *Arterioscler Thromb Vasc Biol, 29*(1), 40-46.

Lee, H. J., Jang, S. H., Kim, H., Yoon, J. H., & Chung, K. C. (2012). PINK1 stimulates interleukin-1beta-mediated inflammatory signaling via the positive regulation of TRAF6 and TAK1. [Research Support, Non-U.S. Gov't]. *Cell Mol Life Sci, 69*(19), 3301-3315.

Lee, T. S., Yen, H. C., Pan, C. C., & Chau, L. Y. (1999). The role of interleukin 12 in the development of atherosclerosis in ApoE-deficient mice. [Research Support, Non-U.S. Gov't]. *Arterioscler Thromb Vasc Biol, 19*(3), 734-742.

Lewis, G. F., & Rader, D. J. (2005). New insights into the regulation of HDL metabolism and reverse cholesterol transport. [Research Support, N.I.H., Extramural Research Support, Non-U.S. Gov't Research Support, U.S. Gov't, P.H.S. Review]. *Circ Res, 96*(12), 1221-1232.

Ley, K. (2003). The role of selectins in inflammation and disease. [Review]. *Trends Mol Med, 9*(6), 263-268.

Li, J., Lau, G. K., Chen, L., Dong, S. S., Lan, H. Y., Huang, X. R., et al. (2011). Interleukin 17A promotes hepatocellular carcinoma metastasis via NF-kB induced matrix metalloproteinases 2 and 9 expression. [Research Support, Non-U.S. Gov't]. *PLoS One, 6*(7), e21816.

Liao, J. K. (2013). Linking endothelial dysfunction with endothelial cell activation. [Research Support, N.I.H., Extramural]. *J Clin Invest, 123*(2), 540-541.

Lichtman, A. H., Clinton, S. K., Iiyama, K., Connelly, P. W., Libby, P., & Cybulsky, M. I. (1999). Hyperlipidemia and atherosclerotic lesion development in LDL receptor-deficient mice fed defined semipurified diets with and without cholate. [Research Support, Non-U.S. Gov't Research Support, U.S. Gov't, P.H.S.]. *Arterioscler Thromb Vasc Biol, 19*(8), 1938-1944.

Lin, D., Sugawara, T., Strauss, J. F., 3rd, Clark, B. J., Stocco, D. M., Saenger, P., et al. (1995). Role of steroidogenic acute regulatory protein in adrenal and gonadal steroidogenesis. [Research Support, Non-U.S. Gov't Research Support, U.S. Gov't, P.H.S.]. *Science, 267*(5205), 1828-1831.

Liu, A. C., Lee, M., McManus, B. M., & Choy, J. C. (2012). Induction of endothelial nitric oxide synthase expression by IL-17 in human vascular endothelial cells: implications for vascular remodeling in transplant vasculopathy. [Research Support, Non-U.S. Gov't]. *J Immunol, 188*(3), 1544-1550.

Lohmann, T., Laue, S., Nietzschmann, U., Kapellen, T. M., Lehmann, I., Schroeder, S., et al. (2002). Reduced expression of Th1-associated chemokine receptors on peripheral blood lymphocytes at diagnosis of type 1 diabetes. *Diabetes, 51*(8), 2474-2480.

Lowes, M. A., Kikuchi, T., Fuentes-Duculan, J., Cardinale, I., Zaba, L. C., Haider, A. S., et al. (2008). Psoriasis vulgaris lesions contain discrete populations of Th1 and Th17 T cells. *J Invest Dermatol, 128*(5), 1207-1211.

Lutgens, E., Faber, B., Schapira, K., Evelo, C. T., van Haaften, R., Heeneman, S., et al. (2005). Gene profiling in atherosclerosis reveals a key role for small inducible cytokines: validation using a novel monocyte chemoattractant protein monoclonal antibody. *Circulation, 111*(25), 3443-3452.

Madhur, M. S., Funt, S. A., Li, L., Vinh, A., Chen, W., Lob, H. E., et al. (2011). Role of interleukin 17 in inflammation, atherosclerosis, and vascular function in apolipoprotein e-deficient mice. [Research Support, N.I.H., Extramural Research Support, U.S. Gov't, Non-P.H.S.]. *Arterioscler Thromb Vasc Biol, 31*(7), 1565-1572.

Madhur, M. S., Lob, H. E., McCann, L. A., Iwakura, Y., Blinder, Y., Guzik, T. J., et al. (2010). Interleukin 17 promotes angiotensin II-induced hypertension and vascular dysfunction. [Comparative Study Research Support, N.I.H., Extramural Research Support, U.S. Gov't, Non-P.H.S.]. *Hypertension, 55*(2), 500-507.

Magoori, K., Kang, M. J., Ito, M. R., Kakuuchi, H., Ioka, R. X., Kamataki, A., et al. (2003). Severe hypercholesterolemia, impaired fat tolerance, and advanced atherosclerosis in mice lacking both low density lipoprotein receptor-related protein 5 and apolipoprotein E. [Research Support, Non-U.S. Gov't]. *J Biol Chem, 278*(13), 11331-11336.

Maor, I., Mandel, H., & Aviram, M. (1995). Macrophage uptake of oxidized LDL inhibits lysosomal sphingomyelinase, thus causing the accumulation of unesterified cholesterol-sphingomyelin-rich particles in the lysosomes. A possible role for 7-Ketocholesterol. *Arterioscler Thromb Vasc Biol, 15*(9), 1378-1387.

May, M. J. (2011). IL-17R signaling: new players get in on the Act1. [Comment News]. *Nat Immunol, 12*(9), 813-815.

Meir, K. S., & Leitersdorf, E. (2004). Atherosclerosis in the apolipoprotein-E-deficient mouse: a decade of progress. [Research Support, Non-U.S. Gov't Review]. *Arterioscler Thromb Vasc Biol, 24*(6), 1006-1014.

Meyrelles, S. S., Peotta, V. A., Pereira, T. M., & Vasquez, E. C. (2011). Endothelial dysfunction in the apolipoprotein E-deficient mouse: insights into the influence of diet, gender and aging. [Research Support, Non-U.S. Gov't Review]. *Lipids Health Dis, 10*, 211.

Minshall, R. D., & Malik, A. B. (2006). Transport across the endothelium: regulation of endothelial permeability. *Handb Exp Pharmacol*(176 Pt 1), 107-144.

Moncada, S., & Higgs, E. A. (2006). *Nitric oxide and the vascular endothelium*: Springer Berlin Heidelberg.

Moseley, T. A., Haudenschild, D. R., Rose, L., & Reddi, A. H. (2003). Interleukin-17 family and IL-17 receptors. [Research Support, U.S. Gov't, Non-P.H.S. Research Support, U.S. Gov't, P.H.S. Review]. *Cytokine Growth Factor Rev, 14*(2), 155-174.

Mosmann, T. R., & Coffman, R. L. (1989). TH1 and TH2 cells: different patterns of lymphokine secretion lead to different functional properties. *Annu Rev Immunol, 7*, 145-173.

Mueller, M. A., Beutner, F., Teupser, D., Ceglarek, U., & Thiery, J. (2008). Prevention of atherosclerosis by the mTOR inhibitor everolimus in $LDLR^{-/-}$ mice despite severe hypercholesterolemia. [Research Support, Non-U.S. Gov't]. *Atherosclerosis, 198*(1), 39-48.

Murphy, N., Grimsditch, D. C., Parkin, S., Vidgeon-Hart, M. P., Overend, P., Groot, P. H., et al. (2002). Hypercholesterolaemia and circulating levels of CXC chemokines in apoE*3 Leiden mice. *Atherosclerosis, 163*(1), 69-77.

Nagy, L., Tontonoz, P., Alvarez, J. G., Chen, H., & Evans, R. M. (1998). Oxidized LDL regulates macrophage gene expression through ligand activation of PPARgamma. [Research Support, Non-U.S. Gov't Research Support, U.S. Gov't, P.H.S.]. *Cell, 93*(2), 229-240.

Nakae, S., Komiyama, Y., Nambu, A., Sudo, K., Iwase, M., Homma, I., et al. (2002). Antigen-specific T cell sensitization is impaired in IL-17-deficient mice, causing suppression of allergic cellular and humoral responses. [Research Support, Non-U.S. Gov't]. *Immunity, 17*(3), 375-387.

Nakae, S., Nambu, A., Sudo, K., & Iwakura, Y. (2003). Suppression of immune induction of collagen-induced arthritis in IL-17-deficient mice. *J Immunol, 171*(11), 6173-6177.

Nilsen, E. M., Johansen, F. E., Jahnsen, F. L., Lundin, K. E., Scholz, T., Brandtzaeg, P., et al. (1998). Cytokine profiles of cultured microvascular endothelial cells from the human intestine. *Gut, 42*(5), 635-642.

Numasaki, M., Fukushi, J., Ono, M., Narula, S. K., Zavodny, P. J., Kudo, T., et al. (2003). Interleukin-17 promotes angiogenesis and tumor growth. *Blood, 101*(7), 2620-2627.

Ogawa, A., Andoh, A., Araki, Y., Bamba, T., & Fujiyama, Y. (2004). Neutralization of interleukin-17 aggravates dextran sulfate sodium-induced colitis in mice. *Clin Immunol, 110*(1), 55-62.

Okazaki, H., Kakurai, M., Hirata, D., Sato, H., Kamimura, T., Onai, N., et al. (2002). Characterization of chemokine receptor expression and cytokine production in circulating CD4+ T cells from patients with atopic dermatitis: up-regulation of C-C chemokine receptor 4 in atopic dermatitis. *Clin Exp Allergy, 32*(8), 1236-1242.

Oppmann, B., Lesley, R., Blom, B., Timans, J. C., Xu, Y., Hunte, B., et al. (2000). Novel p19 protein engages IL-12p40 to form a cytokine, IL-23, with biological activities similar as well as distinct from IL-12. *Immunity, 13*(5), 715-725.

Park, H., Li, Z., Yang, X. O., Chang, S. H., Nurieva, R., Wang, Y. H., et al. (2005). A distinct lineage of CD4 T cells regulates tissue inflammation by producing interleukin 17. *Nat Immunol, 6*(11), 1133-1141.

Park, J. W., Merz, M., & Braun, P. (1998). Effect of HELP-LDL-apheresis on outcomes in patients with advanced coronary atherosclerosis and severe hypercholesterolemia. [Clinical Trial]. *Atherosclerosis, 139*(2), 401-409.

Pickens, S. R., Volin, M. V., Mandelin, A. M., 2nd, Kolls, J. K., Pope, R. M., & Shahrara, S. (2010). IL-17 contributes to angiogenesis in rheumatoid arthritis. [Comparative Study Research Support, N.I.H., Extramural Research Support, Non-U.S. Gov't]. *J Immunol, 184*(6), 3233-3241.

Plump, A. S., & Breslow, J. L. (1995). Apolipoprotein E and the apolipoprotein E-deficient mouse. [Review]. *Annu Rev Nutr, 15*, 495-518.

Plump, A. S., Smith, J. D., Hayek, T., Aalto-Setala, K., Walsh, A., Verstuyft, J. G., et al. (1992). Severe hypercholesterolemia and atherosclerosis in apolipoprotein E-deficient mice created by homologous recombination in ES cells. [Research Support, Non-U.S. Gov't Research Support, U.S. Gov't, P.H.S.]. *Cell, 71*(2), 343-353.

Pober, J. S., & Cotran, R. S. (1990). The role of endothelial cells in inflammation. *Transplantation, 50*(4), 537-544.

Powell-Braxton, L., Veniant, M., Latvala, R. D., Hirano, K. I., Won, W. B., Ross, J., et al. (1998). A mouse model of human familial hypercholesterolemia: markedly elevated low density lipoprotein cholesterol levels and severe atherosclerosis on a low-fat chow diet. [Research Support, U.S. Gov't, P.H.S.]. *Nat Med, 4*(8), 934-938.

Qian, Y., Zhao, Z., Jiang, Z., & Li, X. (2002). Role of NF kappa B activator Act1 in CD40-mediated signaling in epithelial cells. [Research Support, U.S. Gov't, P.H.S.]. *Proc Natl Acad Sci U S A, 99*(14), 9386-9391.

Rabelink, T. J., & van Zonneveld, A. J. (2006). Coupling eNOS uncoupling to the innate immune response. [Comment Editorial]. *Arterioscler Thromb Vasc Biol, 26*(12), 2585-2587.

Rickel, E. A., Siegel, L. A., Yoon, B. R., Rottman, J. B., Kugler, D. G., Swart, D. A., et al. (2008). Identification of functional roles for both IL-17RB and IL-17RA in mediating IL-25-induced activities. *J Immunol, 181*(6), 4299-4310.

Rocha, V. Z., Chacra, A. P., Salgado, W., Miname, M., Turolla, L., Gagliardi, A. C., et al. (2013). Extensive xanthomas and severe subclinical atherosclerosis in homozygous familial hypercholesterolemia. [Case Reports]. *J Am Coll Cardiol, 61*(21), 2193.

Rosenfeld, M. E., Palinski, W., Yla-Herttuala, S., Butler, S., & Witztum, J. L. (1990). Distribution of oxidation specific lipid-protein adducts and apolipoprotein B in atherosclerotic lesions of varying severity from WHHL rabbits. *Arteriosclerosis, 10*(3), 336-349.

Roussel, L., Houle, F., Chan, C., Yao, Y., Berube, J., Olivenstein, R., et al. (2010). IL-17 promotes p38 MAPK-dependent endothelial activation enhancing neutrophil recruitment to sites of inflammation. [Research Support, Non-U.S. Gov't]. *J Immunol, 184*(8), 4531-4537.

Rouvier, E., Luciani, M. F., Mattei, M. G., Denizot, F., & Golstein, P. (1993). CTLA-8, cloned from an activated T cell, bearing AU-rich messenger RNA instability sequences, and homologous to a herpesvirus saimiri gene. [Research Support, Non-U.S. Gov't]. *J Immunol, 150*(12), 5445-5456.

Rubina, K., Talovskaya, E., Cherenkov, V., Ivanov, D., Stambolsky, D., Storozhevykh, T., et al. (2005). LDL induces intracellular signalling and cell migration via atypical LDL-binding protein T-cadherin. [Research Support, Non-U.S. Gov't]. *Mol Cell Biochem, 273*(1-2), 33-41.

Sallusto, F., Lenig, D., Mackay, C. R., & Lanzavecchia, A. (1998). Flexible programs of chemokine receptor expression on human polarized T helper 1 and 2 lymphocytes. *J Exp Med, 187*(6), 875-883.

Schaefer, E. J., Gregg, R. E., Ghiselli, G., Forte, T. M., Ordovas, J. M., Zech, L. A., et al. (1986). Familial apolipoprotein E deficiency. [Case Reports Comparative Study]. *J Clin Invest, 78*(5), 1206-1219.

Schieffer, B., Selle, T., Hilfiker, A., Hilfiker-Kleiner, D., Grote, K., Tietge, U. J., et al. (2004). Impact of interleukin-6 on plaque development and morphology in experimental atherosclerosis. *Circulation, 110*(22), 3493-3500.

Schober, A. (2008). Chemokines in vascular dysfunction and remodeling. *Arterioscler Thromb Vasc Biol, 28*(11), 1950-1959.

Shaposhnik, Z., Wang, X., Weinstein, M., Bennett, B. J., & Lusis, A. J. (2007). Granulocyte macrophage colony-stimulating factor regulates dendritic cell content of atherosclerotic lesions. *Arterioscler Thromb Vasc Biol, 27*(3), 621-627.

Shen, F., & Gaffen, S. L. (2008). Structure-function relationships in the IL-17 receptor: implications for signal transduction and therapy. [Research Support, N.I.H., Extramural Research Support, Non-U.S. Gov't Review]. *Cytokine, 41*(2), 92-104.

Smith, E., Prasad, K. M., Butcher, M., Dobrian, A., Kolls, J. K., Ley, K., et al. (2010). Blockade of interleukin-17A results in reduced atherosclerosis in apolipoprotein E-deficient mice. *Circulation, 121*(15), 1746-1755.

Song, L., & Schindler, C. (2004). IL-6 and the acute phase response in murine atherosclerosis. *Atherosclerosis, 177*(1), 43-51.

Szypula, I., Kotulska, A., Szopa, M., Pieczyrak, R., & Kucharz, E. J. (2009). Adiposis dolorosa with hypercholesterolemia and premature severe generalized atherosclerosis. [Case Reports Letter]. *Wiad Lek, 62*(1), 64-65.

Tabas, I., Williams, K. J., & Boren, J. (2007). Subendothelial lipoprotein retention as the initiating process in atherosclerosis: update and therapeutic implications. [Research Support, N.I.H., Extramural Research Support, Non-U.S. Gov't Review]. *Circulation, 116*(16), 1832-1844.

Tabibiazar, R., Wagner, R. A., Deng, A., Tsao, P. S., & Quertermous, T. (2006). Proteomic profiles of serum inflammatory markers accurately predict atherosclerosis in mice. *Physiol Genomics, 25*(2), 194-202.

Takada, Y., Ye, X., & Simon, S. (2007). The integrins. [Review]. *Genome Biol, 8*(5), 215.

Takahashi, H., Numasaki, M., Lotze, M. T., & Sasaki, H. (2005). Interleukin-17 enhances bFGF-, HGF- and VEGF-induced growth of vascular endothelial cells. *Immunol Lett, 98*(2), 189-193.

Taleb, S., Romain, M., Ramkhelawon, B., Uyttenhove, C., Pasterkamp, G., Herbin, O., et al. (2009). Loss of SOCS3 expression in T cells reveals a regulatory role for interleukin-17 in atherosclerosis. [Research Support, Non-U.S. Gov't]. *J Exp Med, 206*(10), 2067-2077.

Toy, D., Kugler, D., Wolfson, M., Vanden Bos, T., Gurgel, J., Derry, J., et al. (2006). Cutting edge: interleukin 17 signals through a heteromeric receptor complex. *J Immunol, 177*(1), 36-39.

Tran, E. H., Prince, E. N., & Owens, T. (2000). IFN-gamma shapes immune invasion of the central nervous system via regulation of chemokines. *J Immunol, 164*(5), 2759-2768.

Usui, F., Kimura, H., Ohshiro, T., Tatsumi, K., Kawashima, A., Nishiyama, A., et al. (2012). Interleukin-17 deficiency reduced vascular inflammation and development of atherosclerosis in Western diet-induced apoE-deficient mice. [Research Support, Non-U.S. Gov't]. *Biochem Biophys Res Commun, 420*(1), 72-77.

van Es, T., van Puijvelde, G. H., Ramos, O. H., Segers, F. M., Joosten, L. A., van den Berg, W. B., et al. (2009). Attenuated atherosclerosis upon IL-17R signaling disruption in LDLr deficient mice. *Biochem Biophys Res Commun, 388*(2), 261-265.

Vickers, K. C., & Remaley, A. T. (2014). HDL and cholesterol: life after the divorce? [Research Support, N.I.H., Extramural Research Support, N.I.H., Intramural]. *J Lipid Res, 55*(1), 4-12.

Vidal, F., Colome, C., Martinez-Gonzalez, J., & Badimon, L. (1998). Atherogenic concentrations of native low-density lipoproteins down-regulate nitric-oxide-synthase mRNA and protein levels in endothelial cells. [Research Support, Non-U.S. Gov't]. *Eur J Biochem, 252*(3), 378-384.

Wang, L., Yi, T., Kortylewski, M., Pardoll, D. M., Zeng, D., & Yu, H. (2009). IL-17 can promote tumor growth through an IL-6-Stat3 signaling pathway. *J Exp Med, 206*(7), 1457-1464.

Whitman, S. C., Ravisankar, P., & Daugherty, A. (2002). Interleukin-18 enhances atherosclerosis in apolipoprotein E($^{-/-}$) mice through release of interferon-gamma. [Research Support, Non-U.S. Gov't]. *Circ Res, 90*(2), E34-38.

Whitman, S. C., Ravisankar, P., Elam, H., & Daugherty, A. (2000). Exogenous interferon-gamma enhances atherosclerosis in apolipoprotein E$^{-/-}$ mice. [Research Support, Non-U.S. Gov't]. *Am J Pathol, 157*(6), 1819-1824.

WHO. (2011a). *Global atlas on cardiovascular disease prevention and control*. Geneva, Switzerland: World Health Organization.

WHO. (2011b). *Global status report on noncommunicable diseases 2010*. Geneva, Switzerland: World Health Organization.

Yoon, K., Jung, E. J., Lee, S. R., Kim, J., Choi, Y., & Lee, S. Y. (2008). TRAF6 deficiency promotes TNF-induced cell death through inactivation of GSK3beta. [Research Support, Non-U.S. Gov't]. *Cell Death Differ, 15*(4), 730-738.

Zarubin, T., & Han, J. (2005). Activation and signaling of the p38 MAP kinase pathway. [Review]. *Cell Res, 15*(1), 11-18.

Zhang, S. H., Reddick, R. L., Burkey, B., & Maeda, N. (1994). Diet-induced atherosclerosis in mice heterozygous and homozygous for apolipoprotein E gene disruption. *J Clin Invest, 94*(3), 937-945.

Zhang, S. H., Reddick, R. L., Piedrahita, J. A., & Maeda, N. (1992). Spontaneous hypercholesterolemia and arterial lesions in mice lacking apolipoprotein E. [Research Support, Non-U.S. Gov't Research Support, U.S. Gov't, P.H.S.]. *Science, 258*(5081), 468-471.